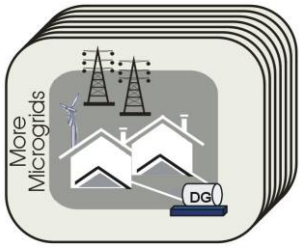

Advanced Architectures and Control Concepts for

MORE MICROGRIDS

Contract No: PL019864

WORK PACKAGE F

TF3. Experimental validation of islanding mode of operation

DF2: Report on field tests for islanded mode

(Kythnos Test site)

Final Version

December 2009

Document Information

Title: Experimental validation of islanding mode of operation

Date: 30-12-2009

Task(s):

Coordination:	Stathis Tselepis	Stathis Tselepis [stselep@cres.gr]
Authors:	Nikos Hatziargyriou	nh@power.ece.ntua.gr
	Aris Dimeas	adimeas@power.ece.ntua.gr
	Spyros Hatzivasiliadis	spyrosxatz@gmail.com
	Michel Vandenbergh	mvandenbergh@iset.uni-kassel.de
	Randolf Geipel	rgeipel@iset.uni-kassel.de
	Stathis Tselepis	Stathis Tselepis [stselep@cres.gr]

Access:

__ **Project Consortium**
_ European Commission
~~X~~ PUBLIC

Status:

_ For Information
_ Draft Version
_ Final Version (internal document)
_ **Submission for Approval (deliverable)**
X Final Version (deliverable, approved on…)

1. Introduction

The electric system in Gaidouromantra, Kythnos initially it was constructed as a 3-phase low voltage system formed by battery inverters. Over the years, for various experimental purposes, it has been modified from 3-phase to 1-phase and recently, in June 2007, it was reconfigured as a 3-phase system for the needs of the EC project "MoreMicrogrids".
The microgrid system is composed of the overhead power lines and a communication cable running in parallel to serve the monitoring and control needs. It is electrifying 12 vacation houses in a small valley in Kythnos, an island in the cluster of Cyclades situated in the middle of the Aegean Sea. The grid and safety specifications for the house connections respect the technical solutions of the Public Power Corporation (PPC), which is the local electricity utility.

Figure 1: The Medium Voltage distribution line (in black) for the island of Kythnos and the location of RES systems and a microgrid powered by RES in Gaidouromantra (red letters) in the south east side of the island.

The settlement is situated about 4 kilometres away from the closest pole of the medium voltage line of the island. A system house of about 30 m2 surface area was built in the middle of the settlement in order to house the battery inverters, the battery banks, the diesel genset and its tank, the computer equipment for monitoring and the communication hardware, called "System Hut or house". The grid electrifying the users is powered by 3 Sunny-island battery inverters, which when they are forming a 1-phase system, they are connected in parallel to form one strong single-phase in a master slave configuration, allowing the use of more than one battery inverter only when more power is demanded by the consumers. Each battery inverter (SI4500) had a maximum power output of 3.6kW.

The battery inverters in the Kythnos system have the capability to operate in both isochronous or droop mode. The operation in frequency droop mode gives the possibility to pass information on to switching load controllers in case the battery state of charge is low and also to limit the power output of the PV inverters when the battery bank is full.

Figure 3: The "system hut or house" where the battery inverters, batteries, diesel generator and monitoring systems are kept.

Until June 2007, the users' system was composed of 10kWp of Photovoltaics divided in smaller PV sub-arrays and a battery bank of nominal capacity 53kWh and a 3-phase diesel genset with a nominal output of 5kVA, when used in 1-phase configuration and 9 kVA when operating in 3-phase configuration. A second system with a 2 kWp PV array is mounted on the roof of the system hut, connected to a Sunny-island inverter and a 32kWh battery bank. This second system provides the power for the monitoring and communication needs of the whole microgrid system. The PV modules are integrated as canopies to various houses of the settlements.

In the first two EC projects, apart from the demonstration of the new battery inverter technology, the main challenge was to control a microgrid with distributed PV generators. Control solutions, based on grid frequency variation (droop control) as communication signal, have been adopted. The battery inverter was able to vary the grid frequency in order to provide simple control information to the distributed PV inverters and to the load controllers installed in each house. The load controllers were developed by E-Connect (UK) and are able to disconnect the whole house as one load. The Sunny island battery inverter, when the battery state of charge is low, mimics the effect of an overloaded generator which is slowing down thus effectively decreasing the microgrid frequency. The E-Connect load controllers are operated in the frequency mode, that is, they sense the grid frequency and they disconnect the house when the frequency drops below a set frequency

(set at 49.14 Hz), provided that the battery state of charge is low or the system is overloaded by the users. The houses "loads" are re-connected randomly when the grid frequency is increased as the battery state of charge is increased. This allows the houses to come back onto the grid progressively, than suddenly coming all together, overloading the system again. Based also on the grid frequency value (when above 50Hz), the PV inverters are able to continuously de-rate their power output, in order to avoid overcharging the battery bank. Finally, a back-up diesel generator was integrated smoothly in the system to charge the batteries.

Figure 4: Wide area view of the Gaidouromantra microgrid in Kythnos island.

This report presents the work within the MORE MICROGRIDS project. More specific the first part includes the description of the simulation tool developed for testing the operation of the Gaidouromantra's Microgrid. The second part included the description of the installation of the load controller and the Multi Agent based control software developed in WPB. Finally the last part presents the results from the system performance monitoring.

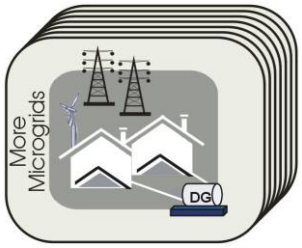

Advanced Architectures and Control Concepts for

MORE MICROGRIDS

Contract No: PL019864

WORK PACKAGE F

DF2. Report on Gaidouromantra microgrid modeling and simulation

Final Version

December 2009

Document Information

Title: Experimental validation of islanding mode of operation

Date: 30-12-2009

Task(s):

Coordination:	Stathis Tselepis	stselep@cres.gr
Authors:	Stathis Tselepis	stselep@cres.gr
	Vangelis Rikos	vrikos@cres.gr

Access:

__	**Project Consortium**
__	European Commission
~~X~~	PUBLIC

Status:

__	For Information
__	Draft Version
__	Final Version (internal document)
__	**Submission for Approval (deliverable)**
X	Final Version (deliverable, approved on…)

1. GENERAL DESCRIPTION-REQUIREMENTS

1.1. Introduction

The main purpose of this report is the description of the simulation tool developed for testing the operation of the Gaidouromantra's microgrid. The specific power system is a pilot one and constitutes the field of many innovative studies and tests, through different projects. In the frame of the specific project, a simulation tool was developed which provides the ability to investigate the operation under different production or load conditions. One of the main scopes of the study was the development of a tool which will be versatile in order to be easily used not only for power flow analysis but also for potential dynamic tests (e.g. short circuit tests). For this purpose the selected platform for this tool was the Matlab/Simulink.

As mentioned above, the main scope of this study is the development of a simulation tool which will describe as accurately as possible the real system mainly in terms of PV production, battery's State of Charge etc. under specific insolation or load conditions. The generation and consumption profiles may be constant or variable, based on realistic data or other desired patterns. As a system, the developed tool receives some inputs (solar irradiance, temperature, loads consumptions) and returns some output quantities (PV power, SOC, Voltage and Frequency). In the next pages a short general description of the microgrid is given. Also, the main assumptions and the points at which this study focuses on are outlined. In the second part, the analytical models for each of the parts are described. Finally, simulation results with discussion on them as well as possible extensions-improvements and perspectives are discussed.

1.2. Basic configuration

The power system of Gaidouromantra is an autonomous microgrid, producing electricity from PVs and using different battery storages for the energy coverage of 13 houses and the control and monitoring systems. The main components of the microgrid are briefly described below:

- PV generators: The system includes 7 PV arrays at different places and angles. The installed power of them is 11kWp. Every PV generator is connected to one of the three phases of the microgrid through inverters.
- Battery storage: The main storages of the system are two battery banks. The battery cells are Lead-Acid (FLA) batteries. The main bank is 800Ah, 48V (400kWh) while the back-up system consists of cells 480Ah while the total voltage is 60V (30kWh). The

main system is regulated through three single phase battery inverters (SI5048) forming a three phase voltage system. The secondary battery is controlled through one single phase inverter (SI4500). During the day, the two banks are connected together at the AC side in order to cover the energy demands of the houses. At night, the two banks are disconnected and the secondary system covers the needs of all the control and monitoring equipment.

- Diesel back-up generator: the system is equipped with a three-phase 9kVA diesel generator, which operates only in case of emergency, when the main batteries are discharged (SOC<30%). In this case, the battery inverters trigger the diesel startup and the generator charges the battery until the SOC becomes 80%.
- Three-phase overhead lines for the connection of loads and generators.
- Energy consumers which are considered as ohmic and inductive loads for the representation of houses' and control systems consumption.
- Load controllers: these devices are used for the protection of the system against overloading. The main feature of them is the fact that according to the frequency, a load shed can take place preventing so overload of the microgrid or deep discharge of the batteries. The frequency limit for load shed is 49.14Hz. The load reconnection becomes after two minutes and randomly in order to prevent instant reconnection of all the consumers.

1.3. Main features of the developed simulation model

As it is obvious the studied system appears an important complexity in its modeling since it consists of many devices and subsystems with a variety of parameters and features. In this study, we focused on some specific characteristics which where integrated in the model of each subsystem. These characteristics are outlined below:

- First of all the microgrid was modeled as a 3-phase system with many devices connected to different phases. It is important to mention that in case that is necessary the configuration can be easily changed to single phase.
- Considering the PV units, in our study each PV array and inverter were modeled as one device, which present an I-V curve based on known mathematical model. The effects of irradiance and temperature are also taken into consideration. Another important feature of the developed simulation model is the existence of an MPP algorithm. The selected algorithm is based on the open-circuit voltage, and as described in a following section was used in order to reduce the simulation time. Also,

the feature of power derate versus frequency was modeled. As in the real system, the PV inverters have the ability to reduce the output power linearly versus the frequency, if the latter varies from 51 to 52Hz. This feature is used from the battery management system in order to prevent battery overcharge. Finally, the model PV systems have unity power factor.

- Battery storage: The battery model includes three main features: Calculation of the terminal voltage, calculation of the remaining Ampere-hours and calculation of the maximum available capacity. These parameters are modeled through the kinetic battery model as described in the next paragraphs.
- Battery inverters: One of the most complicated parts due to the variety of operations and control that perform. The main features on which the study focused are: the ability for grid-forming or grid-tied operation. In other words, the battery inverters can change their mode from voltage to current source with constant or variable frequency. Moreover, the battery SOC calculation which is crucial for the management. The battery management is divided mainly into two parts. The first one involves frequency regulation according to the battery SOC. The detail frequency control is given in the next paragraphs. In addition, the inverter selects the battery charging voltage according to specific parameters which determine the charging phase.
- Diesel generator: This subsystem is modeled as a simplified current source which charges the battery bank. During its operation the frequency varies according to the load which is taken into account into our study. Also, one parameter which will be modeled in the diesel genset is the oil consumption which is a linear equation of the operation time.
- Load controllers: the main features of this device are the load shed for frequency under 49,14Hz and the reconnection of loads when f>49,14Hz. In this case, the minimum and maximum reconnection times are 2 and 4min while the reconnection is random.

1.4. Basic Assumptions

The development of the simulation models demands some assumptions which are necessary in order to determine the model abilities and to reduce as much as the simulation time. Focusing on the operation of the system, the simulation model should be tested in time intervals of some days. This means that we need to simplify some critical points of the model and the solution method. The simplification deals with transients

because simulation models with high transients appear demand longer simulation times. Because of this the assumptions were the following:

- Use of continuous linear sources (current or voltage) wherever a power converter exists. This, in other words means that, the PV as well as the battery inverters are not model as Switch Mode Power Converters but as linear sources which give the same output. This assumption was made because the switching behavior of power inverters increases dramatically the simulation time while does not provide important information from the system's point of view.
- Use of phasor solution. This technique was selected in order to have high simulation speed because it calculates only the angles and the magnitudes of the electrical quantities. In contrast, the calculation of continuous quantities would increase dramatically the simulation time without giving important details about the system's operation.

2. MODEL DEVELOPMENT

Based on the aforementioned specifications and assumptions, discrete models for each of the microgrid's parts were developed. The models were based either on literature of on manufacturer datasheets. In the following paragraphs, detailed description of the used models as well as the final Matlab/Simulink model for each component is given.

2.1. PV System Model

A. PV Module

In general, a PV cell can be represented by the equivalent circuit shown in fig. 1.

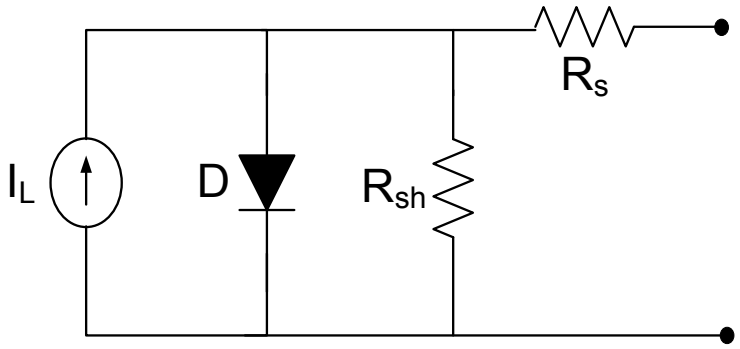

Fig. 1: Equivalent circuit of a PV cell

The above model although it is accurate and can be used in various simulation tests, it has the disadvantage of incorporating quantities which are very difficult to be determined and are not given by manufacturers. Because of this a more appropriate model should be used.

The selected model for our simulation was the known from literature "interpolation model" [1] which compared to other mathematical models is more advantageous, because all the parameters apart from the series resistance (R_s) are given. The most important feature of the model is the fact that the parameters are directly those given in the data sheet and there is no necessity for adaptation or other calculations. The selected model is described by the following equation set:

$$I=I_{SC}\left[1-C_1\left(\exp\left(\frac{V_R}{C_2 V_{oc}}\right)-1\right)\right]+D_I \quad (1)$$

Where:

$$C_1=\left(1-\frac{I_{mp}}{I_{sc}}\right)\exp\left(-\frac{V_{mp}}{C_2 V_{oc}}\right) \quad (2)$$

$$C_2=\left(\frac{V_{mp}}{V_{oc}}-1\right)\Big/\ln\left(1-\frac{I_{mp}}{I_{sc}}\right) \quad (3)$$

$$V_R=V+\beta\left(T-T_{ref}\right)+R_s D_I \quad (4)$$

$$D_I=\alpha\Phi\left(T-T_{ref}\right)+I_{sc}\left(\Phi-1\right) \quad (5)$$

V_{mp}=Maximum Power Point Voltage
I_{mp}=Maximum Power Point Current
V_{oc}=Open Circuit Voltage
I_{sc}=Short Circuit Current
Φ=Solar Irradiance
T=Cell Temperature
T_{ref}=Reference Temperature (25 ^{o}C)
α, β=Coefficients of Isc and Voc variation depending on temperature.
R_s=Series Resistance.

The above equation set describes the I-V curve, taking as I the dependent and V as the independent variable. In addition, this model provides a relationship of the voltage as a function of the current. In our case it was considered that the PVs supply the loads (Sunny boy inverters) with current. Thus, the used model was the one of eq. 1. In fig. 2, the Matlab/Simulink block diagram is depicted.

B. PV Inverter Model

In addition to the modules a model for the PV inverters was developed. The inverters installed in the microgrid are the SMA-Sunny Boy. The main features taken into account for the modeling are:

- Maximum Power Point Tracking (MPPT) in order to obtain always the maximum power from the PVs.
- Operation as current sources.

Power vs. Frequency derate through a specific pattern in order to prevent the battery overcharging.

More specifically, for the MPPT a specific algorithm based on literature was selected. Compared with other algorithms the selected one is the most simplified and the fastest which was considered critical for the simulation speed [2]. This algorithm is based on the calculation of the MPP voltage from the open circuit voltage as given below:

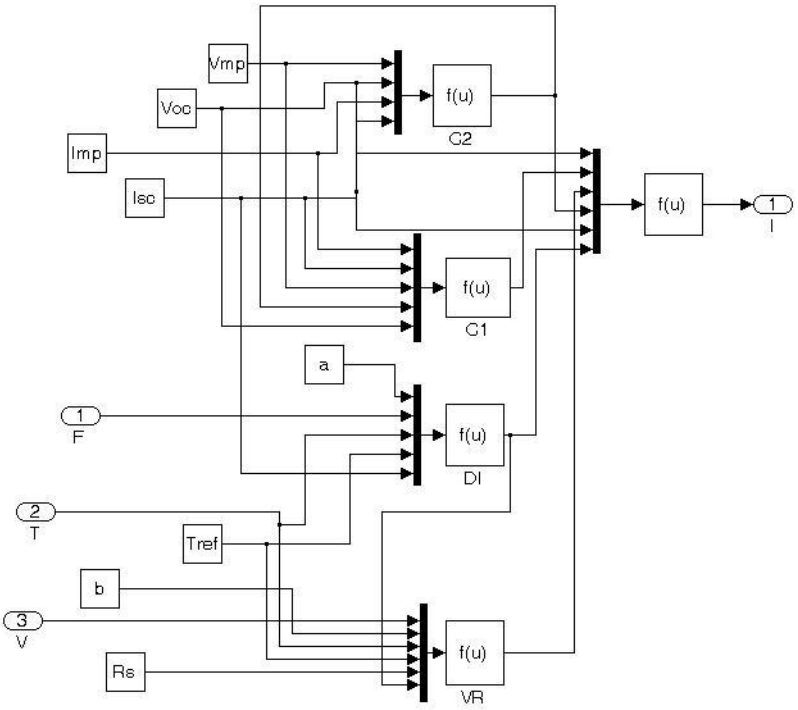

Fig.2: Matlab/Simulink model for a PV panel

$$V_{mp}^{*}=0.79V_{oc}^{*} \tag{6}$$

$$V_{oc}^{*}=C_2V_{oc}\ln\left(\frac{\left(1-\left(I-D_I\right)/I_{sc}\right)}{C_1}+1\right)-\beta\left(T-T_{ref}\right)-R_SD_I \tag{7}$$

It is important to mention that in a real system the V_{oc} can be determined through measurement. In our case the calculation through eq.7 was selected in order to achieve reduction of the computational time.

Concerning the power vs. frequency derate, the specific series of inverter provide the ability of reducing the PV generated power linearly from frequencies between 51 and 52 Hz according to the formula:

$$P_{ac}=\begin{cases}P_{pv,\,max}, & f \le 51Hz \\ P_{pv,max}\,(52\text{-}f), & 51<f \le 52Hz \\ 0, & f>52Hz\end{cases} \quad (8)$$

Where P_{ac} the output power, $P_{pv,max}$ is the maximum power from the PVs and f the frequency. The power derate is used in order to prevent battery overcharging.

In fig. 3 the simulink model for the MPPT is shown. This subsystem receives as input the PV operating as well as the open circuit voltage and controls the current in order to achieve the voltage reference. This block yields as outputs the current and the power. The first is used as a feedback to the PV model while, the latter is driven to the power derate subsystem which is shown in fig. 4.

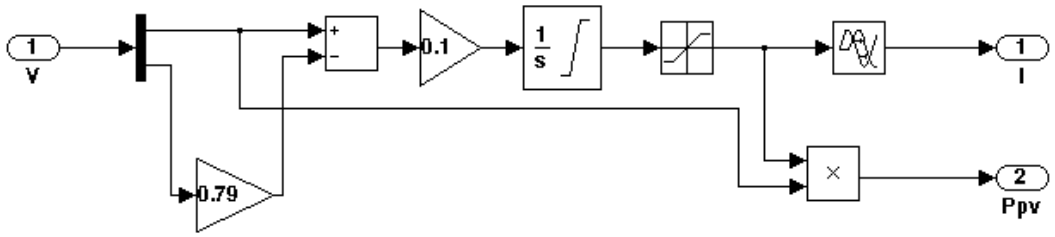

Fig.3: Matlab/Simulink model for the MPP Tracker

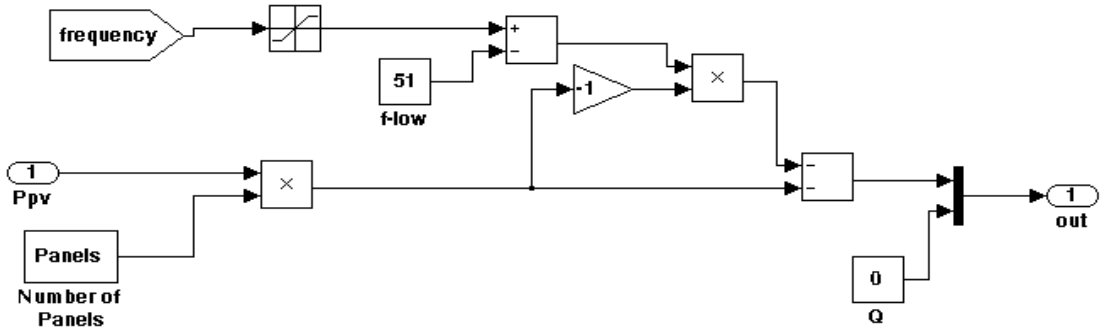

Fig.4: Matlab/Simulink model for the power derate

2.2. Battery Storage System

A. Battery model

The implemented model for all the batteries is the known from literature Kinetic Battery Model [3]. According to this paper the battery can be described by an equivalent circuit shown in fig. 5.

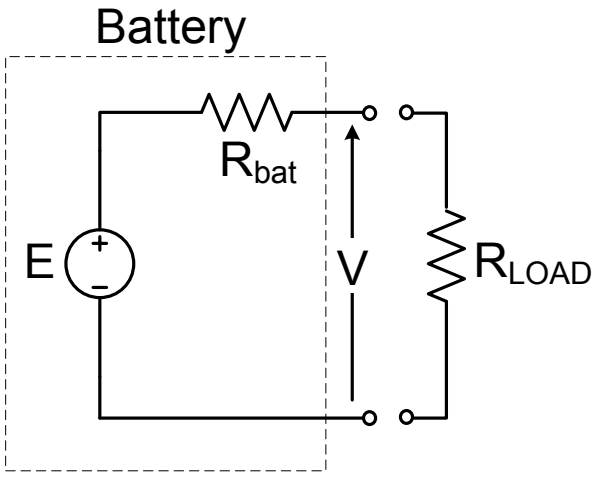

Fig.5: Thevenin equivalent circuit for the Kinetic Battery Model

In our study, two major components of the battery model were developed. These are the remaining capacity q and the battery terminal voltage V. The battery capacity is calculated from the following set of equations:

$$q = q_1 + q_2 \tag{9}$$

$$\frac{dq_1}{dt} = -I - k(1-c)q_1 + kcq_2$$
$$\frac{dq_2}{dt} = k(1-c)q_1 - kcq_2 \tag{10}$$

q=remaining capacity

q_1=available charge

q_2=bound charge

I=battery current

k=rate constant

c=Ratio of available charge capacity to total capacity.

In addition to the above, the following equation set for the terminal voltage was adopted:

$$V = E - IR_{bat} \tag{11}$$

$$E=E_o+AX+CX/(D-X) \tag{12}$$

$$X=\begin{cases} q/q_{max}(I), & \text{charging} \\ (q_{max}-q)/q_{max}(I), & \text{discharging} \end{cases} \tag{13}$$

$$q_{max}(I)=\frac{q_{max}kc(q_{max}(I)/I)}{1-e^{-k(q_{max}(I)/I)}+c\left(k(q_{max}(I)/I)-1+e^{-k(q_{max}(I)/I)}\right)} \tag{14}$$

E_o= fully charged/discharged internal battery voltage.

A= Parameter reflecting the initial linear variation of internal battery voltage with state of charge.

C, D=Parameters reflecting the decrease/increase of battery voltage during charging discharging.

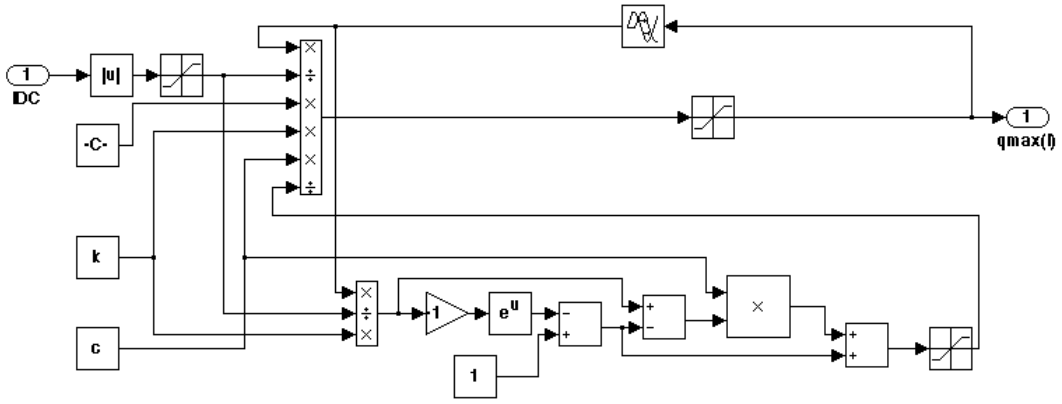

Fig.6: Matlab/Simulink model for the qmax(I) calculation

B. Battery inverters

One of the most complicated parts during modeling was the battery inverters. The developed model was used for both main and secondary battery system. The main features of the model are:

- State Of Charge (SOC) calculation. This is important for the battery management, the selection of charging phases and the frequency regulation.
- Frequency regulation according to the battery SOC.
- Initialization of the Diesel Genset.

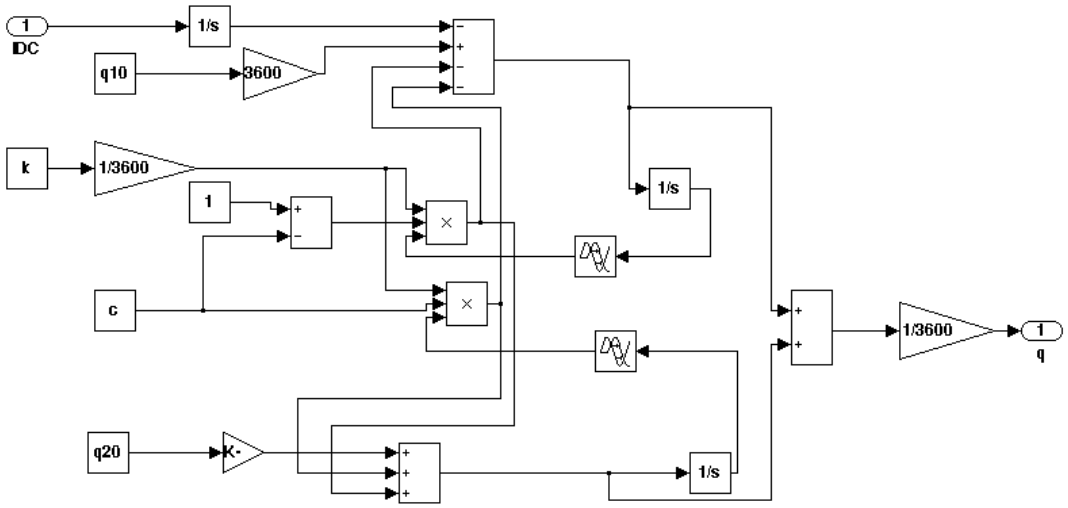

Fig.7: Matlab/Simulink model for the remaining Ah calculation

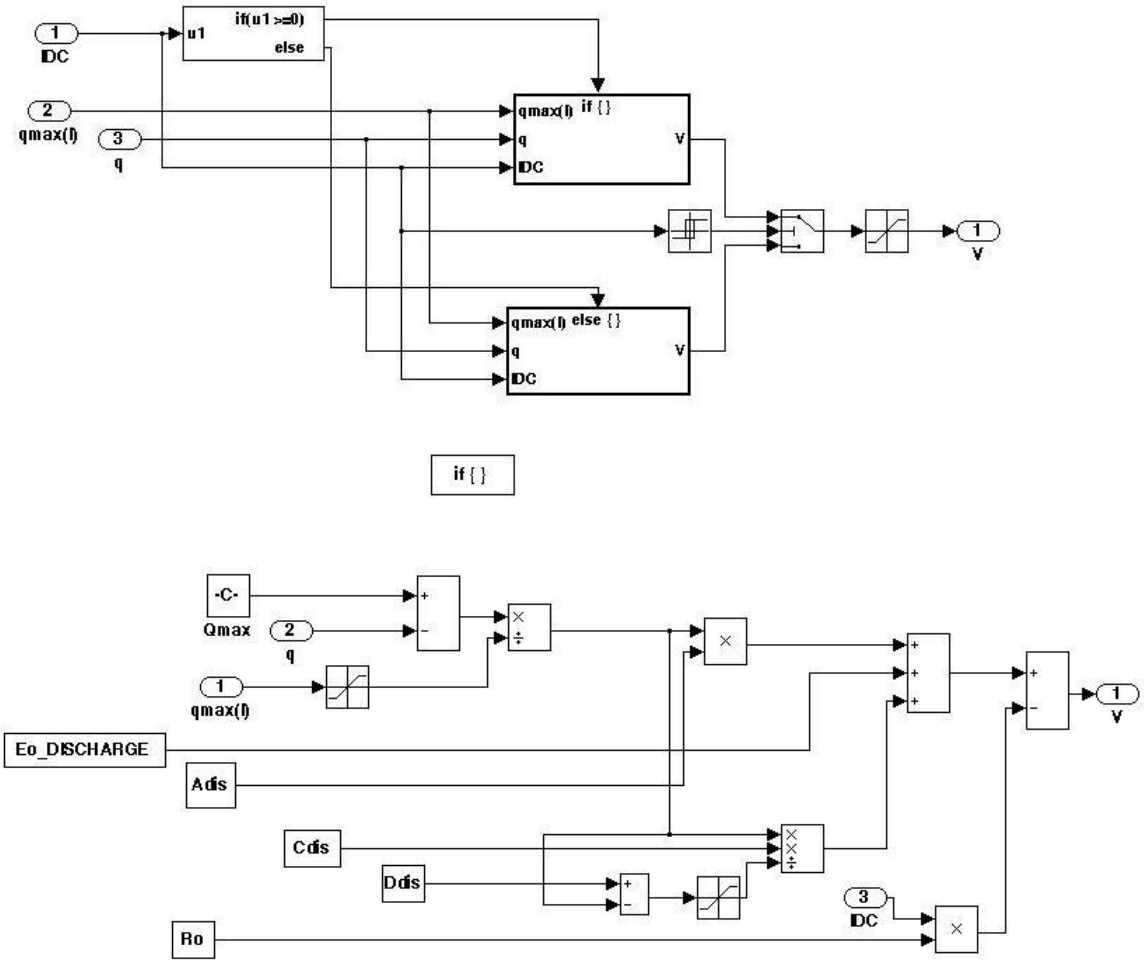

Fig.8: Matlab/Simulink model for the battery terminal voltage

- Selection of the maximum battery voltage according to the charging phase.
- Finally, depending on the operation mode (grid forming or charging through the diesel genset) the inverters were modeled as controlled voltage/current sources.

Below the main features of the battery inverters are outlined.

SOC calculation

The accurate calculation of the battery SOC is very critical in order to achieve the proper management which includes diesel startups, load sheds and charging phase selection. Among different calculation methods in the literature, the specific method selected in our study was the one based on the Ah-balancing. This method takes into account the charging/discharging current and the respective time. In our case, in order to increase the accuracy the method of Ampere-hour included also losses due to gassing [4]. This model is described from the following equation set:

$$SOC=\frac{1}{C_{10}}\int\left(I_{bat}-I_{gas}\right)dt \quad (15)$$

$$I_{gas}=\frac{I_{go}}{100Ah}\exp\left[C_V\left(V_{cell}-2.23V\right)+C_T\left(T-20^oC\right)\right] \quad (16)$$

C_{10}=Battery capacity for 10-hour discharging.

I_{go}=Normalized gassing current.

C_V=Voltage coefficient.

V_{cell}=Battery cell voltage.

C_T=Temperature coefficient.

T=Cell temperature.

In fig.9 the developed Simulink diagram for the SOC calculation is depicted.

Frequency regulation

During the operation the battery inverter is regulating the frequency in order to control the generated/consumed energy and hence to maintain the battery health. The parameters which determine the operating frequency are the battery SOC and terminal voltage. According to these, the frequency is kept constant at 50Hz until the SOC falls under the critical limit of 15%. Under this limit the inverter causes a step decrease in the frequency from 50 to 47Hz. This results to activation of the installed load controllers which will

immediately disconnect the loads until the battery SOC increases to 50%. When this happens, the frequency returns to the nominal value of 50Hz and the loads are reconnected. The other leg of frequency regulation includes linear change of frequency between 51 and 52Hz. This aims to battery protection against overcharging. The parameter in this case is the battery voltage. During charging the battery voltage should be less or equal to a limit value, the charge voltage, which is determined from the charging phase and the battery temperature. If during the operation the real voltage becomes higher than the reference value, a PI controller changes the frequency so as to derate the output power from the PV inverters. Similarly, the frequency decreases when the real voltage becomes lower than the reference value. Summarizing the previous description in one formula we have:

$$f = \begin{cases} 50\text{Hz}, & \text{for SOC}>15\% \\ 47\text{Hz}, & \text{for SOC}<15\% \text{ and until reaches } 50\% \\ 51\text{-}52\text{Hz}, & \text{for } V_{bat} > V_{charge} \end{cases} \quad (17)$$

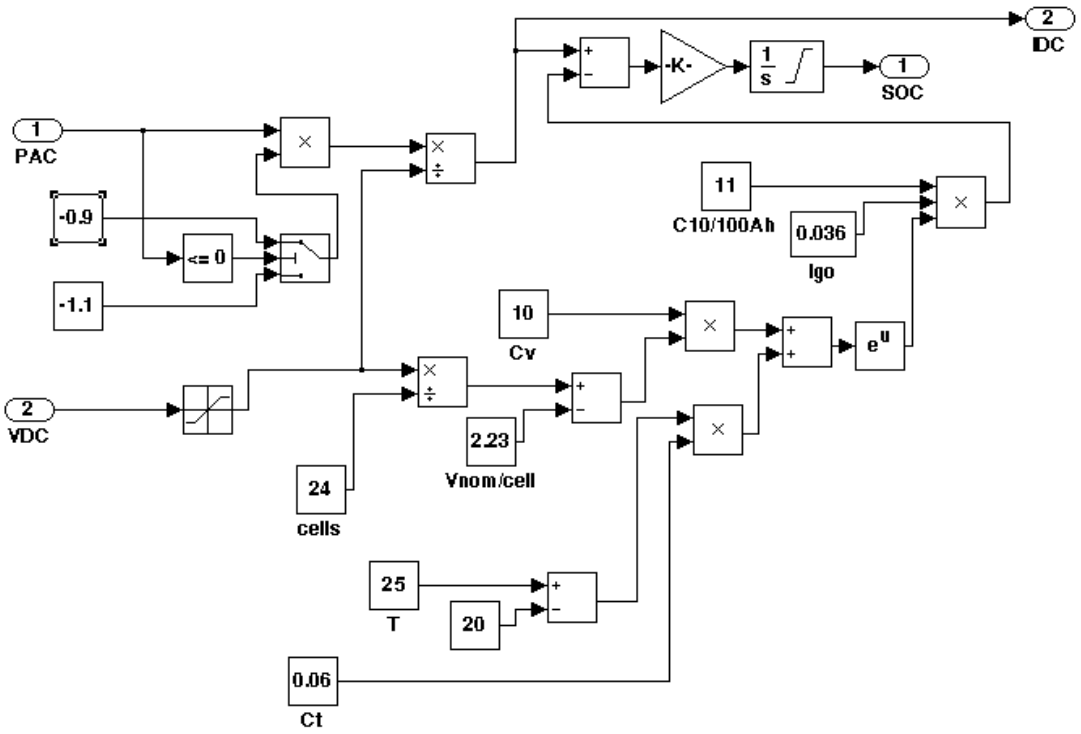

Fig. 9: Matlab/Simulink model for the battery SOC calculation

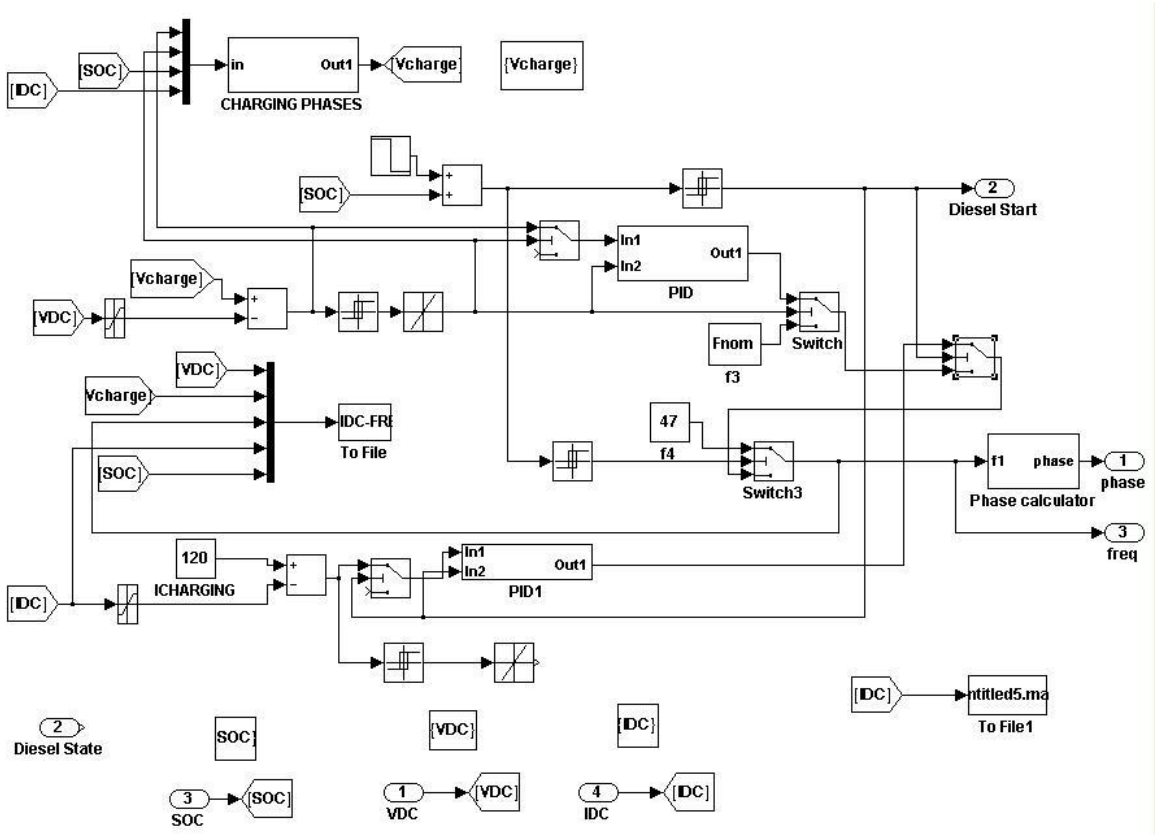

Fig. 10: Matlab/Simulink model for the battery inverter frequency regulation

Diesel genset control

An additional feature of the battery inverter modeled in this study was the control of the diesel generator. This unit is used only as an emergency backup when the battery are deeply discharged (SOC<30%). This means that before the critical limit of 15% with the load shed, the inverter starts up the diesel generator in order to charge the batteries. During this operation the frequency decreases continuously between 49 and 50 Hz. The procedure continues until the SOC value becomes 80%. Then the inverter deactivates the generator and the systems returns to the normal state. This feature is also depicted in fig.10.

Charging phases and temperature compensation

This feature includes the selection of the charging voltage according to the phase and the battery temperature. The real system includes four charging phases with different reference voltage. The first phase is the Boost charging which has maximum duration 90 min. After that time the control passes to float charging until SOC becomes 70% or more

than 30% of the nominal capacity has been used. When this happens the system returns to the boost charging. The other two phases take place instead of boost charging after 14days (or 8 charging throughputs) for the phase of full charging and every 180 days (or 30 charging throughputs). From all the above phases the developed model focuses on boost and float charging. The voltage/cell for each of the previous phases is: 2,55V for boost and 2,23V for float charging. This values in the real system as well as in the developed model change according to the battery temperature with a coefficient of -0,4% for each cell.

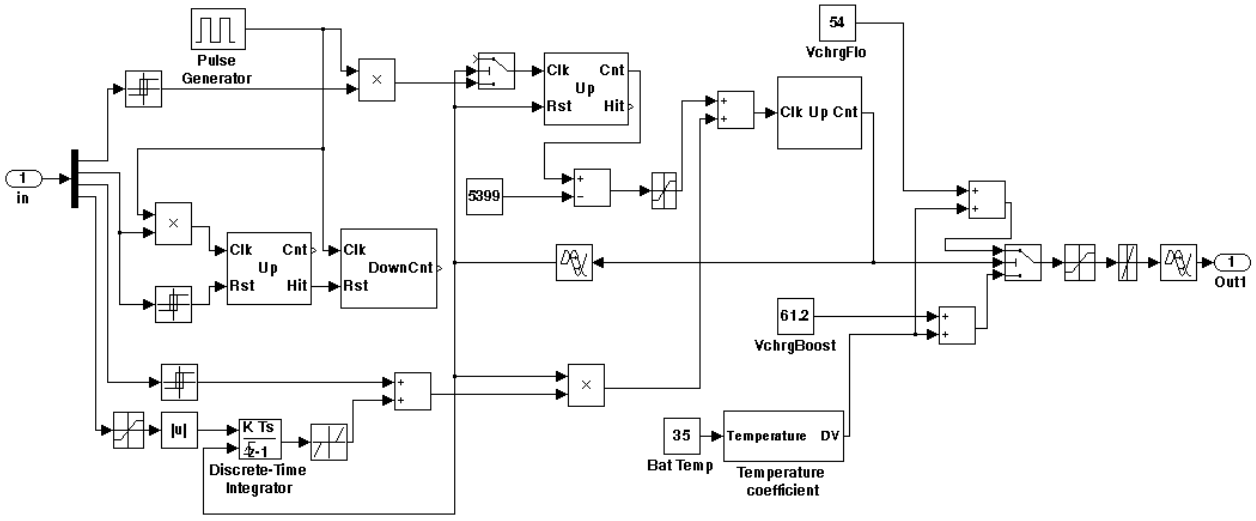

Fig. 11: Matlab/Simulink model for the battery charging phases and temperature compensation

2.3. Other parts

A. Power consumers

The 13 houses, that constitute the power consumers of the microgrid, are modeled as resistive and inductive loads. More specifically, each house was modeled as a combination of static and dynamic load. This combination is depicted in fig.12. The use dynamic loads provides the ability of using external data for the power consumption while the static components are used in order to increase the reliability of the simulation and to eliminate convergence problems. Each house consist a single phase consumer and all the houses are distributed into the three phases of the microgrid.

B. Load controllers

Each house is provided with a load controller, a device which is programmed to shed specific loads when the frequency falls under the value of 49,14Hz. The controller will

remain in this state until the frequency becomes higher that that value. When this happens, a minimum 2-min interval passes before the load is reconnected. The reconnection of all loads will take place within maximum 2 min with a random sequence so as to prevent the instant reconnection of all loads. These features are modeled and depicted in fig. 13.

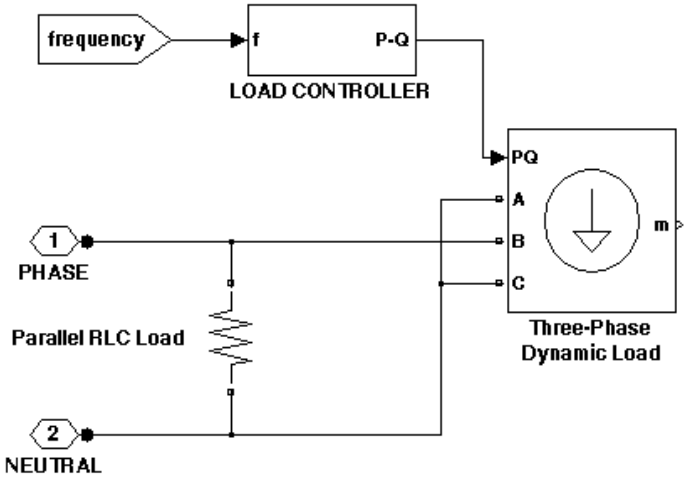

Fig. 12: Matlab/Simulink model for the energy consumers

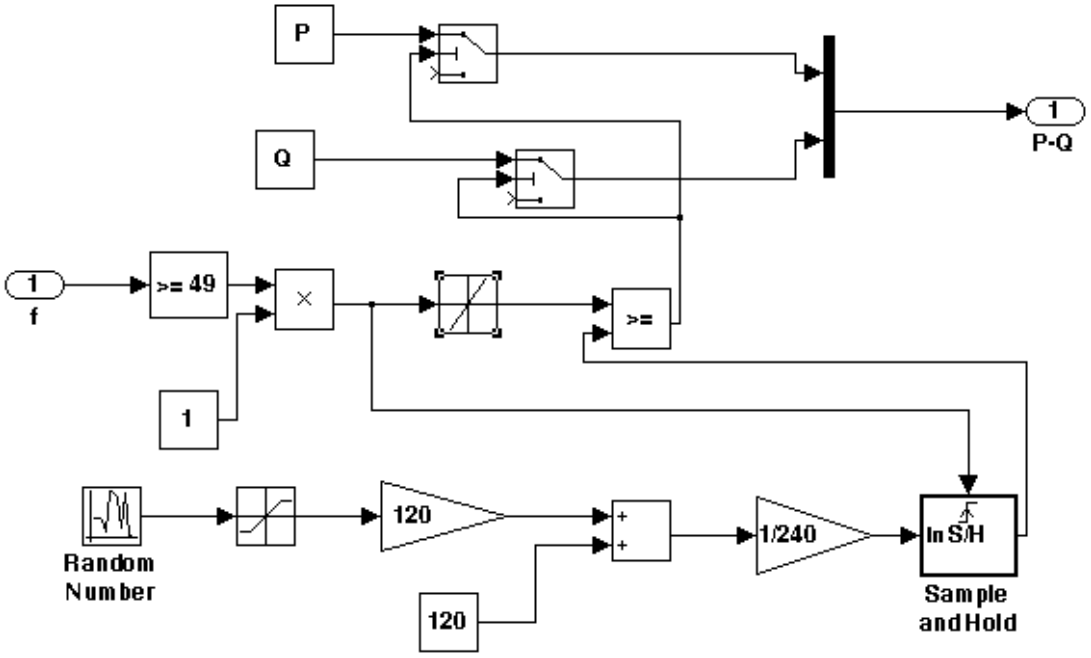

Fig. 13: Matlab/Simulink model for the load controllers

3. SIMULATION MODEL VALIDATION

3.1. Introduction

The third step of the present study included validation and improvements of the developed model so as to simulate the operation of the real system as accurately as possible. Validation tests took place during the development of each part individually, in order to make sure that the used models are correct. These first tests were performed for the I-V model of the PVs, for the load controllers etc. Since these results are intermediate ones are not included in the present document. In this report results from test concerning the total system are given. It is important to mention that the tests focus mainly on the energy flow and not on transient phenomena. In the following lines results concerning one and more than one days of operation, extracted from the simulation tool as well as comparison with real measurements are illustrated.

3.2. Simulation results for 24-hour operation

In these tests the operation of the system during 1 day (24 hours) was examined. The irradiation profile was selected from real measurements conducted at CRES and the consumption profiles were rather randomly selected since the main scope was the investigation of the system in not explicitly specified conditions.

More analytically, the irradiation profile is given in fig. 14a. This profile represents a sunny day with almost smooth solar irradiance, apart from some deviations in the afternoon due to scattered clouds. The selected load profile for this test is shown in fig. 14b. This figure illustrates the consumption for two of the thirteen houses. It is important to make clear that the consumption of the rest of the loads was taken asconstant. The implementation of the above input data leads to the simulation results of fig. 14c-14g. More specifically, these diagrams show quantities regarding the battery (Voltage, Current, Power, SOC) and the microgrid (frequency). From the results it is obvious that the simulation model appears the expected operation like the real system for these conditions. More analytically, when the battery terminal voltage reaches the value of 60V (the value for boost charging and 35^{o}C battery temperature-red curve in fig. 14c) at around 13:00 the control of the SI inverter modifies the frequency (fig. 14f) so as to derate the PV power.

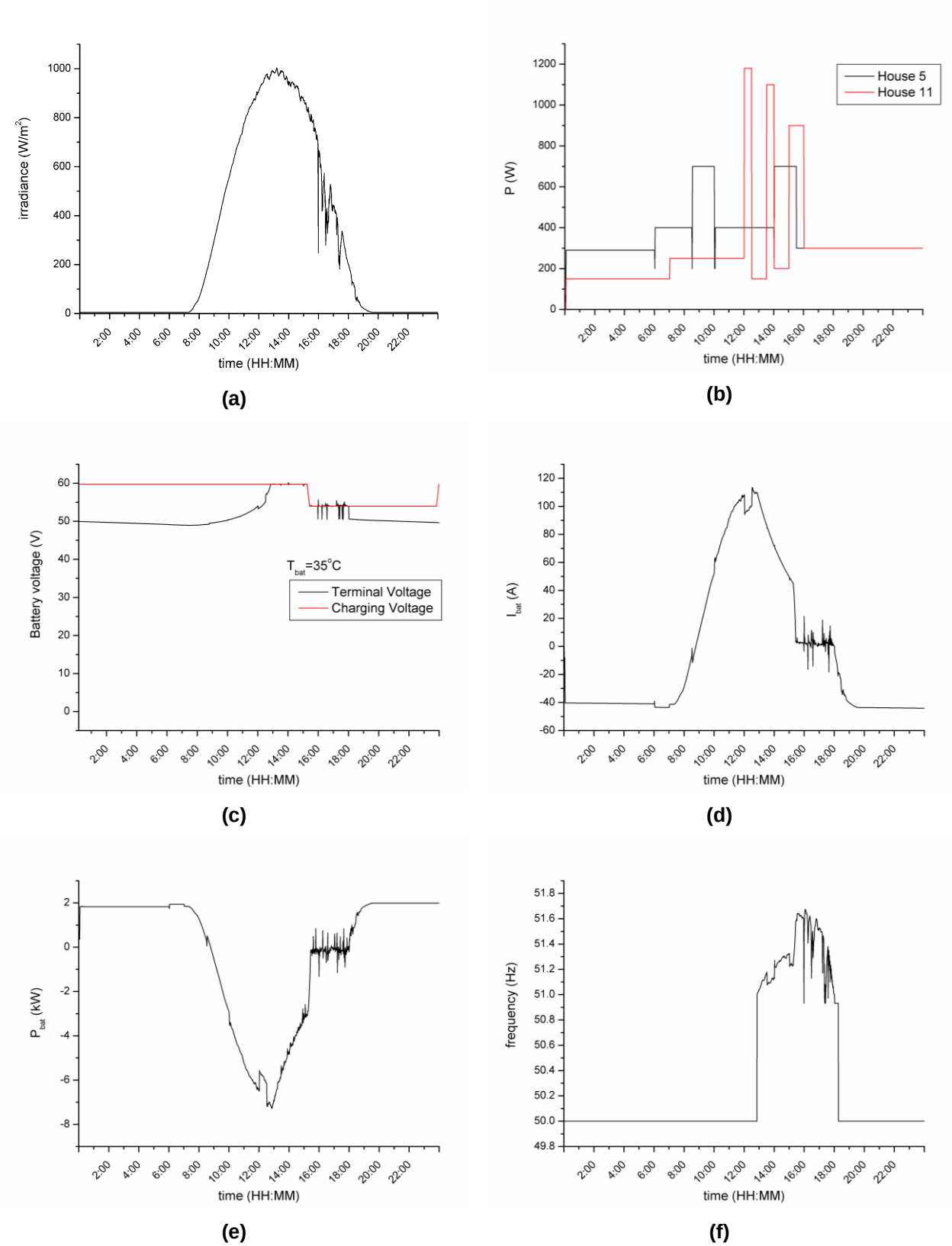

Fig. 14: 24-hour simulation test: a) insolation profile, b)house consumption, c)battery voltage, d)battery current, e)battery power, f)microgrid frequency and g)battery SOC

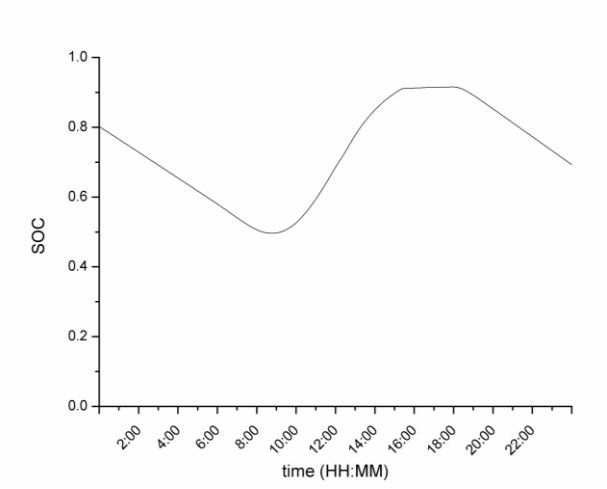

(g)

Fig. 14: 24-hour simulation test: a) insolation profile, b)house consumption, c)battery voltage, d)battery current, e)battery power, f)microgrid frequency and g)battery SOC **(continued)**

Progressively, the battery current reduces and the voltage is kept constant until the time of boost charging elapses. After that, the charging voltage reduces to 53,5V (floating charge phase).

3.3. Simulation results for 4 continuous days of operation

During this test the system was examined during four successive days of operation. The solar irradiance profile selected for the test is shown in fig. 15a. The profile reveals a smooth curve with maximum value at around 1000W/m^2. It is important to mention that the power consumption was assumed similar to the 24-hour test. The difference here is that the consumption varies for more than two houses with the same profile as in fig. 14b so as to have deep battery discharge. The results are shown in fig. 15b-15d. The battery SOC during the operation is shown in fig. 15d. It is obvious that SOC reaches the critical value of 30% every day of the simulation. It should be mentioned that this is a rather extreme case because of the selected power consumption profile which presents extreme values, something evident from fig. 15b which depicts the battery current. From fig. 15c it is clear that each time the SOC becomes 30% the diesel generator starts up and the

battery is recharged. During the operation of the generator, a frequency droop appears (fig. 15d).

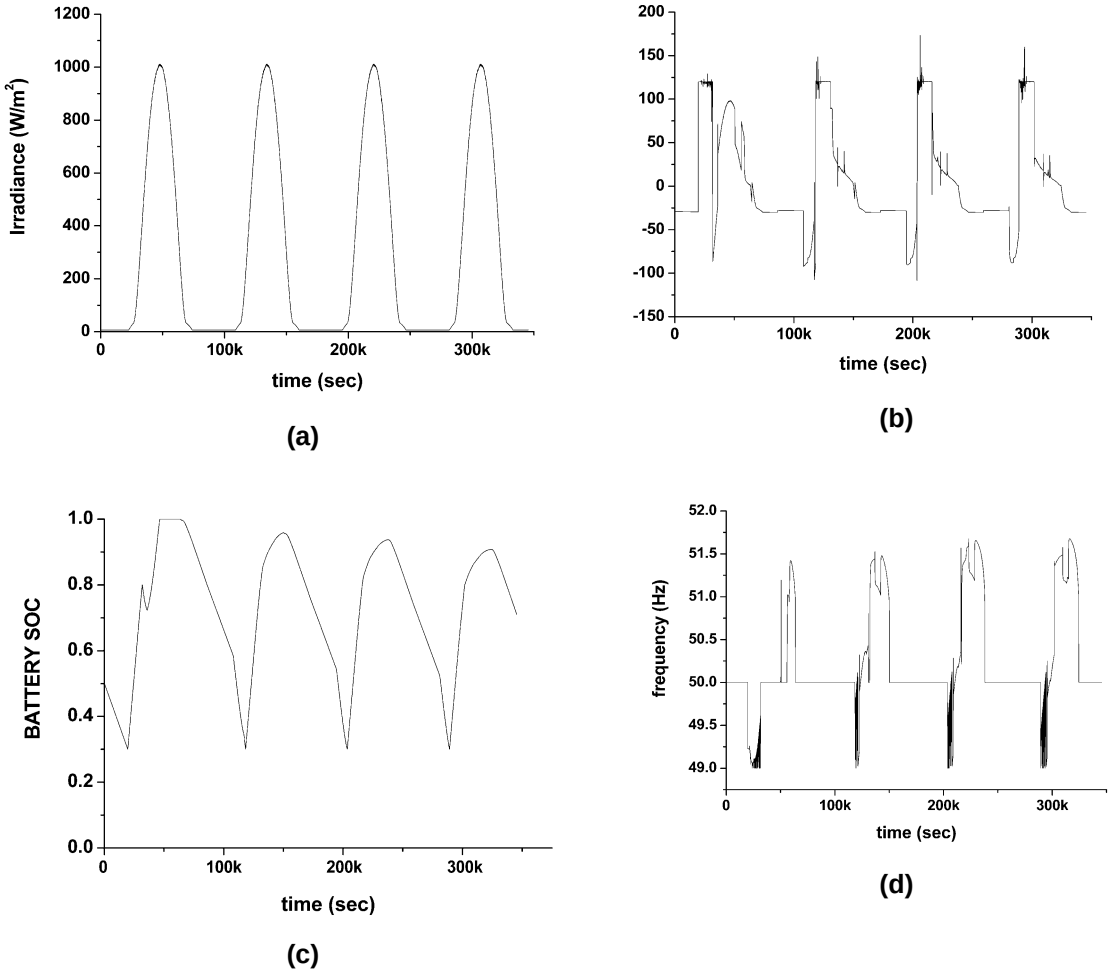

Fig. 15: 4-day simulation test: a)Insolation profile, b)Battery current, c)Battery SOC and d) Microgrid frequency

3.4. Comparison with real data

In fig. 16 a comparison between simulation results and real measurements are depicted. These diagrams reveal similarities and some deviations. The latter exist due to the fact that the load consumption used in the simulation was only a rough estimation of the real load and not exactly the specific load curve.

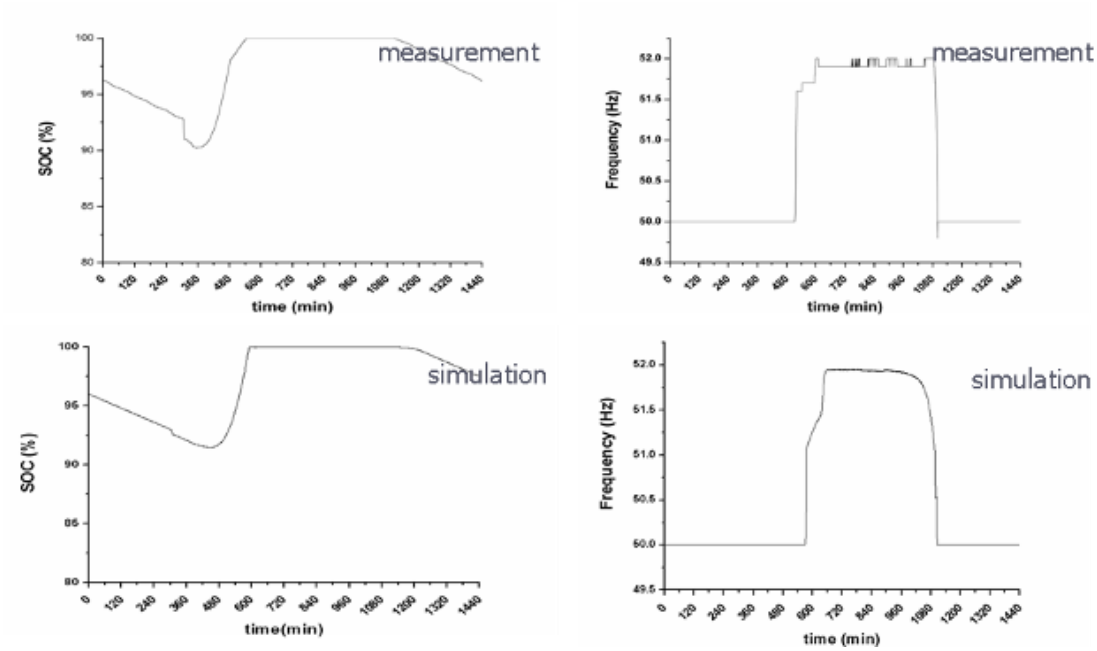

Fig. 16: comparison between simulation results and real measurements

4. CONCLUSION

This subtask focused on the development of a simulation tool which gives the ability to estimate the system behavior under various operating conditions. By using a simulation model we can achieve an accurate calculation of different electrical quantities such as Battery voltage and SOC, grid voltage and frequency etc. not only under static but also under conditions with rapidly changing insolation. The platform used for the development of this model was Matlab/Simulink. The model was divided into parts following the real system configuration. This means that separate models were developed for PVs, batteries, inverters, loads and load controllers, generator etc. all of which were based on literature models or manufacturer datasheets.

Through some tests, the results of which are presented above, it was proven that the system operates according to the estimated behavior and is similar to the real system. However, though the models are accurate enough, the absence of necessary analytical data sets which would be useful for the calculation of unknown parameters of models like batteries makes the coincidence of simulation and real data rather difficult.

There are also some additional points which could be subject of study for the model extension like the integration of a dynamic diesel generator model and the development of an interconnection to the public utility. The first point would be necessary in case of

dynamic states examination (i.e. faults, diesel or load connection-disconnections), while the second part could provide the ability of extending the simulation tests from the level of the Microgrid to a higher level where a Medium Voltage power grid delivers or receives power to and from island grids. The last case would demand the integration of a static switch and appropriate control which will monitor the public and microgrid conditions and will decide the connection-disconnection of the microgrid to the mains.

REFERENCES

[1]. K. Khouzam, and K. Hoffman, “Real-Time Simulation of Photovoltaic Modules”, Solar Energy, Vol. 56, No. 6, pp. 521-526.

[2]. D. P. Holm, and M. E. Ropp, “Comparative Study of Maximum Power Point Tracking Algoritmhs”, Progress in Photovoltaics: Research and Applications, Vol. 11, April, 2003, pp. 47-62.

[3]. J. F. Manwell, J. G. McGowan, I. Baring-Gould, W. Stein, “Recent Progress in Battery Models for Hybrid Wind Power Systems”, Proc 1995 AWEA Annual Conference, March 1995.

[4]. S. Duryea, S. Islam, and W. Lawrence, “A Battery Management System for Stand-Alone Photovoltaic Energy Systems”, IEEE Industry Applications Magazine, May/June 2001, pp. 67-72.

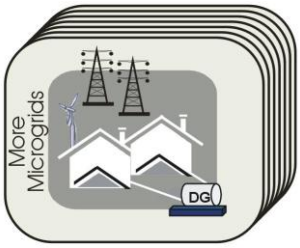

Advanced Architectures and Control Concepts for

MORE MICROGRIDS

Contract No: PL019864

WORK PACKAGE F

DF2. Installation of the MAS in the island of Kythnos

Final Version

December 2009

Document Information

Title: Installation of the MAS in the island of Kythnos

Date: 30-12-2009

Task(s):

Coordination:	Aris Dimeas	adimeas@power.ece.ntua.gr
Authors:	Nikos Hatziargyriou	nh@power.ece.ntua.gr
	Aris Dimeas	adimeas@power.ece.ntua.gr
	Spyros Hatzivasiliadis	spyrosxatz@gmail.com

Access:

__ **Project Consortium**
_ European Commission
~~X~~ PUBLIC

Status:

_ For Information
_ Draft Version
_ Final Version (internal document)
_ **Submission for Approval (deliverable)**
X Final Version (deliverable, approved on…)

1. Introduction

This part of the report includes the description of the technical installation of the Intelligent Load Controller in the Kythnos Test Site. In this report we will not provide detailed description of the MAS system and the controller since this was done in DA6 and DB3. Only short description will be provided in order to make the report easy to read. The report will focus on the specific details and measurements for the Kythnos test site. More specific in the first section information will be provided regarding the installation of the Load Controllers in the Kythnos test site. Next the implemented algorithm will be described followed by the measurements in the test site. Finally, the last section concludes with technical and non technical results.

2. Technical installation

The pilot Microgrid in the island of Kythnos electrifies 12 houses in a small valley of Kythnos, an island in the Aegean Sea, Greece [4], [10]. The generation system comprises 10 kW of PV, a nominal 53-kWh battery bank, and a 5-kW diesel genset. A second PV array of about 2 kW, mounted on the roof of the control system building (System House), is connected to an SMA inverter and along with a 32-kWh battery bank provide power for monitoring and communication. Residential service is powered by three SMA battery inverters, connected in a parallel master-slave configuration, forming one strong single-phase circuit. More than one of the 3.6-kW battery inverters is used only when more power is demanded by consumers. The battery inverters can operate in frequency droop mode, allowing information flow to switching load controllers if the battery state of charge is low, and limiting the power output of the PV inverters when the battery bank is full.

The core of the system is based on the Intelligent Load Controller (developed in WP A). The ILC is a system that can be used to monitor the status of a power line and take Voltage, Current and Frequency measurements. In addition it can remotely control up to 256 PLC A10 devices (PLC load switches) connected to the power line. As far as the houses of the settlement are concerned each ILC will control two PLC switches.

Main objective of this application is to control the operation of non-critical loads. Each house in the Kythnos Microgrid is equipped with a water pump, which is responsible for replenishing a water tank and in this way supplying water to the residents of the house. The water pump is considered as a non-critical load and therefore, in case of power shortage, it should be disconnected if needed. Therefore, the first PLC Switch controls the water pump, while the second PLC Switch controls a power socket and any load connected to it (e.g. air-conditioning unit).

Additionally, the ILC features a Wi-Fi interface that enables it to wirelessly connect to a Local Area Network. This eliminates the need of a data-cabling infrastructure and simplifies the installation of the units.

The core of the unit is an integrated computer module that runs the Windows CE 5.0 operating system. The integrated computer module is driven by the powerful Intel® XscaleTM PXA255 processor at 400MHz and features 64MB of RAM and 32MB FLASH Memory (instead of a hard disk drive). Thus, it is suitable for demanding applications.

The operating system supports the installation of a Java Virtual Machine. Therefore, an agent environment based on the JADE platform [11] can be easily

embedded in the controller. In this way, along with the MGCC installed in the System House in the Kythnos Microgrid, we schedule to perform the first actual field test of Multi-Agent Systems in a Microgrid.

The ILC hosts an integrated Web Server, as shown in Figure 2.1, through which we are able to control the operation of each controller.

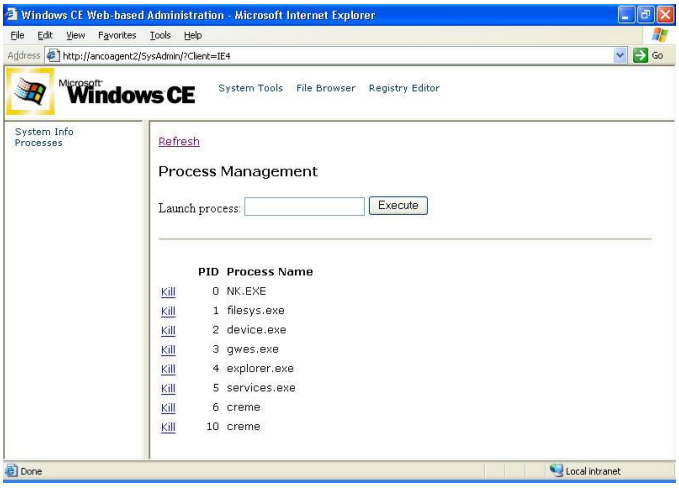

Fig. 2.1. ILC Integrated Web Server

During the installation in the Kythnos Microgrid, a broadband Internet connection will allow for remote control through a Virtual Private Network. As a result, commands can be sent and data can be exchanged among the ILCs, the MGCC and authorized users who are not required to be on-site. It should be noted that an ILC communicates with the MGCC through a Local Area Network and the Wi-Fi interface they both feature.

Figure 2.2 shows how the ILCs are connected in the electricity grid. Each ILC unit is connected to the Power Line outside the house, before the kWh-meter and the house's electrical panel. After the electrical panel and near the loads, the PLC switches are installed. Each PLC switch has a unique address, so that it can receive commands from the Intelligent Load Controller.

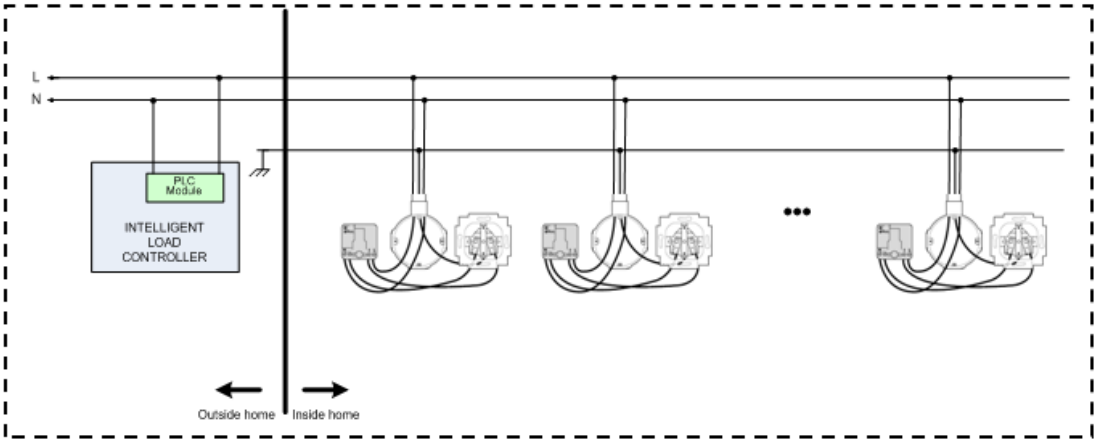

Fig. 2.2. Typical Installation of an ILC Unit

The Intelligent Load Controller built-in software provides the following functionalities regarding the power line measurements:

- Frequency measurement.
- Voltage RMS measurement.
- Current RMS measurement.
- Sag events detection and announcement.
- Overvoltage events detection and announcement.
- Overcurrent events detection and announcement.

The RMS values are calculated by sampling the power line at a rate of 3,500 SPS (samples/second). As far as the events detection functionalities are concerned, the controller announces the event start and termination, records the duration of the event and, depending on the event, records the maximum or minimum value measured. It is important that, with the software we have developed, the controller is capable of processing these measurements. As a result, the agent who is implemented in the controller is able to identify certain events and take the relevant actions. For example, the agent can recognize an overcurrent event resulting from an engine start and can distinguish it from an overcurrent event due to a failure.

The installation of the equipment included three main steps:

1. The installation of the Controllers
2. The installation of the PLC Switched
3. The installation of the Communication

Figure 2.3 presents photos of the installed load controllers. 5 houses were selected and one controller was installed in the System House where the Sunny

Islands are also installed. The controller was installed outside the house and electrically just after the electric meter.

Fig. 2.3 The installed controllers

Figure 2.4 provides an overview of the system while Figure 2.5 provides detailed description of the system topology.

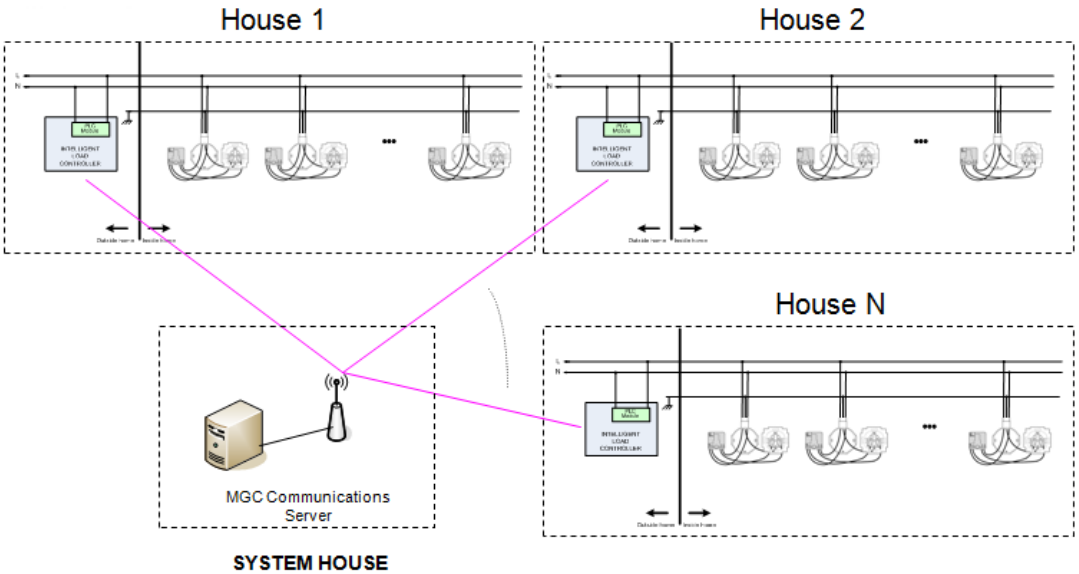

Fig 2.4 The Load Controllers have the ability to communicate with each other.

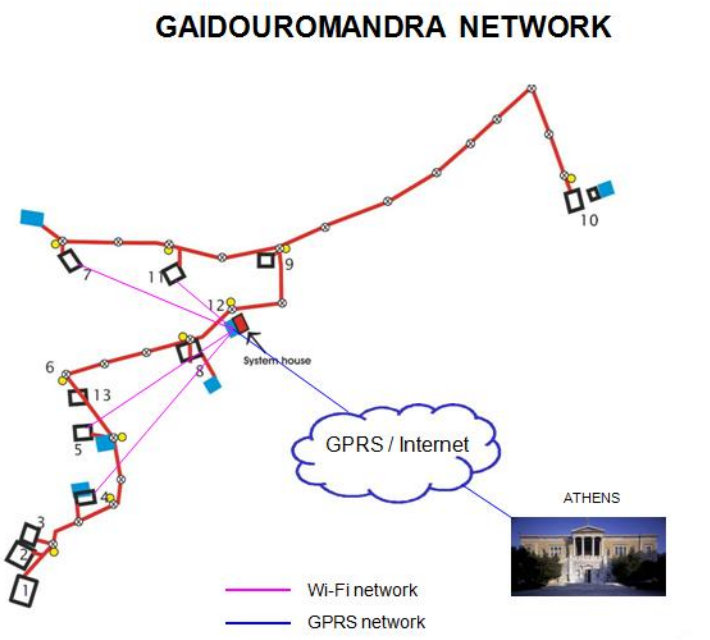

Fig 2.5 The system topology.

4. Installation of the software

The significant part of the system is the agent based software developed in WP B as well a software with centralised capabilities developed for monitor and centralised control.

JADE (Java Agent Development Framework) is a software development framework aimed at developing multi-agent systems and applications conforming to FIPA standards for intelligent agents. It includes two main products: a FIPA-compliant agent platform and a package to develop Java agents. JADE has been fully coded in Java and an agent programmer, in order to exploit the framework, should code his/her agents in Java, following the implementation guidelines described in this programmer's guide.

Every control system provides services in order to manipulate the various processes of the system and to achieve its tasks or goals. A service could be the minimization of the total consumption within a group of units, the provision of reserve to the grid or the management of a battery bank. The various services have two main characteristics:

1. Local or global. The battery management is a local procedure but the consumption minimization of a group of units is not.
2. Contradictory. Consumption minimization is contradictory to reserve provision. The control system should decide the hierarchy of the services' satisfaction.

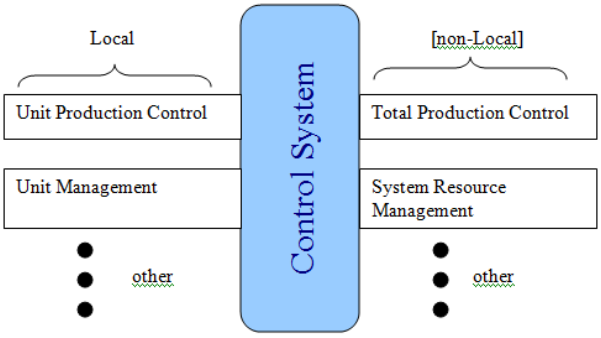

Fig. 2.6 The services provided by the control system.

The two categories mentioned above, also reveal the main problem with Microgrid control: the complexity of the system. Figure 2.6 generally presents some of the several operations that should be adopted for the electrical control of the system. As an example we could consider two of these operations: the control of total production and the control of a specific unit. Although the similar control process in

the main grid would have been described as central, it is actually not, since the central SCADA does not take into account local information (e.g. temperature of a boiler) in order to decide the set point for a specific Power Station. The central SCADA has knowledge of only two values, frequently updated by the Power Station personnel: the Maximum and the Minimum production capability. Thus, it sends a set point between these two values. Several people may however urge that the DG units are very simple and therefore simple rules and models can be inserted in the central control system. This is wrong if we consider the operation of hundreds of DGs (scalability) the system becomes significantly complex or even infeasible to solve (computational complexity).

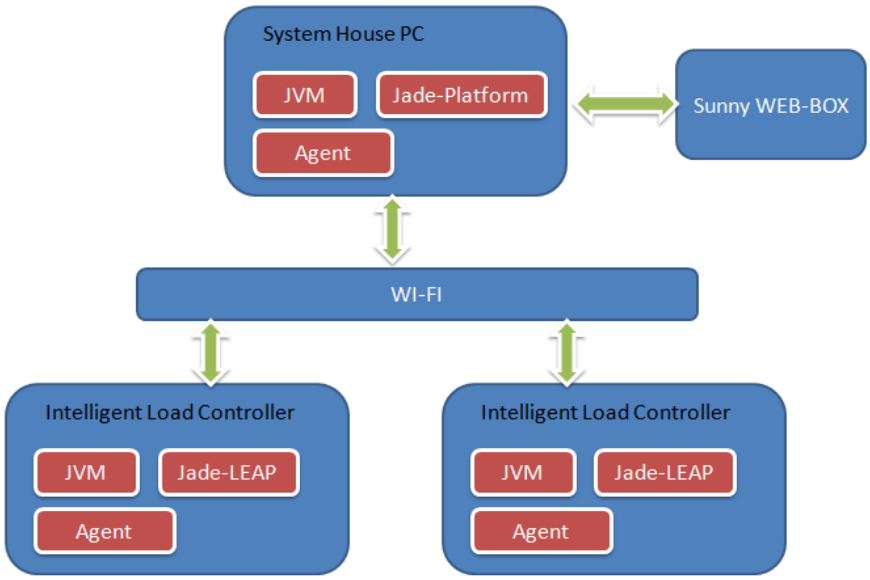

Figure 2.7 The agent based software topology.

Figure 2.7 presents the agent based software topology. More specific each ILC hosts an agent and the PC in the system house host the agent platform as well some software developed in VB.NET for communication with the Sunny Web-BOX. All these pieces of software form the multi agent system.

Furthermore a centralized control software was developed for monitoring and even centrally controlling the system. As it was mentioned in the beginning, the system is quite simple and the central control software has very limited functionalities. This software is based on simple “if-then-else” rules and some functionalities for estimating the available energy in the system. Figure 2.8 presents the basic graphic used interface of this software.

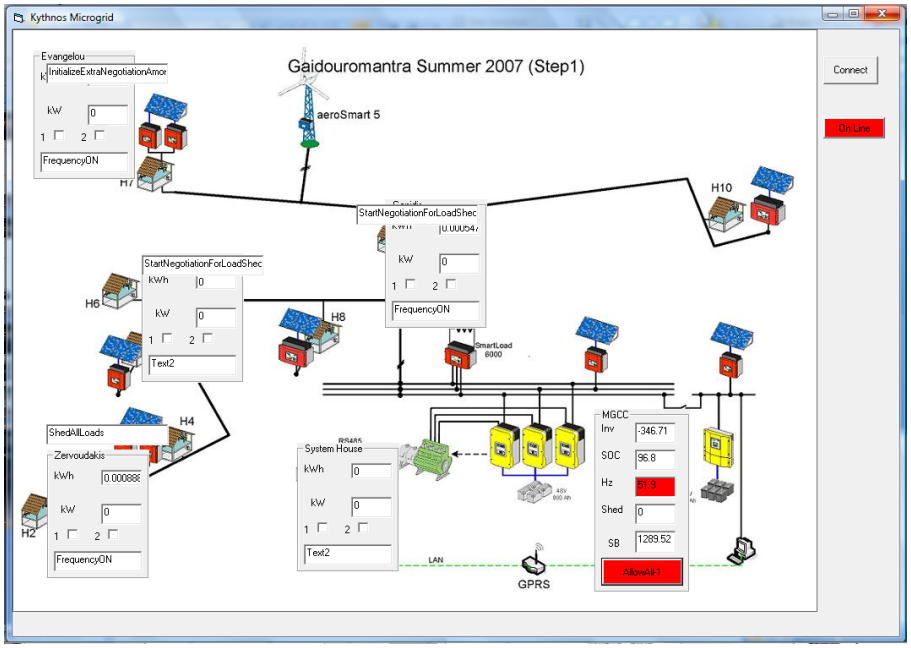

Figure 2.7 the graphic user interface of the central software.

Theoretical background & Measurements

The general goal of the system installed in the Kythnos test site is to increase the energy efficiency and this can be done with several methods. The primary goals can be separated in two sections the technical and the electrical:

Technical goals:

The technical goal is to check a quite complex system in a real environment. This means that the complex Multi Agent System with all the functionalities (Ontology, Yellow Pages Capabilities, Negotiation Algorithm, Coordination Algorithm) should be installed and run smoothly for a long period of time.

An important property of the JADE platform needs to be acknowledged. JADE platform provides the agents with a Yellow Pages service. This characteristic becomes important, if we need to offer the “plug and play” capability to the agents. A Yellow Pages service allows agents to publish one or more services they provide so that other agents can find and successively exploit them. Every agent who comes into operation (i.e. a load or a production unit is connected to the grid) is registered in the Yellow Pages service. For example, when a battery bank is connected to the grid, it informs the Yellow Pages service accordingly. When another agent desires to communicate with agents controlling a battery, it refers to the Yellow Pages service, which, in turn, provides information about all agents performing such a service. As a result, an agent does not need to be reprogrammed or notified every moment a load

or a production unit connects or disconnects from the grid. Instead, whenever it needs to be informed, the agent consults the Yellow Pages service. This procedure was also followed for the implementation of the Multi-Agent System in our application. The ILC agents and the MGCC are registered in the Yellow Pages service when the units they control connect to the grid, and they respectively de-register when they disconnect.

Electrical goals

The electrical operation of the system focuses in two main goals:

1. Minimize the usage of the diesel generator
2. Shift the loads to operate during the hours where PV energy is rejected.

Our main objective in this application is the minimization of the use of the diesel generator. For this goal to be accomplished, the agents are required to cooperate so that they make efficient use of the power supplied from the PV units and the battery banks.

The MGCC is responsible for monitoring the operation of the Microgrid and coordinating the Local Controllers. Therefore, it gathers information from the Intelligent Load Controllers and the inverters who control the PVs output and the batteries, regarding the amount of energy consumed and the amount of energy produced respectively. The MGCC is also informed about which controllable loads are in operation every moment. (Controllable loads comprise the two loads in each house equipped with a PLC switch). If the production units of the Microgrid (i.e. the PVs and the batteries) are able to supply the requested power, then the MGCC takes no action. If the PVs are capable of producing more power than the loads request, then the MGCC sends a message to the batteries informing the relevant agents that there is a surplus of power. The agents controlling the batteries are able to decide if there is need for the batteries to be charged, according to their state of charge.

If, on the other hand, the loads on operation demand more power than the production units can offer, the MGCC informs the Intelligent Load Controllers that there is need for load shedding. The ILCs, equipped with intelligent agents, and, hence, with communication skills, are required to interact with each other and most probably negotiate in order to decide which load is going to be disconnected from the grid. Finally, the possibility the produced power not to be sufficient, while all the non-important loads have already been disconnected, should also be anticipated. In this case, the diesel genset is started to supply the additional power. Figure 2.8 illustrates the course of action of the algorithm presented.

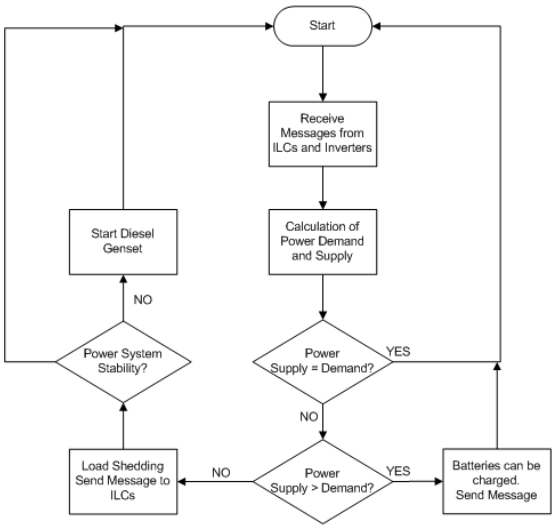

Figure 2.8. Flow Chart of the MGCC Algorithm

The algorithm for the implementation of the intelligent agent in the ILC has as main objectives the collection of measurements and the development of negotiation skills. Thus, every ILC agent has been programmed to collect periodically voltage, current and frequency measurements and inform the MGCC. Furthermore, the ILC agent has the ability to negotiate with fellow ILC agents in order to decide, when needed, which load will be disconnected.

Goal of this part of the algorithm has been the minimal intervention with the residents' decisions. Therefore, if a resident has decided that he needs to operate the water pump, or another controllable appliance (load), the agents are required to interfere to the minimum possible extent with this decision. On this account, the algorithm developed can be illustrated as a baton passed from one agent to another. When an agent has the baton in its possession, then it is not allowed to operate its non-critical loads (i.e. the water pump). The baton is passed from one agent to another in predefined time intervals (e.g. 10 minutes). In this way, load shedding does not burden only one house, but is equally divided among the whole settlement. In case more than one load needs to be disconnected, an additional "digital baton" is created, also following the aforementioned cyclic behavior.

Finally, regarding the energy shift, the system allows the operation of the loads when it detects a frequency over 51Hz (or SOC>90%). According to the main principle of the islanded operation of the system, when the batteries are full the system increases the frequency and limits the production of the PV inverters. So, a high frequency is a strong indication that the system rejects energy production.

3. Measurements

In this section the measurements gathered from the Sunny Web-Box, as well the load controllers are presented. As mentioned in the conclusions, some technical problems did not allow us to have complete continuing measurements for long periods. However, the data are sufficient for general conclusions.

Figures 2.9-11 provide the production of the PV inverters during some selected days. The key conclusion from these results is that when the SOC of the batteries is very high then the PV production is limited, thus lost. So the system should force the water pumps to work during this time.

Finally Figures 2.12-15 provides data from the load controller during the operation in August 2009. The data include also tests during this session.

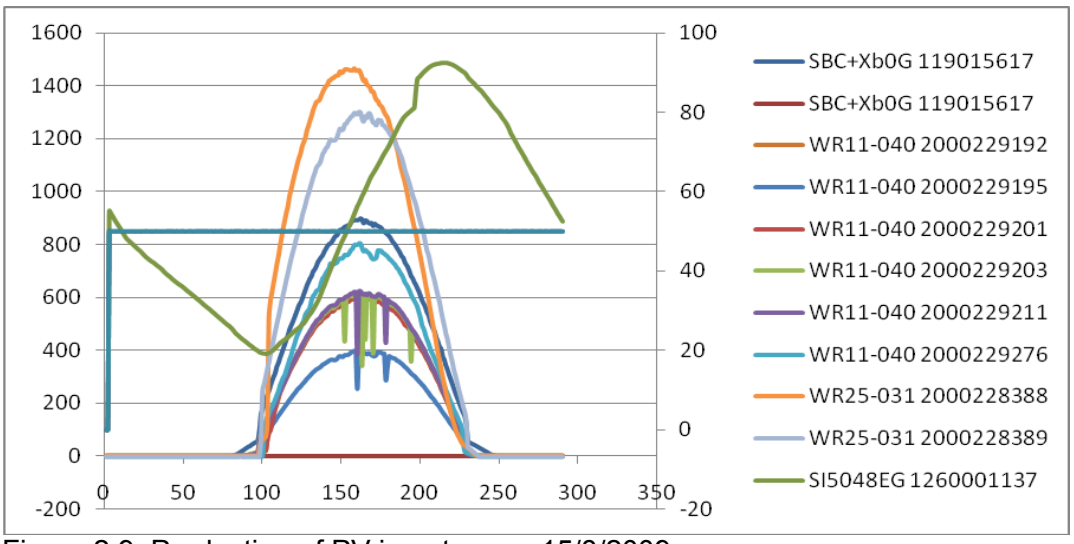

Figure 2.9. Production of PV inverters on 15/8/2009.

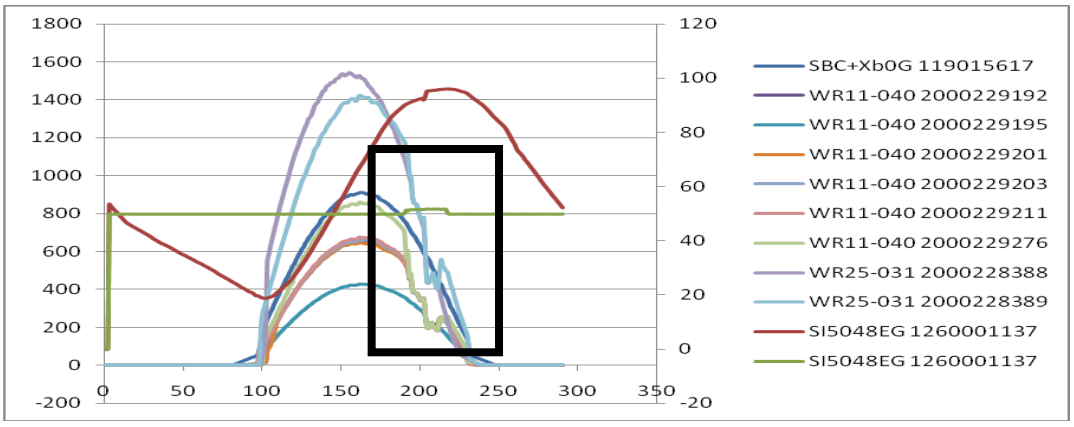

Figure 2.10. Production of PV inverters on 09/8/2009

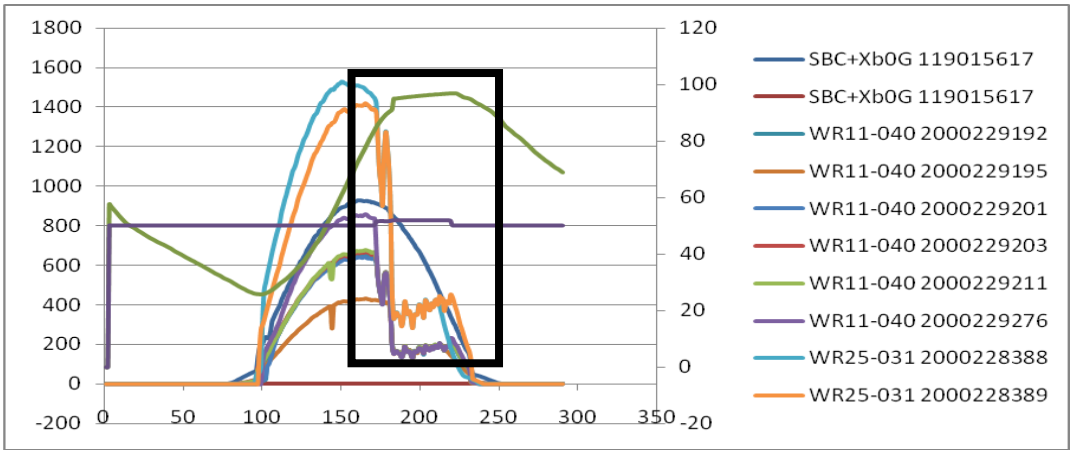

Figure 2.11. Production of PV inverters on 1/8/2009

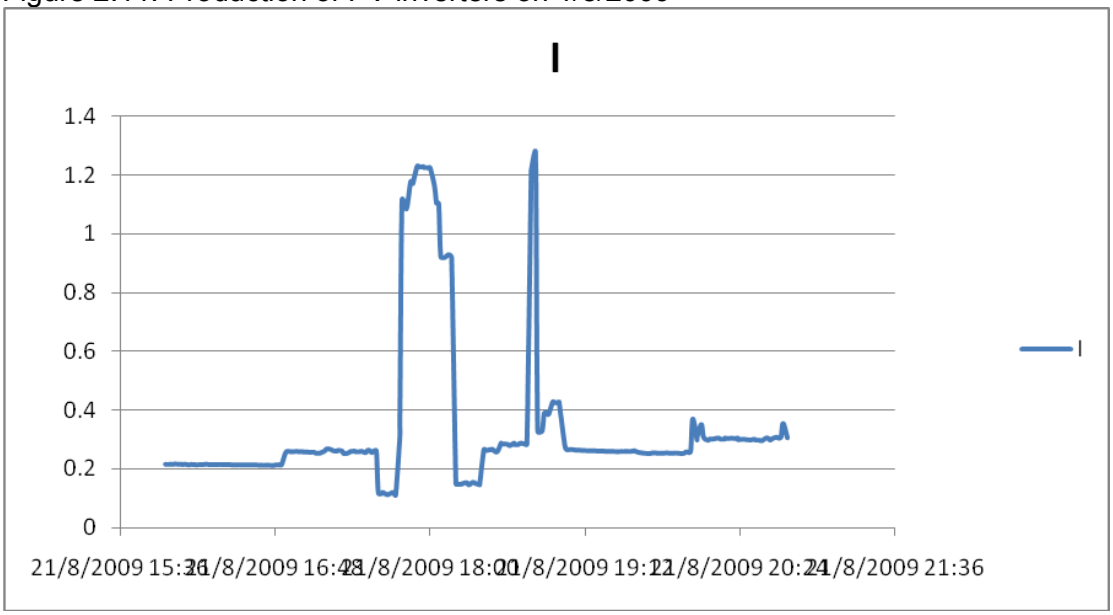

Figure 2.12. Current Consumption of House Nr. 4.

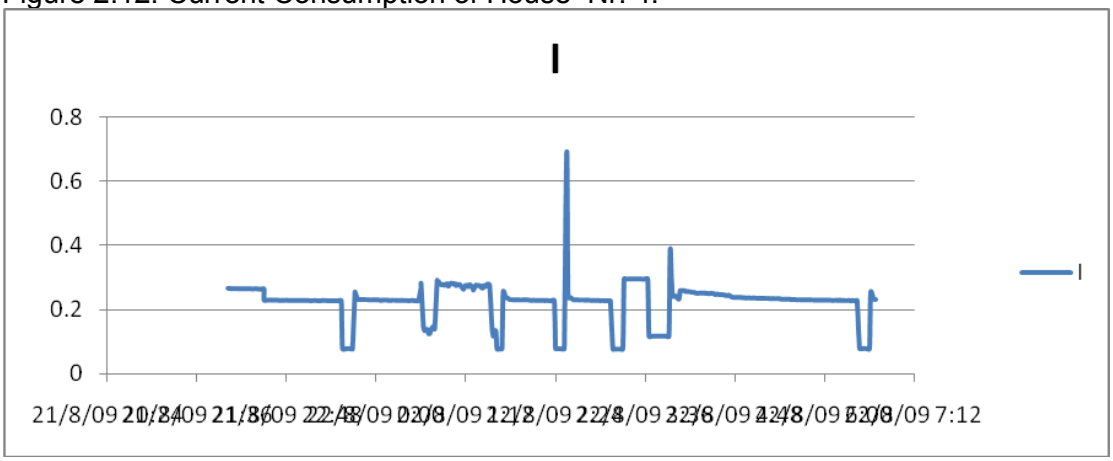

Figure 2.12. Current Consumption of House Nr. 4.

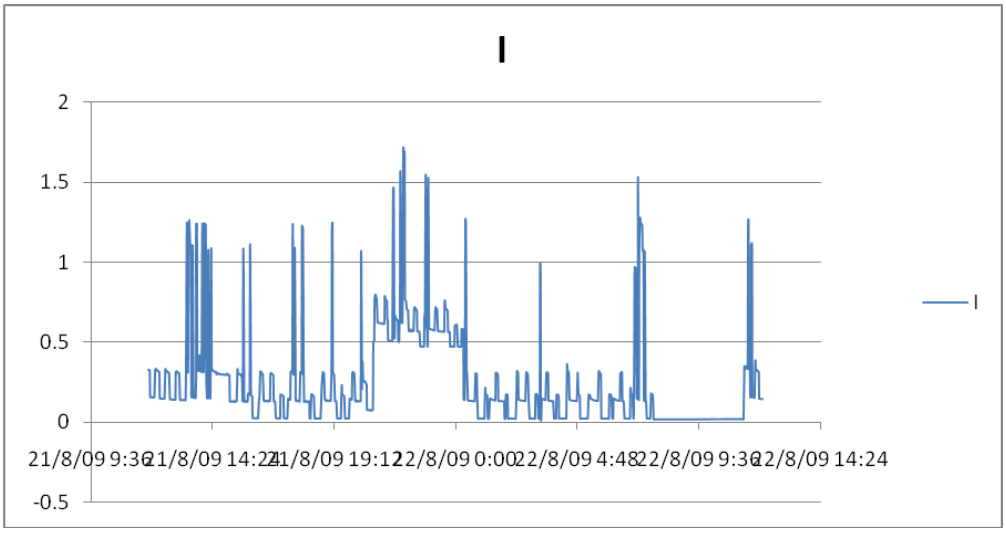

Figure 2.13. Current Consumption of House Nr. 5.

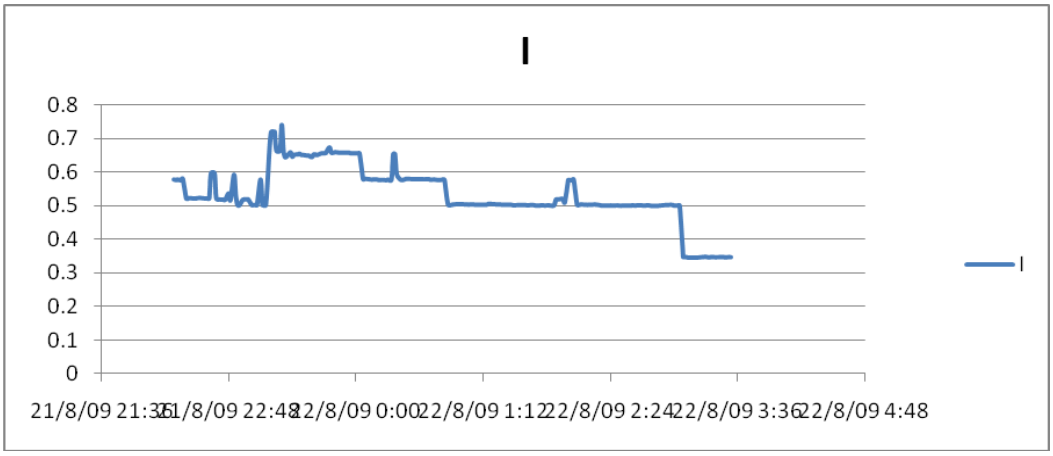

Figure 2.14. Current Consumption of House Nr. 7.

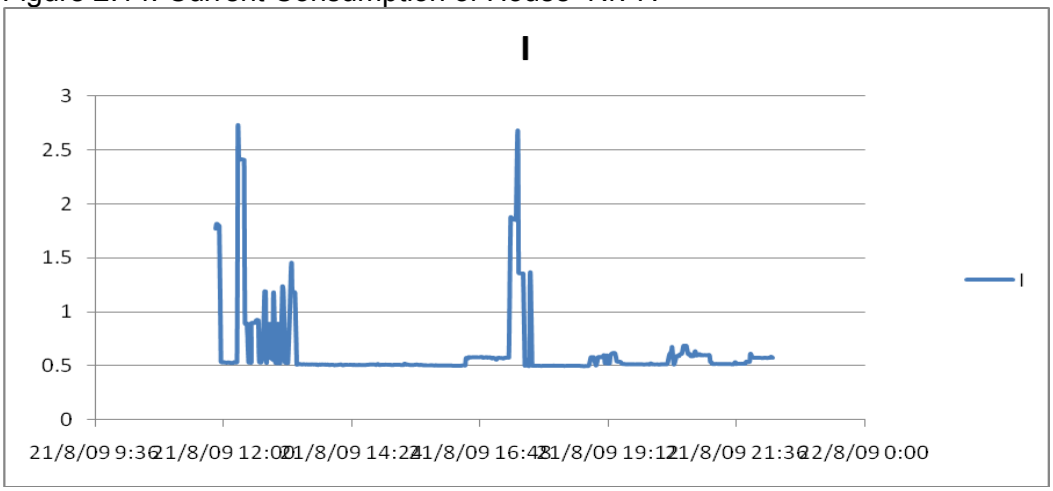

Figure 2.16. Current Consumption of House Nr. 11

4. Reliability Tests

The algorithms and the application presented in this document were tested in the Power Systems laboratory of NTUA, in order to investigate their reliability. The application of the described control system in the Kythnos Microgrid must be as reliable as possible, since it is tested under real-life conditions and affect the residents' daily routine. The rate of message exchange capability has already been tested and found that two agents are able to exchange more than 5,000 messages per minute. The actual operating conditions in Kythnos require a rate of no more than 100 messages per minute.

5. Evaluation

The evaluation of the system has several parts:

Hardware Evaluation.

The hardware performance was good and the algorithms could be processed fast enough. However three minor problems occurred. The first problem with the controller was some unexpected "reboots", especially during the start up of the system caused probably by insufficient memory. The problem was partially solved by reducing the size of the loaded libraries and the complexity of the ontology. The second problem occurred with the PLC switches, which could not operate when the system frequency was above 52Hz and this problem was solved by proper software modifications. The final problem occurred with the main WI-FI antenna which was sensitive to the humidity and finally was ruined. This part of the system has been replaced.

Communication Evaluation

The WI-FI system seems to be insufficient for the environment of Kythnos. The humidity level leads to signal losses and as mentioned before, the main antenna finally broke down. However the new antenna during the last period worked correctly.

Software Evaluation.

The Jade platform and the Agent Based control software installation in Kythnos was the first test in a non laboratory environment. In order to ensure smooth operation, system reboot was taking place once a day. This way the system operated correctly without any critical bug, although this is not the correct approach.

Furthermore, this approach created some complications taking into account the fact that sometime the controller was unstable during the start up.

Performance of the Algorithm.

The results of the performance of the algorithm were as expected, although it is not easy to calculate the exact benefit of the system. The operation was not continuous due to technical problems. It should be mentioned that the system is too complicated for controlling only 5 houses and the architecture is more appropriate for a larger number of agents. The primary goal of the experiment however was the testing of the software libraries and the controllers and this was successfully fulfilled. The above means that a similar system with a simple set of if then else rules and simplified control and decision tools could have similar results.

Acceptance by the Citizens.

Most of the citizens accepted the system well and were very cooperative during the tests. However some of them requested the removal of the PLC switches. Furthermore, during the tests, the main concept of the system was presented to them. This is the main idea of the user interface presented in Figure 2.7, which will be publicly available to demonstrate to the citizens the concept that the optimization process is based on collaboration among them.

3. Conclusions

Although small test sites like the one of Kythnos cannot be the base for an accurate economic evaluation of the solution, several critical conclusions can be drawn. The first question is whether a solution is better that using a centralized approach. In mathematical point of view if both systems monitor the same variables, and have the same amount of information then they should converge in the same solution with probability one and considering deterministic algorithms. For example it is proven that the algorithm for the auction algorithm developed in WP B has bounded complexity at $O(n^2 \max_{(i,j)}|a_{ij}|/\varepsilon)$ considering that a_{ij} is an integer and converges to the optimal solution with probability 1.

However the previous answer is misleading since a straight forward compare is not correct. The critical parameter is the amount of information the two systems can handle. To further analyze this, the system overview as presented in figure 2.17 should be considered. This figure presents comparison of several aspects of the system operation: LV vs MV network as well market operation vs electrical. In the center of the figure is the ICT infrastructure for the Enterprise management. According to this figure the MV network will have the existing structure based on DMS system as well Substation automation. However this infrastructure is not sufficient to manage LV consumers. It is not possible to include in the functionalities of the DMS the management of the LV consumers/prosumers (in terms of MV network sections this suggests thousands of consumers/households).

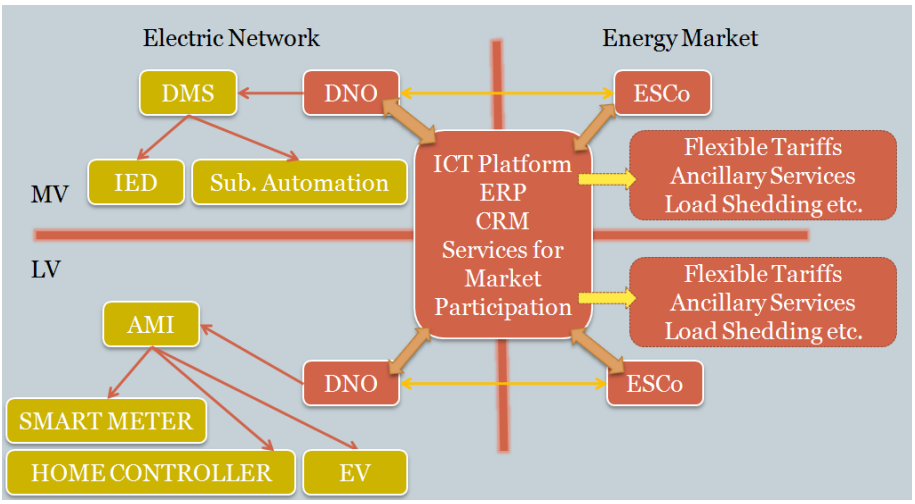

Figure 2.17. General View of the system structure.

Thus according to our approach as presented in WP B the decentralized control is suggested as a feasible approach. The main principal is that the agregator sends

price schedules and policies to the LV consumers. Next the LV consumers will decide their actions as presented in the next figure.

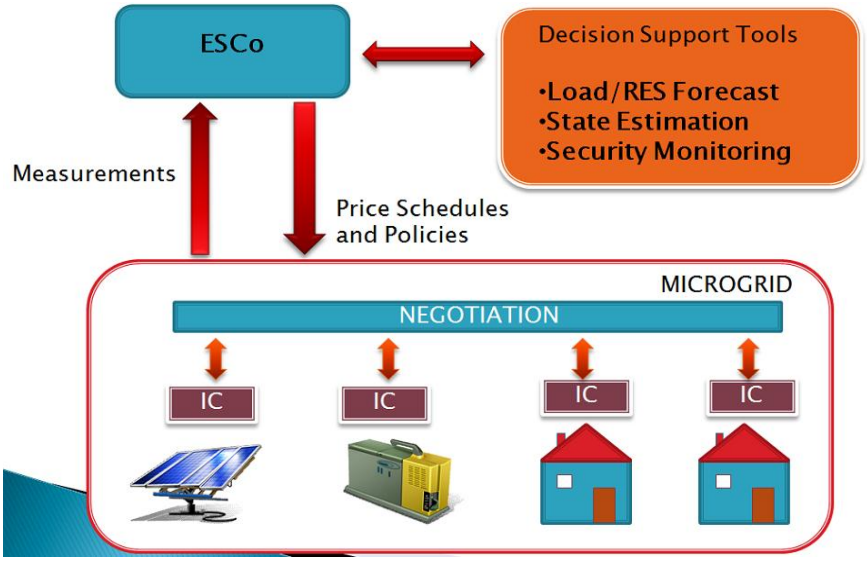

Figure 2.18. General View of the system structure.

According to this approach the load controller has minimum interaction with the aggregator and does not need to send large amount of data to the aggregator. The data include total consumption of the household, consumption per device and depending on the application voltage and frequency measurements. In order to prove this it should be mentioned that in this application the ratio of the data (values) exchanged to the total data stored is 1 to 5. This ratio includes only the values and not the coordination signals or the predefined parts of the messages according to the ACL and FIPA specification. This suggests that a central control system should process and exchange more than double data. (it is mentioned more than double since the calculation for the ratio is only considered for the installation in Kythnos)

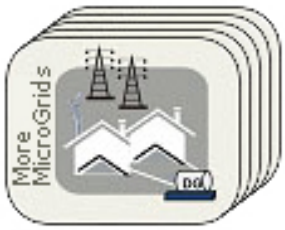

Advanced Architectures and Control Concepts for

MORE MICROGRIDS

Contract No: SES6-019864

WORK PACKAGE F

DF2: Report on field tests for islanded mode (Kythnos Test site)

TASK TF3: Experimental Validation of Islanding mode of operation

Final Version

25 November 2009

Document Information

Title: Data monitoring on Kythnos

Date: 25-Nov-09

Task(s): TF3 Experimental Validation of Islanding mode of operation

Coordination:	Michel Vandenbergh	mvandenbergh@iset.uni-kassel.de
Authors:	Michel Vandenbergh	mvandenbergh@iset.uni-kassel.de
	Randolf Geipel	rgeipel@iset.uni-kassel.de
	Unchalee Parinyacupt	

Access:

__	Project Consortium
_	European Commission
X	PUBLIC

Status:

__	For Information
__	Draft Version
__	Final Version (internal document)
__	Submission for Approval (deliverable)
X	Final Version (deliverable, approved on.)

Table of content

1. Executive summary

In the framework of the task F of the European project More-Microgrids, ISET is responsible for the monitoring of the minigrid Gaidouromantra in Kythnos.

In a first step, the existing ISET monitoring system has been upgraded by the addition of the WEBBOX from SMA, of the power quality analyzer HAAG, of a local communication network allowing easy integration of additional components (eg. the load management PC from NTUA) and of a new GPRS link.

Upon request from project partners, monitoring data from summer 2004 has been made available. This data is useful to evaluate the load evolution and the difference of management strategies between the first and second generation of battery inverters.

For the evaluation of the performance of the Gaidouromandra supply system, a dedicated software tool based on Visual Basic language has been designed and used for the evaluation of the data. The energy performance analysis in summer 2008 leads to the following results:

- Additional loads could be included for increasing the performance ratio
- The battery inverters should be coupled on a single phase for a better efficiency
- Additional pyranometers for measuring the tilted irradiance in each PV field would increase the accuracy for the performance evaluation
- A common database should be used for storing the data from all 3 logging systems.
- Some maintenance checks should be organized (PV inverter at house 7, module temperature sensor)

Analyze of measurement of power quality in the minigrid presents a few weaknesses according to EN50160.
Grid frequency is above threshold because of the derating of PV inverters, which is proportional to the frequency value above 51 Hz. High values for voltage flicker and for some harmonics are due to non optimal distribution of load between three phases (e.g. single phase water pumps). High values for some voltage harmonics have also been measured when the PV inverters are operating in de-rating mode.

2. Introduction

The electric system in Gaidouromantra, Kythnos is currently a 3-phase low voltage system formed by battery inverters. Over the years, for various experimental purposes, it has been modified from 3-phase to 1-phase and recently, in June 2007, it was reconfigured as a 3-phase system for the needs of the EC project “More-Microgrids”. The minigrid system is composed of the overhead power lines and a communication cable running in parallel to serve the monitoring and control needs. It is electrifying 12 vacation houses in a small valley in Kythnos, an island in the cluster of Cyclades situated in the middle of the Aegean Sea. The grid and safety specifications for the house connections respect the technical solutions of the Public Power Corporation (PPC), which is the local electricity utility. The reason for such a decision was taken on grounds that potentially the minigrid may be connected with the rest of the island grid. Each house has an electricity counter meter of the type provided by PPC and is supplied with one-phase current, limited by a 6A fuse. This means that each home can have lighting, a refrigerator, water pump and small electrical appliances. The residents were asked from the beginning to use high-performance appliances, such as fluorescent lamps and refrigerators with good insulation.

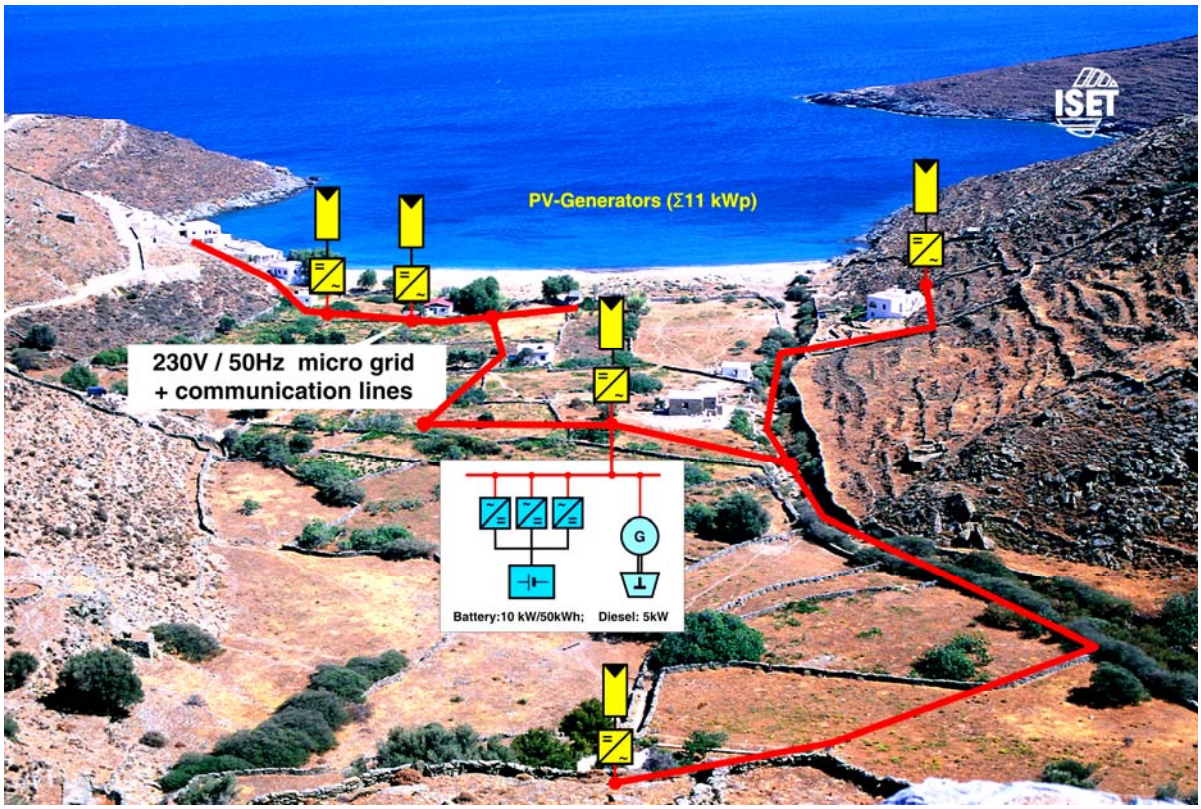

Figure 1: **The Gaidouromantra minigrid in Kythnos island**

The settlement is situated about 4 kilometers away from the closest pole of the medium voltage line of the island. A system house of about 30 m2 surface area was built in the middle of the settlement in order to house the battery inverters, the battery banks, the diesel genset and its tank, the computer equipment for monitoring and the communication hardware, called “System Hut”. The grid electrifying the users is powered by 3 Sunny-island battery inverters, which when they are forming a 1-phase system, are connected in parallel to form one strong single-phase in a master slave configuration, allowing the use of more than one battery inverter only when more power is demanded by the consumers. Each battery inverter (SI4500) has a maximum power output of 4.5 kW. The battery inverters in the

Kythnos system have the capability to operate in both isochronous or droop mode. The operation in frequency droop mode gives the possibility to pass information on to switching load controllers in case the battery state of charge is low and also to limit the power output of the PV inverters when the battery bank is full.

Figure 2: **The "system hut" where the battery inverters, batteries, diesel generator and monitoring systems are kept**.

Until June 2007, the users' system was composed of 10 kWp of Photovoltaics divided in smaller PV sub-arrays and a battery bank of nominal capacity 53 kWh and a 3-phase diesel genset with a nominal output of 5 kVA, when used in 1-phase configuration and 9 kVA when operating in 3-phase configuration. A second system with a 2 kWp PV array is mounted on the roof of the system hut, connected to a Sunny-island inverter and a 32 kWh battery bank. This second system provides the power for the monitoring and communication needs of the whole minigrid system. The PV modules are integrated as canopies to various houses of the settlements. The grid and the systems were installed in 2001, in the framework of two European projects (PV-MODE, JOR3-CT98-0244 and MORE, JOR3CT98-0215). The projects were co-funded by the European Commission.
The main partners in the two projects were CRES, SMA and ISET e.V. They invested in the systems and they are responsible for the maintenance of and repairs to the systems for 10 years. After that period, it is planned to hand over the system's operation to a local organisation. One electrician in the island of Kythnos was trained during the project and is still in charge to service and maintain the system, according to the projects' needs. In order to ensure good management and maintenance of the system, contracts have been drawn up between CRES, the Municipality of Kythnos and the house owners concerning the responsibilities and rights of all parties. CRES is responsible for the book-keeping and management of the systems (incomes and expenses for maintenance and reparations).
In the first two projects, apart from the demonstration of the new battery inverter technology, the main challenge was to control a minigrid with distributed PV generators. Control solutions, based on grid frequency variation (droop control) as communication signal, have been adopted. The battery inverter was able to vary the grid frequency in order to provide simple control information to the distributed PV inverters and to the load controllers installed in each house. The load controllers were developed by E-Connect (UK) and are able to

disconnect the whole house load. The Sunny island battery inverter, when the battery state of charge is low, mimics the effect of an overloaded generator which is slowing down thus effectively decreasing the minigrid frequency. The load controllers are operated in the frequency mode, that is, they sense the grid frequency and they disconnect the house when the frequency drops below a set frequency, provided that the battery state of charge is low or is overloaded by the users. The houses are re-connected randomly when the grid frequency is increased as the battery state of charge is increased. This allows the houses to come back onto the grid progressively, avoiding that they suddenly come all together and overload the system again. Based also on the grid frequency value (when above 50 Hz), the PV inverters are able to continuously de-rate their power output, in order to avoid overcharging the battery bank. Finally, a back-up diesel generator was integrated smoothly in the system to charge the batteries.

In the framework of the European project More-Microgrids, CRES, ISET, NTUA and SMA are responsible to upgrade the minigrid system. By using the LV grid of Gaidouromantra in Kythnos, they will demonstrate centralized and decentralized control strategies in islanding mode. This report presents the results from the system performance monitoring.

3. Minigrid overview

Figure 3 presents the layout of the minigrid, indicating the location and serial numbers of the distributed PV inverters. The three PV inverters located in the system house (in red colour) are providing electricity only to the monitoring system.

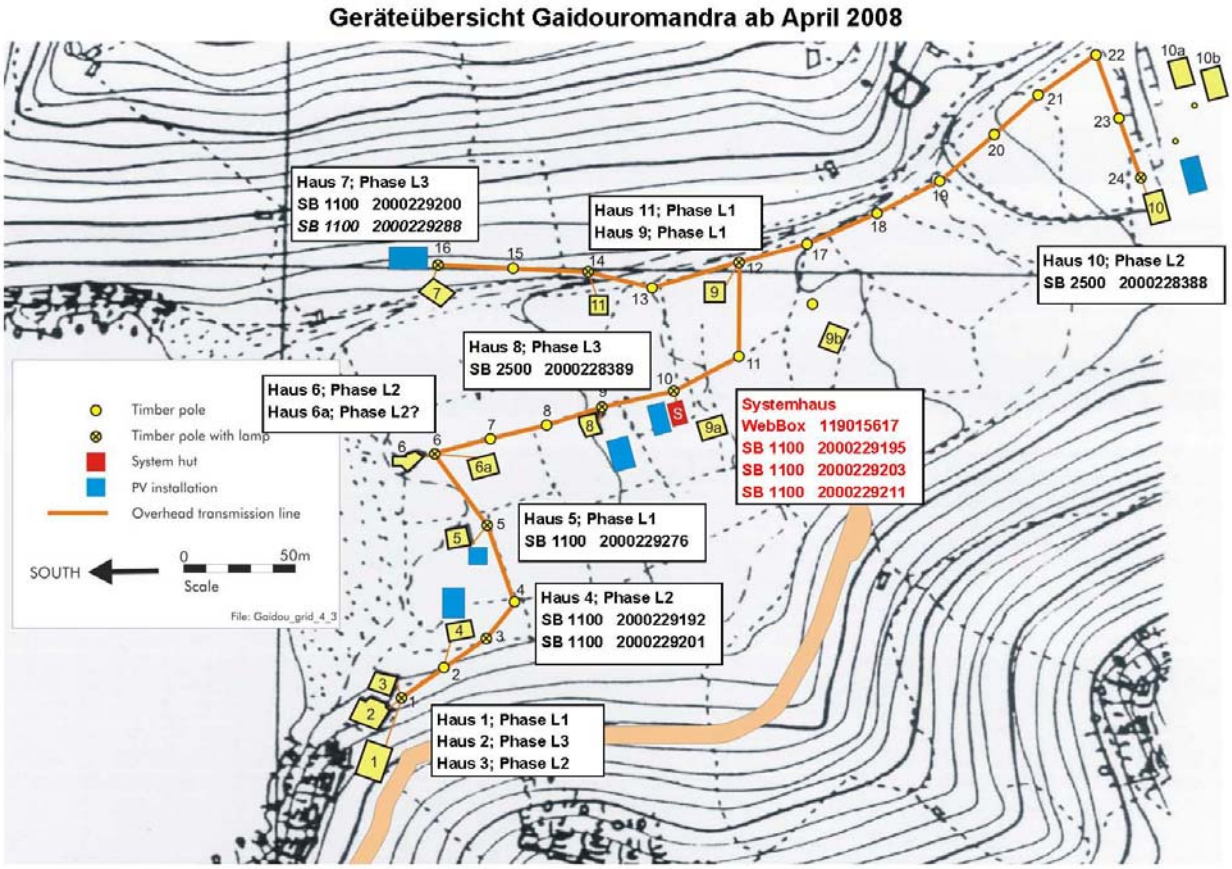

Figure 3: Minigrid layout

4. Description of the monitoring equipment

Within the frame of the MoreMicrogrids project, the Gaidoroumandra minigrid monitoring system has been upgraded by the installation of a WEBBOX from SMA, a HAAG power quality meter and a new GPRS communication link.
The monitoring equipment of the Gaidoroumandra minigrid is divided in 3 independent complementary subsystems :

1. WEBBOX monitoring from SMA, which is logging, via the inverters, the parameters of the distributed PV fields and of the battery storage system. Additionally, meteorological and some diesel generator parameters are collected. The logging rate is 5 min.
2. INTOUCH monitoring from ISET, which is logging data via AC power meters distributed at different locations in the minigrid. The logging rate is 1 second.
3. HAAG monitoring for high accuracy power quality measurements at the minigrid centre, in the system house. The logging rate is 1 second.

All the 3 systems have an independent data storage capacity. They are interconnected via a LAN to a GPRS router for remote communication. Remote download of data can be realized via different web or ftp servers.

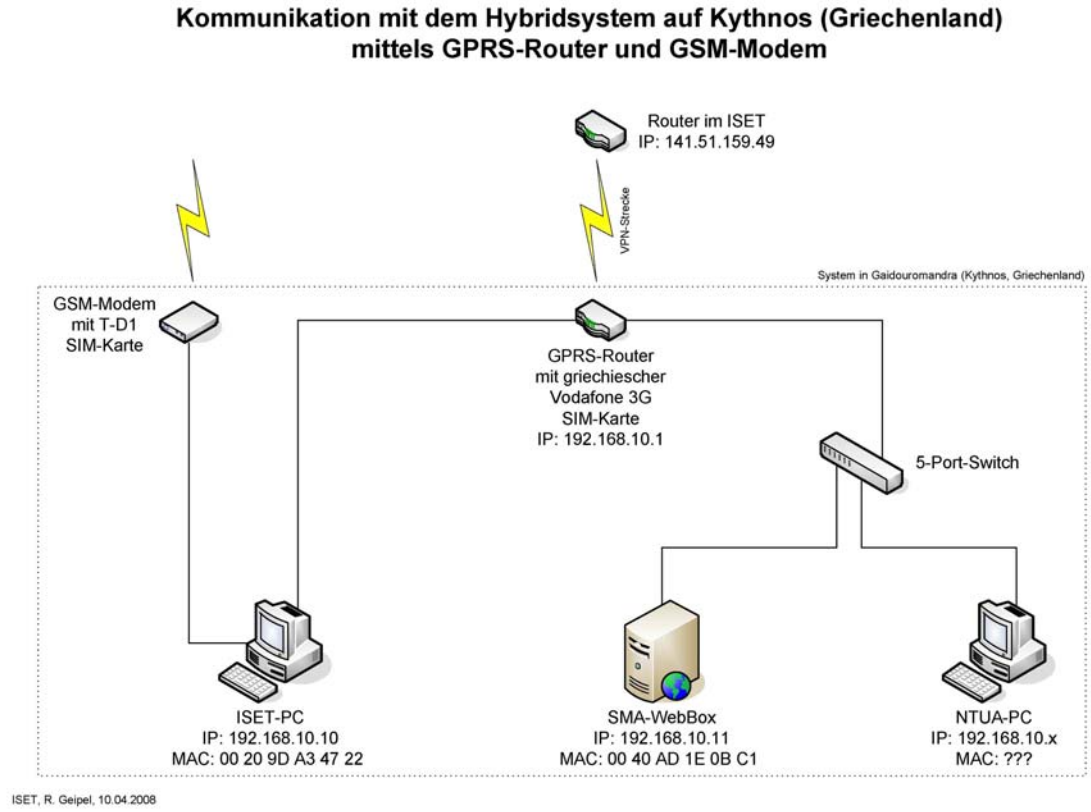

Figure 4: Local and remote communication system for the monitoring

4.1. WEBBOX monitoring from SMA

Table 1 lists the components of the minigrid whose parameters are logged by the WEBBOX.

Inverter	Serial number	House number
SB 1100a	2000229192	4
SB 1100b	2000229201	4
SB 1100c	2000229200	7
SB 1100d	2000229276	5
SB 1100e	2000229288	7
SB 2500a	2000228388	10
SB 2500b	2000228389	8
SBC+	119015617	
SI 5048	1260001137	

Table 1: SMA components connected to the WEBBOX

In addition, the webbox also monitors the 3 PV inverters and the Sunny island of the monitoring system.
The size of the daily monitoring data file is 350 kbytes/day (73 kbytes/day compressed)

4.2. HAAG monitoring for power quality

A power quality analyser of the type HAAG Combi-Quant has been installed in june 2008 in the system house. The device is used for measuring AC voltages and AC currents at the central point of the mini-grid. The monitored data allows to evaluate power quality according to standards like EN50160. The RMS values (Mean, max, min) are stored in the local storage at a rate of 1 Hz. No trigger for recording transients has been implemented.

The size of the daily monitoring data file is 21 Mbytes/day (18 Mbytes/day compressed).

4.3. INTOUCH monitoring from ISET

In order to monitor the performance of the system there are several measurements of electrical values. In detail these different types of values are listed in Table 2.

Electrical data
PV-production
Diesel production
Consumption of the system house
Public lightning
Consumption of the individual users
Grid frequency

Table 2: Measured electrical and meteorological data

Figure 5 shows the energy and power measurement system. Every house has its own unidirectional one phase energy-counter (EC). Also every PV-generator has got a one phase energy-counter at the ac-side and the consumption of the public lightning is also measured by one energy-counter, placed at the system house. The values of these energy-counters are transmitted via the S_0-bus to three aggregators. From these aggregators, the values are submitted via a LON-bus to the system-house where a PC with a LON-Interface collects and logs the data from these energy counters.
In the system house there are 3 three-phase multifunctional power meters. One power meter is measuring the energy flow for charging and discharging the battery by the Sunny Island cluster. The other one collects the amount of the produced energy by the diesel generator. The last one determines the power consumption of the external grid. The values of these 3 power meters are also sent via LON-Bus to the PC where the data is logged.
In order to be evaluated, the data has to be sent to ISET. The former GSM-connection was updated to a GPRS-connection. A new GPRS-router with a Vodafone-Card was installed at the system house. The counterpart of this new GPRS-router is located at ISET.

The size of the daily monitoring data file is 61 Mbytes/day (1.3 Mbytes/day compressed)

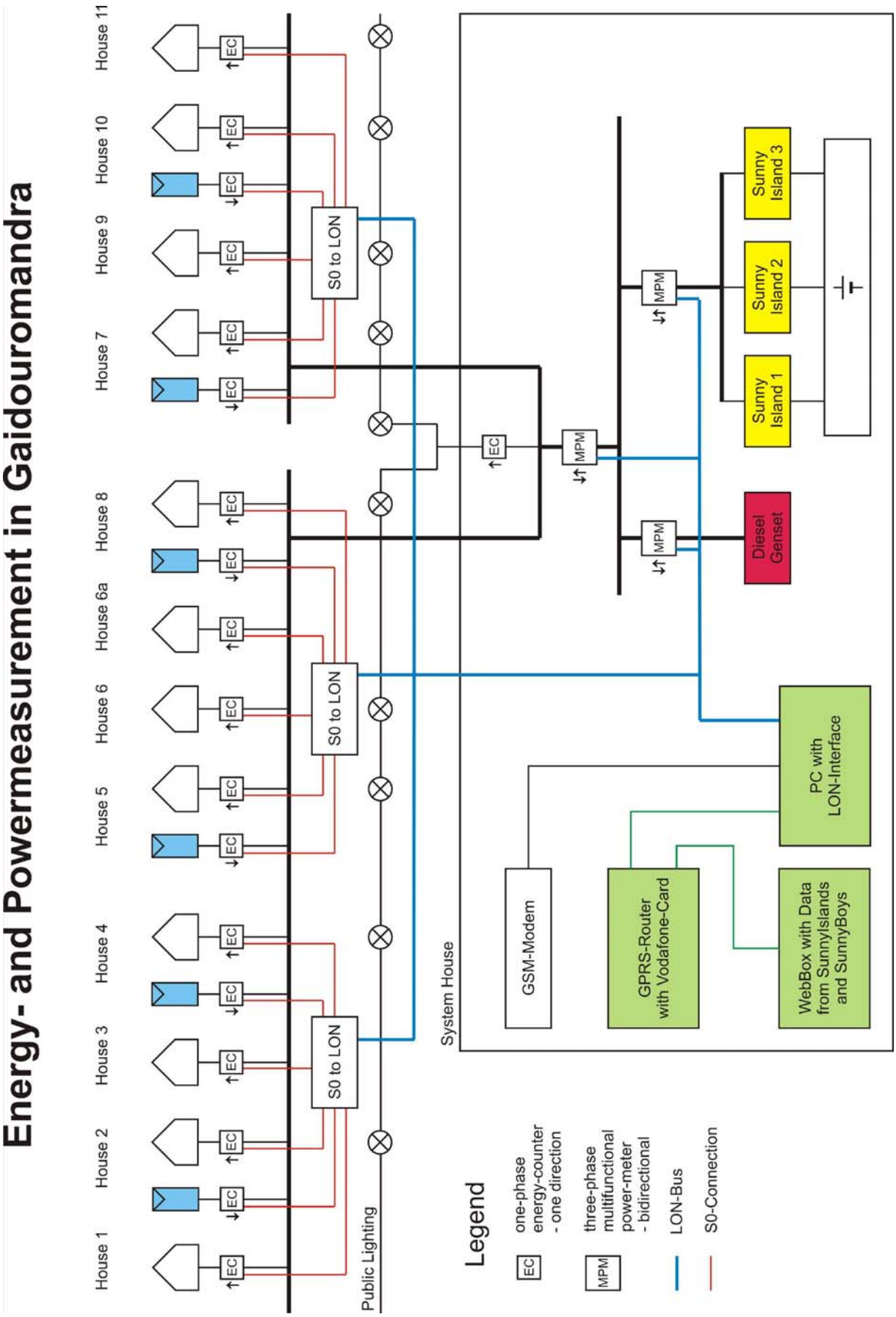

Figure 5: Energy and power measurement in Gaidouromandra

5. Data availability

The new monitoring devices have been installed and configured in different steps, since June 2007. Some design updates were necessary in April and June 2008. Initially the GPRS link was aimed at periodic download of the monitoring data. However, some difficulties in the remote communication occurred for big files and not all the data could be transferred to ISET in Germany. The GPRS transfer rate is limited to about 1 kbytes/s, which is enough for the WEBBOX data but not for the rest of the data.
The main steps in the installation of the monitoring system were:

1. 19.06.2007: new PV and battery inverters are installed, together with a WEBBOX from SMA. The webbox is monitoring the data from the PV inverters and from the SBC+. The data of the battery inverters is logged directly on SD memory cards.
2. 24.04.2008: The webbox is monitoring the data from the PV inverters, from the SBC+ and from the battery inverters.
3. 05.06.2008: The HAAG power quality meter is installed

Figure 6 presents the data which has been downloaded by ISET until 02.02.2009. More data should however be available from the local hard-disks.

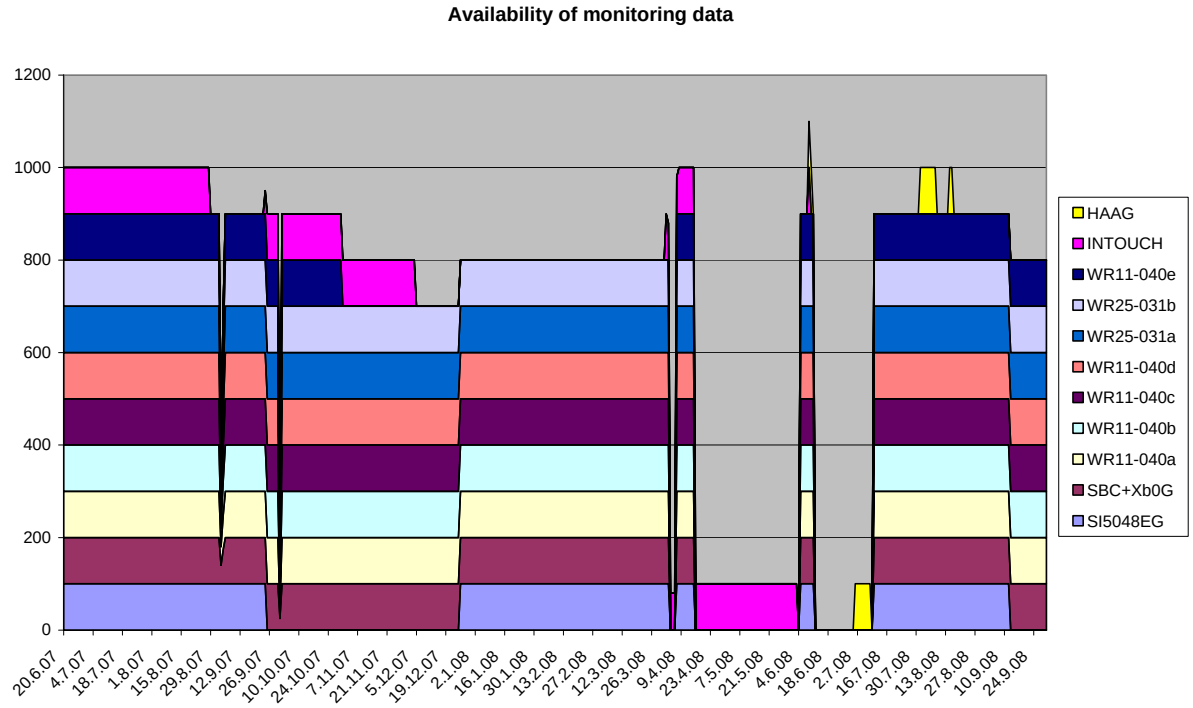

Figure 6: Data available at ISET (as of 24.11.2008)

Several reasons explain the loss of data:

- Broken SD card of the webbox
- Max. file size for the INTOUCH monitoring
- Hard disk full for the HAAG
- Broken communication to some components (eg. between the Webbox and the battery inverter or a PV inverter

All the files generated could not be remotely downloaded because of the relatively bad quality of the GPRS connection available on the island.

6. Comparison of data accuracy

The three monitoring systems have a different accuracy. Although the INTOUCH system is logging with a one second time step, its monitoring data is actualized only after about 6-7 seconds. This is illustrated in Figure 7. A short term peak power of 1 kW is logged by the HAAG on phase L1 the 09.06.2008 at 00:10:09. This peak is only partially visible on the INTOUCH logging.

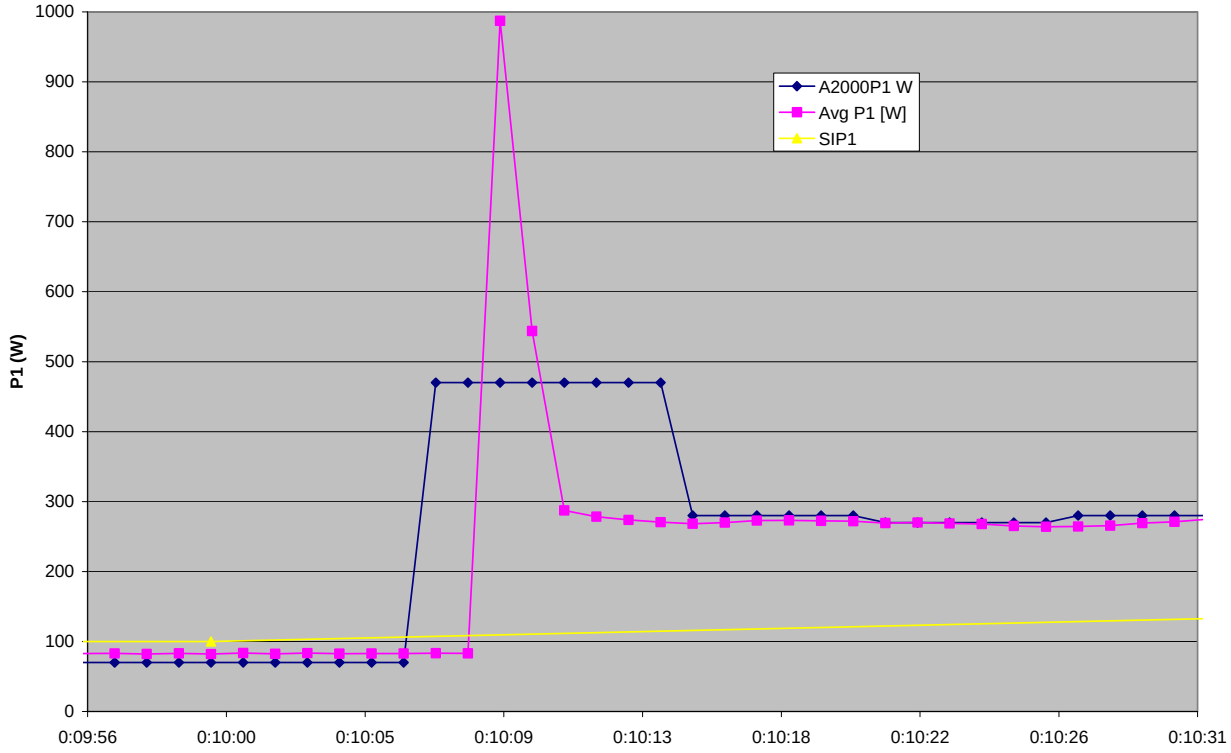

Figure 7: Gaidoroumandra 09.06.2008: active power on phase L1, measured by INTOUCH(A2000P1 in dark blue), HAAG(Avg P1 in pink) & Webbox(SIP1 in yellow)

In Figure 8, it can also be seen that the INTOUCH system does not log synchronously the active power and the current. Indeed, the current peak is completely invisible. For these reason, it was decided to install the power quality HAAG. This system has also the following advantages: it records the min., max, and averages during the one second step. On the contrary, the INTOUCH system can only record the average value for the last 0.3 seconds.

Only one HAAG logger has been installed closed to the battery inverters and this power quality information should be complemented by the voltage measurements provided by the distributed PV inverters.

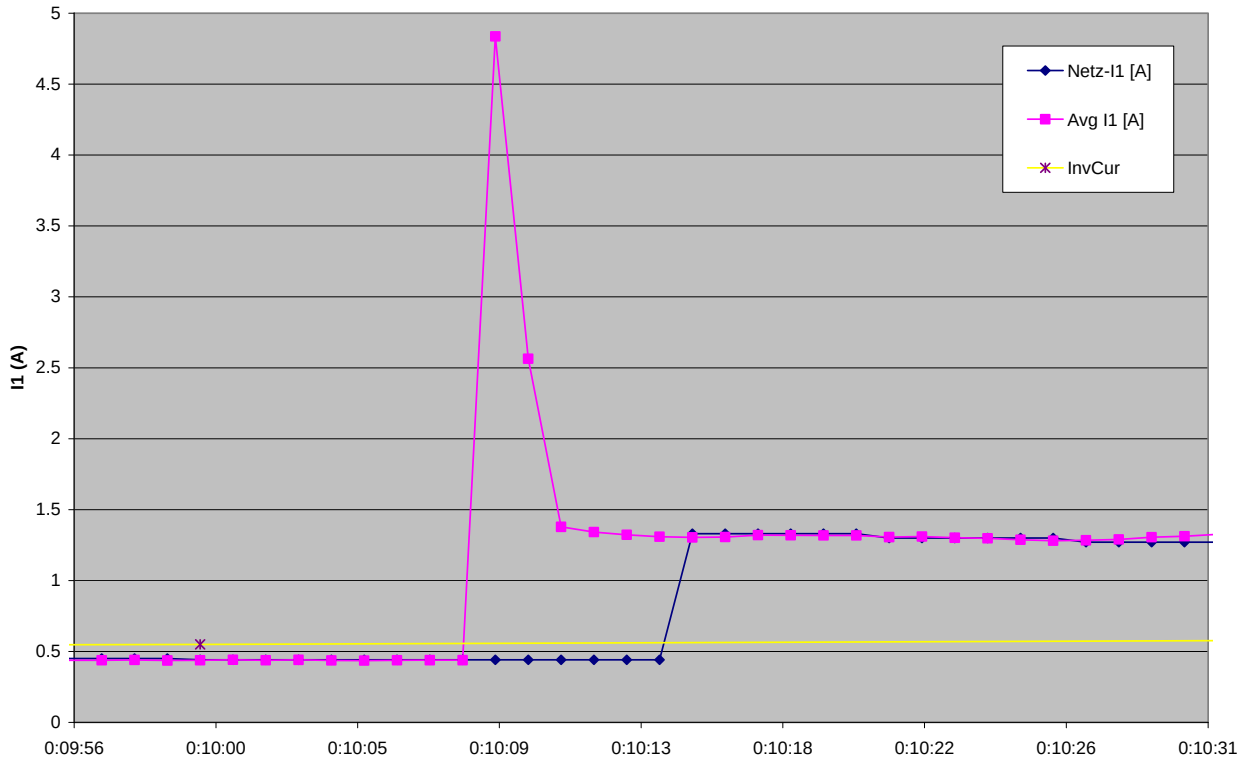

Figure 9: Gaidoroumandra 09.06.2008: current on phase L1, measured by INTOUCH(Netz-I1 in dark blue), HAAG(AVG I1 in pink) & WEBBOX(InvCur in yellow)

7. Performance analysis tool

A software tool based on “Microsoft Visual Basic”, has been developed for analysing the daily performance of the minigrid. This tool allows to supervize the operation of each PV field (each having different tilt and azimuth angles), the power quality and the monitoring system itself. In its present version, the tool is reading the WEBBOX daily data files (5 min time step).

7.1. Graphical user interface (GUI)

The GUI is designed to provide a daily summary of the most important performance indicators.

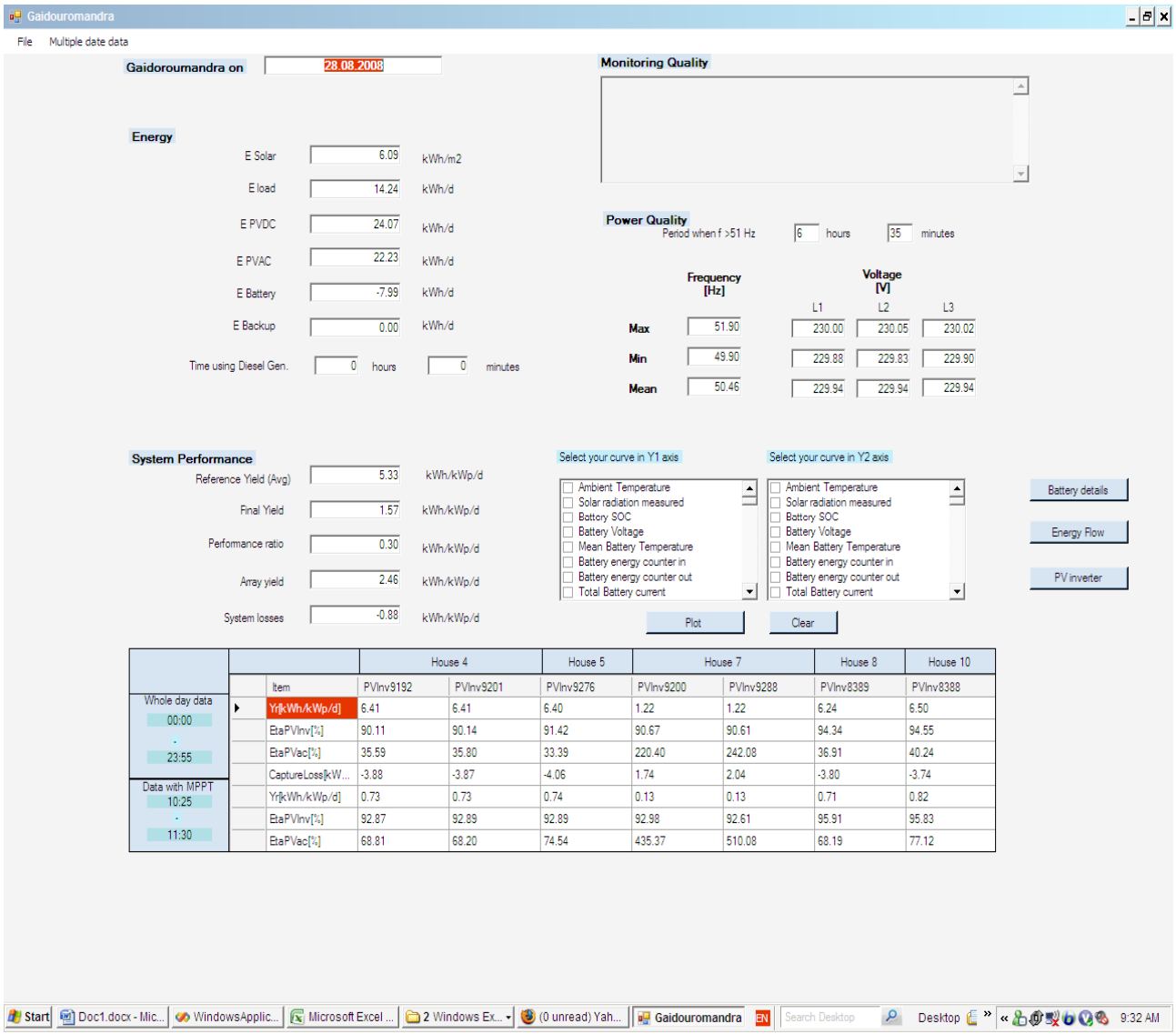

Figure 10: Graphical user interface

7.2. Program features

7.2.1. Monitoring Quality

The program can check the data measured and tells users which and how many data are missing in the specific date.

7.2.2. Energy

The program can calculate the solar energy, energy to the load, PV energy production (AC and DC), Battery energy, and energy from the diesel generator.
Moreover, the time using diesel generator is calculated.

7.2.3. Power Quality

The program can provide power quality information about the system by checking maximum, minimum and mean of system's frequency and also of voltage in each phase (Phase1, 2 and 3). Moreover, the program can show how long the system frequency was over 51 Hz.

7.2.4. System performance

The program can calculate the averaged reference yield, final yield, performance ratio, array yield, and losses of the system.

7.2.5. Each PV field and PV inverter Performance

In this part, the program can calculate each PV field and PV inverter performance in two time periods:

1. **Whole data**. Here, the program can calculate reference yield, PV inverter, PV efficiency and capture losses of each PV inverter from whole data available.
2. **Data with MPPT**. Here, the program can calculate reference yield, PV inverter's efficiency, PV's efficiency of each PV inverter only when PV field worked with maximum power point tracking. (data is limited to 1hour before the frequency step over 51 Hz)

7.2.6. Plotting curves

The program can help users with plotting curves easily. Users can select the data needed in both axes (Y1 and Y2) and click the plot button to plot the selected data or click the clear button to clear all check marks. However, users have to check that all data must have the same unit for plotting in the same axis.

7.2.7. Battery Details

The program can show the starting SOC, Ending SOC of data available. Battery efficiency can be calculated on the assumption that in the time concerned the starting SOC and the ending SOC have the same value.

7.2.8. Energy flow

The program can show an energy flow diagram. However, the energy flow diagrams are from 2 static pictures. Only the calculated number are changed by the program.

7.2.9. PV and inverter performance

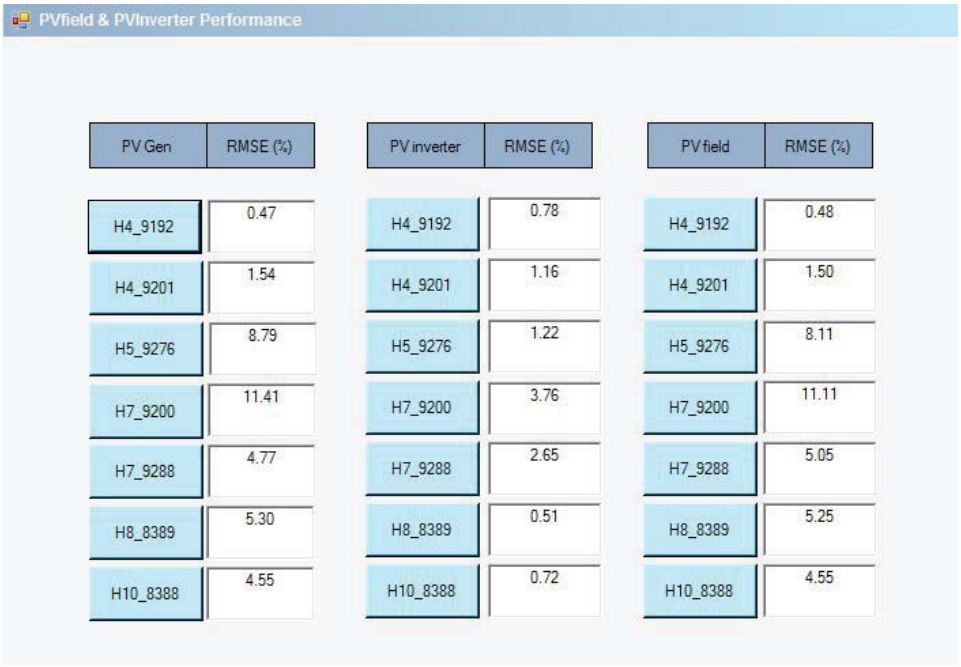

Figure 11: PV filed, PV inverter and PV generator Performance

In this section, the PV modules, PV inverter, and whole PV generator (PV module and Inverter) efficiency are calculated compared to the reference efficiency. Users can select each device to see its graphical efficiency as in the Figure 12. The RMSEs next to the equipment show their Root Mean Square Error in percentage.

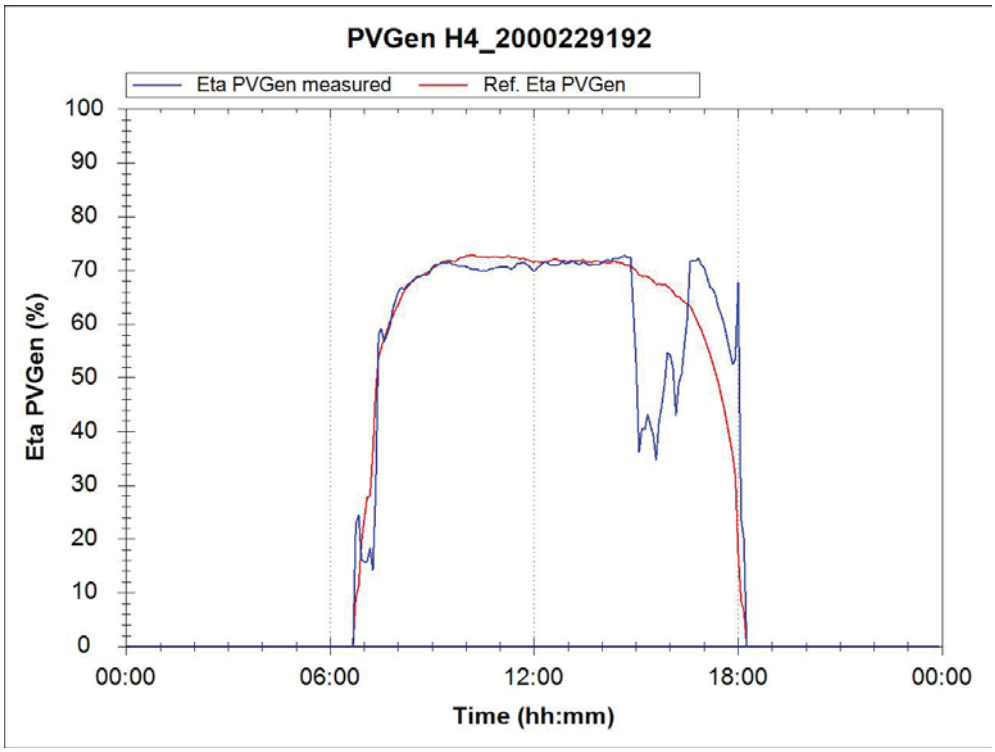

Figure 12: Comparing the PV Generator efficiency measured at House 4 to the reference PV Generator efficiency calculated

7.2.10. Multiple date

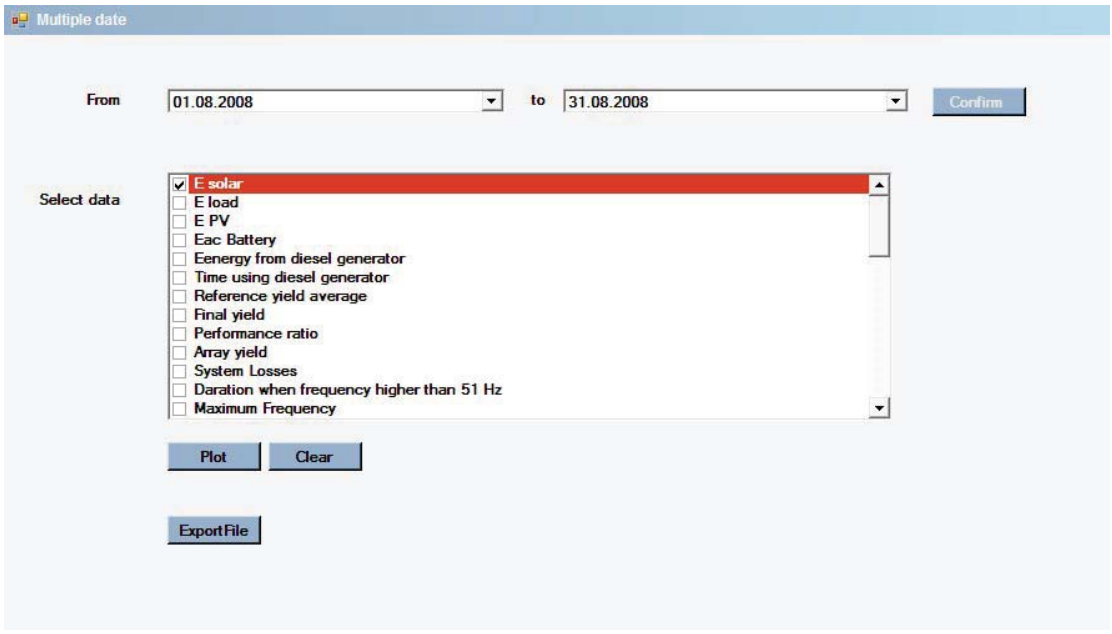

Figure 13: The multiple date page

In this section, users can select the starting date and the ending date, then click confirm. However, the files must be in the correct format and stored in the right place. Every file name must be saved in YYYY-MM-DD.csv and stored in c:\Kythnos\. Furthermore, multiple dates' data can be plotted. User can also export the results.

7.2.11. Input Variables

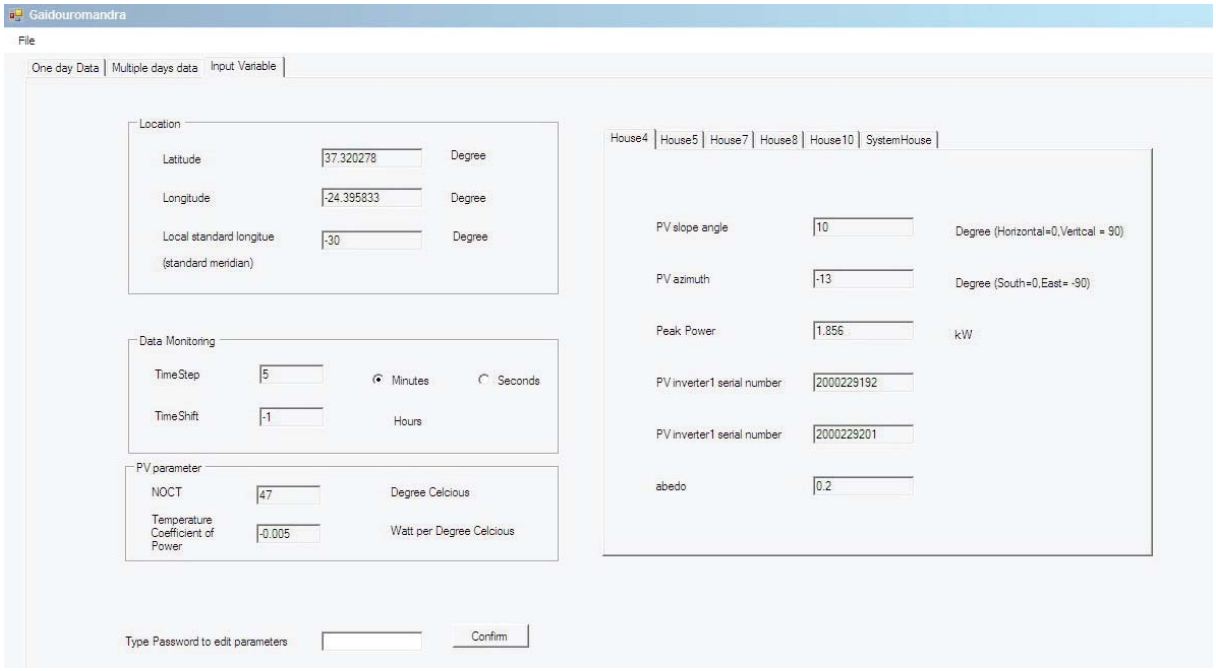

Figure 14: The input variables

Input Variables of the Gaidouromandra minigrid were put in the software as in the Figure 14. For example, latitude, longitude, local standard longitude, time step, NOCT, temperature coefficient of power, and all data of the distributed PV can be specified in this page.

8. Re-analysis of 2004 measurements

Monitoring data from 2004 has been provided to the More Microgrid consortium.
The data cover 5 months from 01.06.2004 to 31.10.2004, with a time step of 5 minutes.
The data represent spot values, logged asynchronously with an interval of 5 minutes from three logging devices (Sunny Island Master and 2 SunnyBoyControlplus from the company SMA).
The following parameters are provided:

- **DateTime** (SunnyIsland)
- **UnixTime** (SunnyIsland)
- **Uconv eff** (SunnyIsland): RMS voltage at the AC connection point of the battery inverter
- **Fconv** (SunnyIsland): frequency at the AC connection point of the battery inverter
- **Pconv Sum** (SunnyIsland): Total active power provided by the battery inverter
- **Qconv Sum** (SunnyIsland): Total reactive power provided by the battery inverter
- **Ubat mean** (SunnyIsland): Average battery voltage
- **SOC act** (SunnyIsland): Battery state of charge
- **DateTime** (SBC1): Following parameters logged by SBC 1 (sn:114362468)
- **PacPV2** (SBC1): Total active power of the PV inverters logged by SunnyBoyControlplus 114362468
- **Radiation** (SBC1): solar radiation horizontal
- **Temp. Ambiente** (SBC1): air temperature
- **Temp. Module** (SBC1): module temperature
- **DateTime** (SBC2): Following parameters logged by SBC2 (sn: 114362467)
- **PacPV1** (SBC2): Total active power of the PV inverters logged by SunnyBoyControlplus114362467
- **Pdiesel** (SBC2): active power produced by diesel generator

The different loads are not measured directly but can be calculated. The total load can be computed from the above parameters as:
Pload= Ppv1+Ppv2+Pdiesel+Pbat
However, it is to be noted that due to the unsynchronized logging, uncorrected time difference in the data can lead to errors (eg. Negative loads), especially if the sky is cloudy.

The following sections illustrate the seasonal variation of the parameters, the frequency variation concept used for controlling the PV inverters and the parallel operation of the battery inverters on a single phase.

8.1. Seasonal variation

Example of plots are shown hereafter for:

- Grid frequency (5 x 1 month)
- Grid voltage (5 x 1 month)
- Battery voltage (2 x 2.5 month)
- Horizontal radiation (2 x 2.5 month)

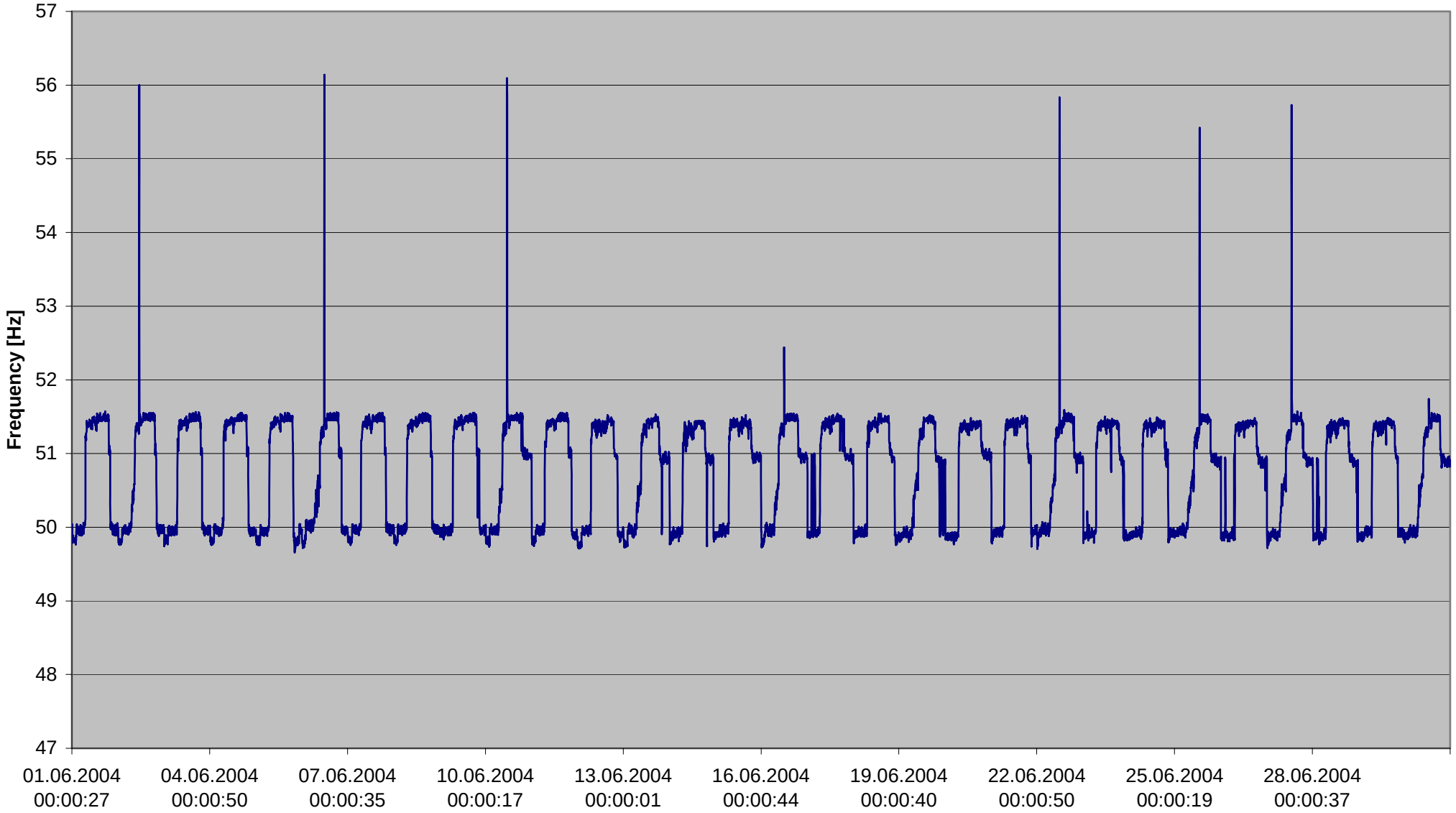
Frequency [Hz]
57
56
55
54
53
52
51
50
49
48
47
01.06.2004 00:00:27
04.06.2004 00:00:50
07.06.2004 00:00:35
10.06.2004 00:00:17
13.06.2004 00:00:01
16.06.2004 00:00:44
19.06.2004 00:00:40
22.06.2004 00:00:50
25.06.2004 00:00:19
28.06.2004 00:00:37

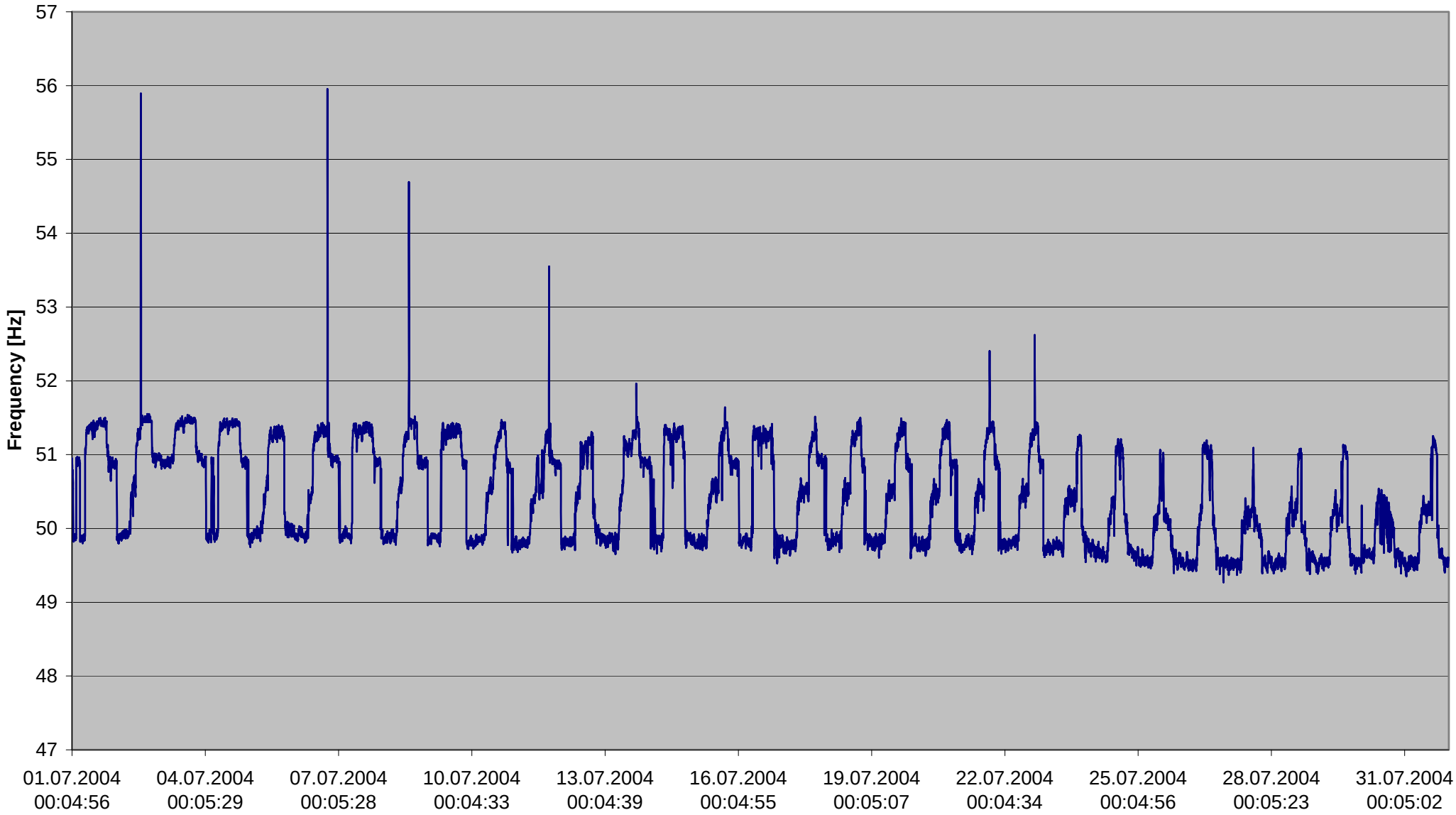
Frequency [Hz]
57
56
55
54
53
52
51
50
49
48
47
01.07.2004 00:04:56
04.07.2004 00:05:29
07.07.2004 00:05:28
10.07.2004 00:04:33
13.07.2004 00:04:39
16.07.2004 00:04:55
19.07.2004 00:05:07
22.07.2004 00:04:34
25.07.2004 00:04:56
28.07.2004 00:05:23
31.07.2004 00:05:02

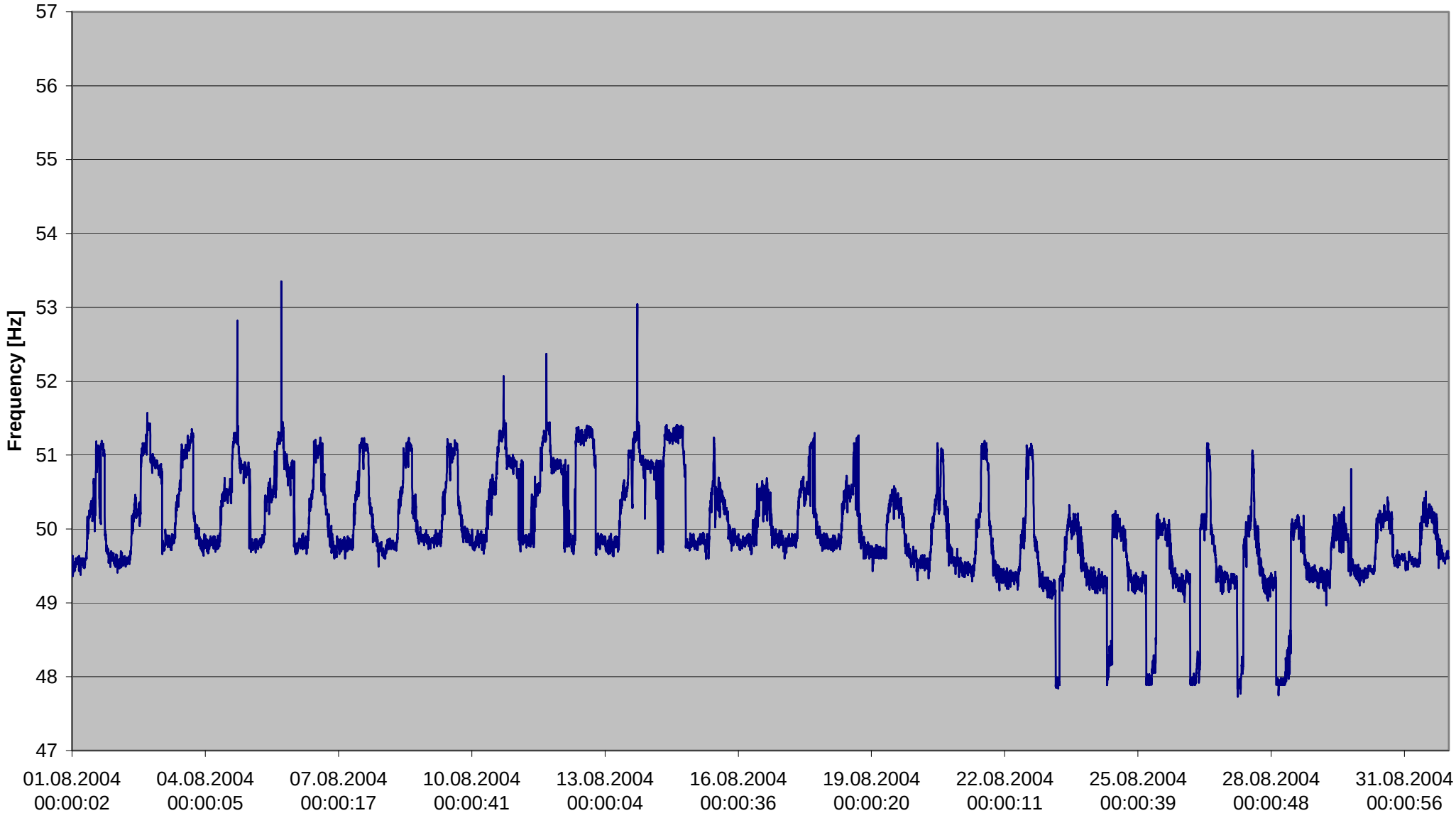
Frequency [Hz]
57
56
55
54
53
52
51
50
49
48
47
01.08.2004 00:00:02
04.08.2004 00:00:05
07.08.2004 00:00:17
10.08.2004 00:00:41
13.08.2004 00:00:04
16.08.2004 00:00:36
19.08.2004 00:00:20
22.08.2004 00:00:11
25.08.2004 00:00:39
28.08.2004 00:00:48
31.08.2004 00:00:56

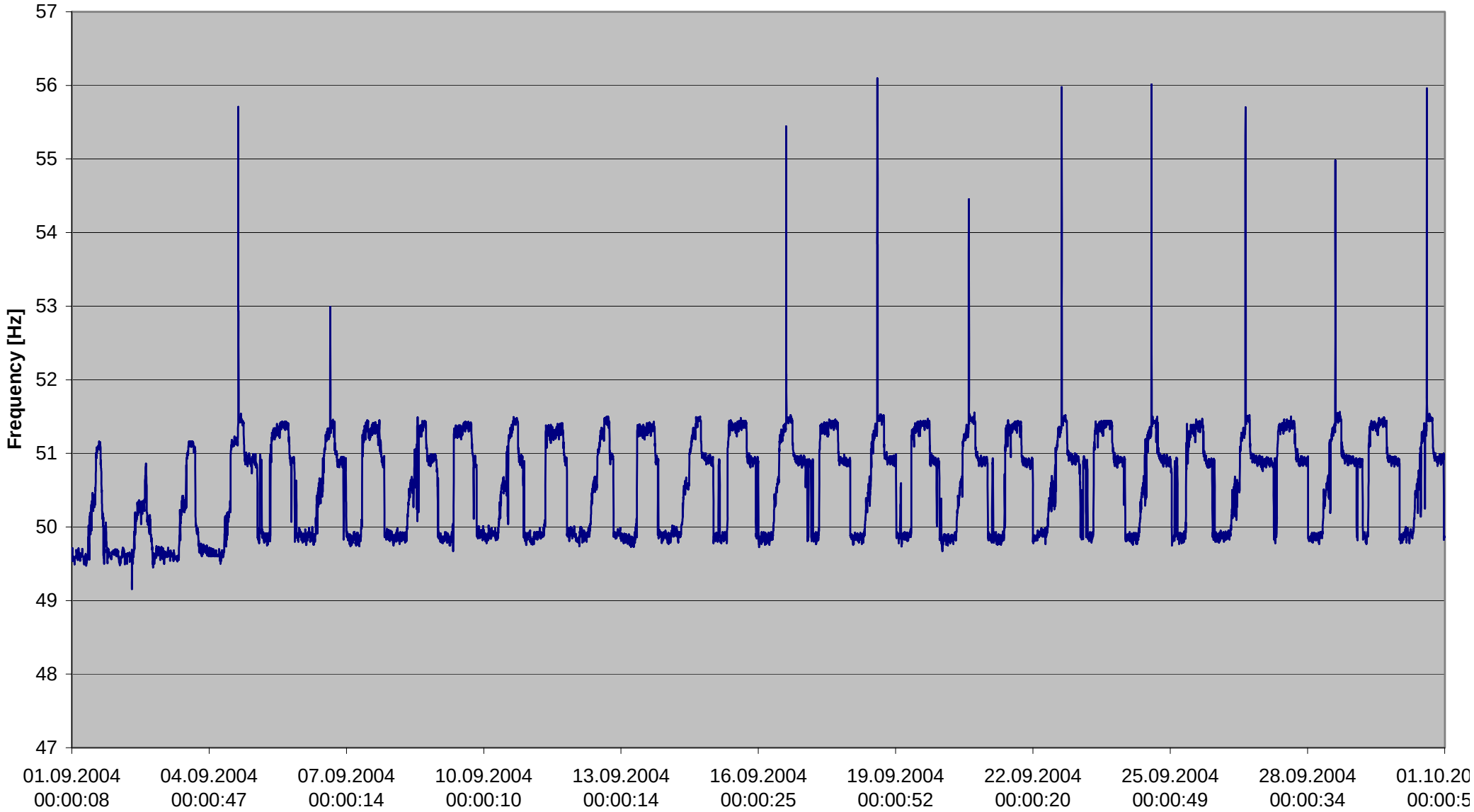
Frequency [Hz]
57
56
55
54
53
52
51
50
49
48
47
01.09.2004 00:00:08
04.09.2004 00:00:47
07.09.2004 00:00:14
10.09.2004 00:00:10
13.09.2004 00:00:14
16.09.2004 00:00:25
19.09.2004 00:00:52
22.09.2004 00:00:20
25.09.2004 00:00:49
28.09.2004 00:00:34
01.10.20 00:00:5

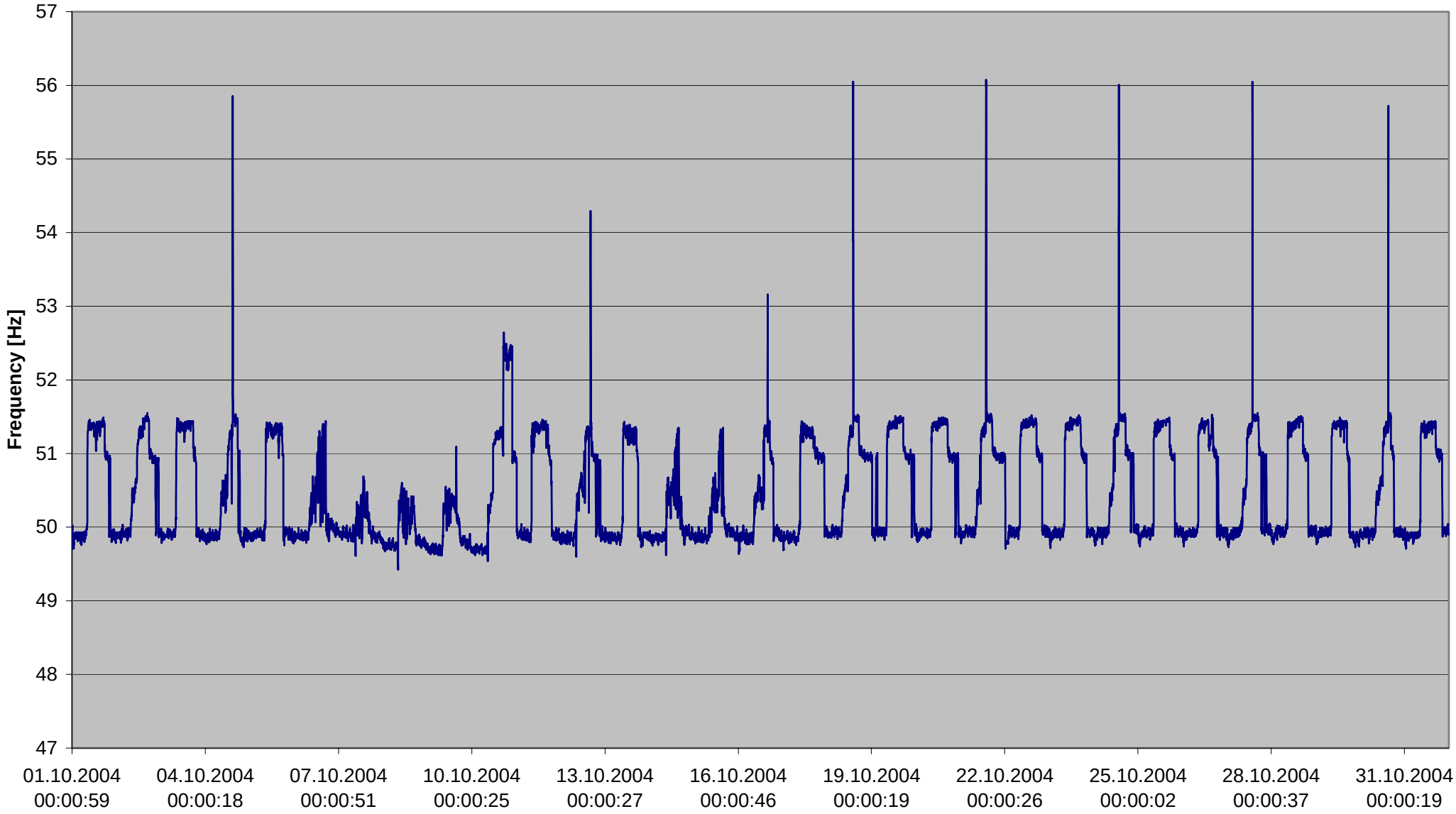
Frequency [Hz]
57
56
55
54
53
52
51
50
49
48
47
01.10.2004 00:00:59
04.10.2004 00:00:18
07.10.2004 00:00:51
10.10.2004 00:00:25
13.10.2004 00:00:27
16.10.2004 00:00:46
19.10.2004 00:00:19
22.10.2004 00:00:26
25.10.2004 00:00:02
28.10.2004 00:00:37
31.10.2004 00:00:19

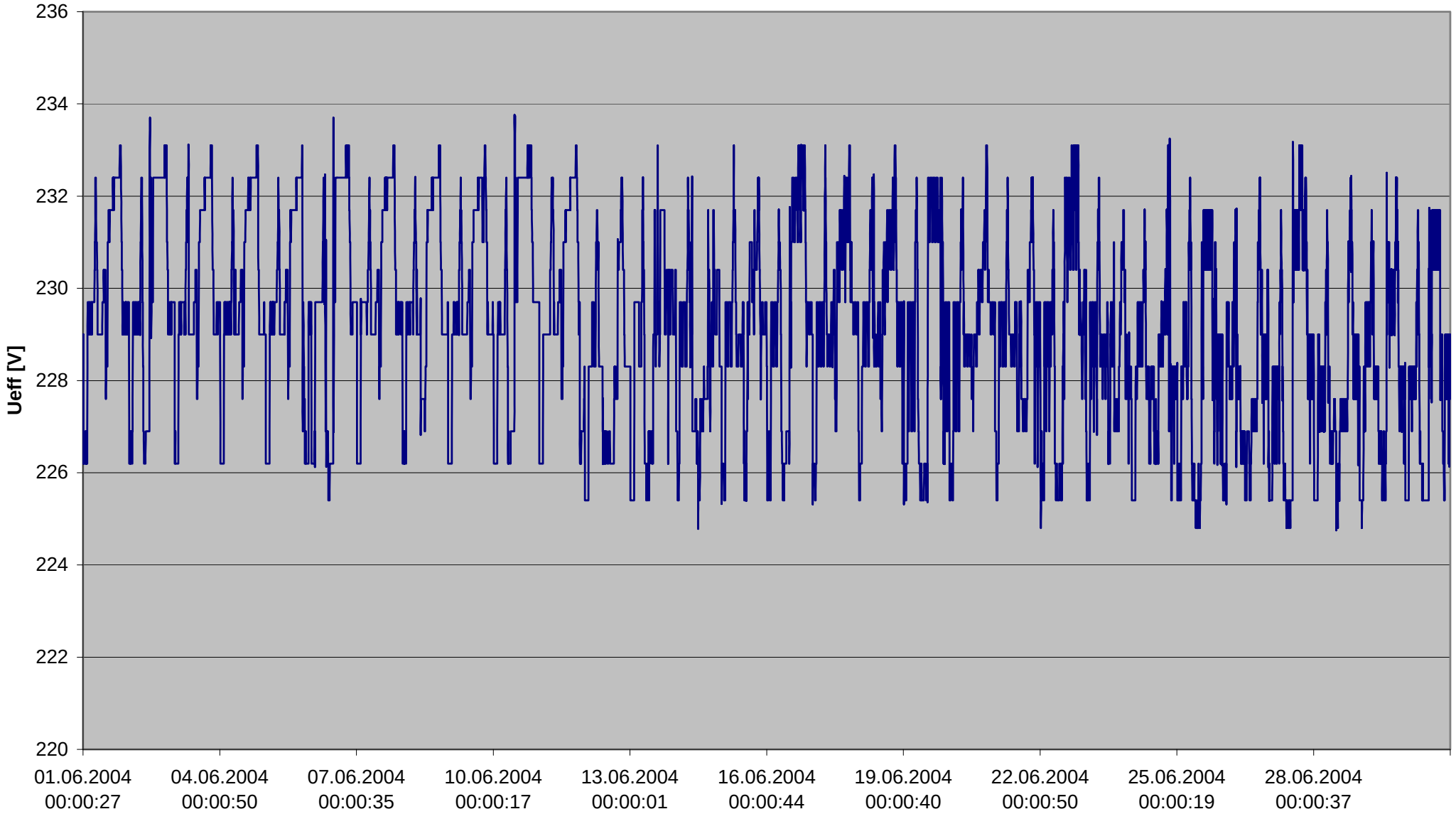
Ueff [V]
236
234
232
230
228
226
224
222
220
01.06.2004 00:00:27
04.06.2004 00:00:50
07.06.2004 00:00:35
10.06.2004 00:00:17
13.06.2004 00:00:01
16.06.2004 00:00:44
19.06.2004 00:00:40
22.06.2004 00:00:50
25.06.2004 00:00:19
28.06.2004 00:00:37

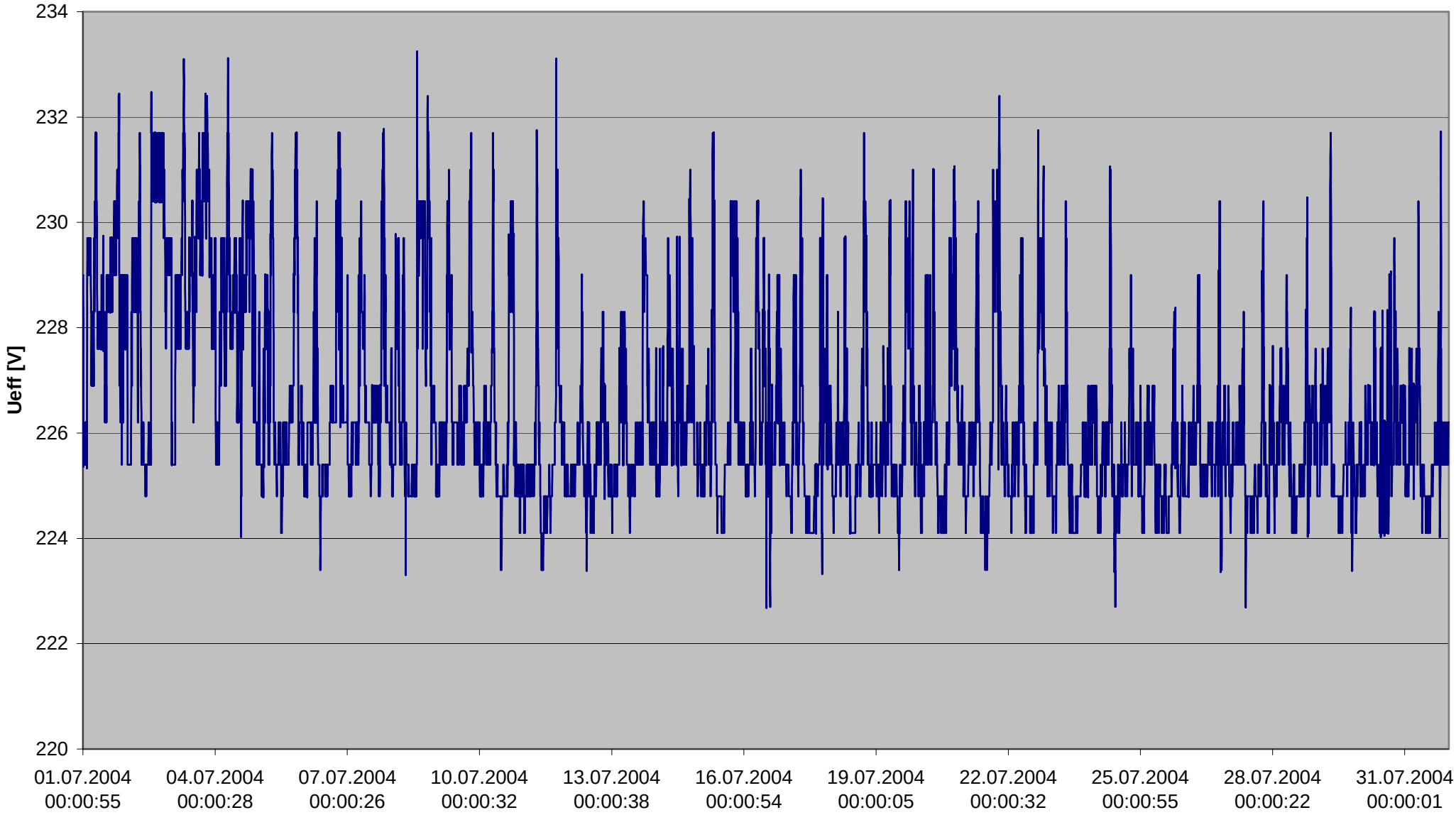
234
232
230
228
226
224
222
220
Ueff [V]
01.07.2004 00:00:55
04.07.2004 00:00:28
07.07.2004 00:00:26
10.07.2004 00:00:32
13.07.2004 00:00:38
16.07.2004 00:00:54
19.07.2004 00:00:05
22.07.2004 00:00:32
25.07.2004 00:00:55
28.07.2004 00:00:22
31.07.2004 00:00:01

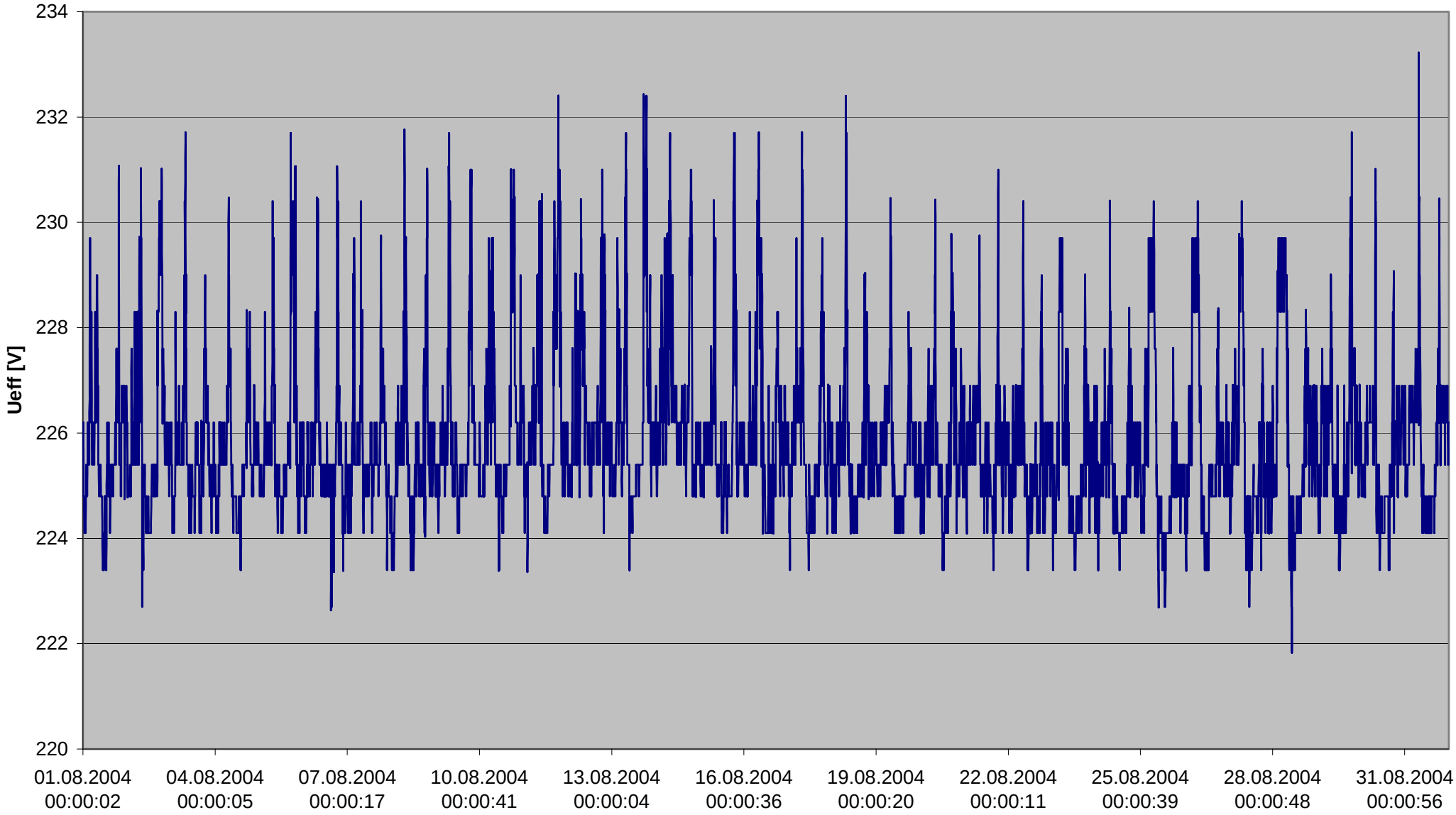
234
232
230
228
226
224
222
220
Ueff [V]
01.08.2004 00:00:02
04.08.2004 00:00:05
07.08.2004 00:00:17
10.08.2004 00:00:41
13.08.2004 00:00:04
16.08.2004 00:00:36
19.08.2004 00:00:20
22.08.2004 00:00:11
25.08.2004 00:00:39
28.08.2004 00:00:48
31.08.2004 00:00:56

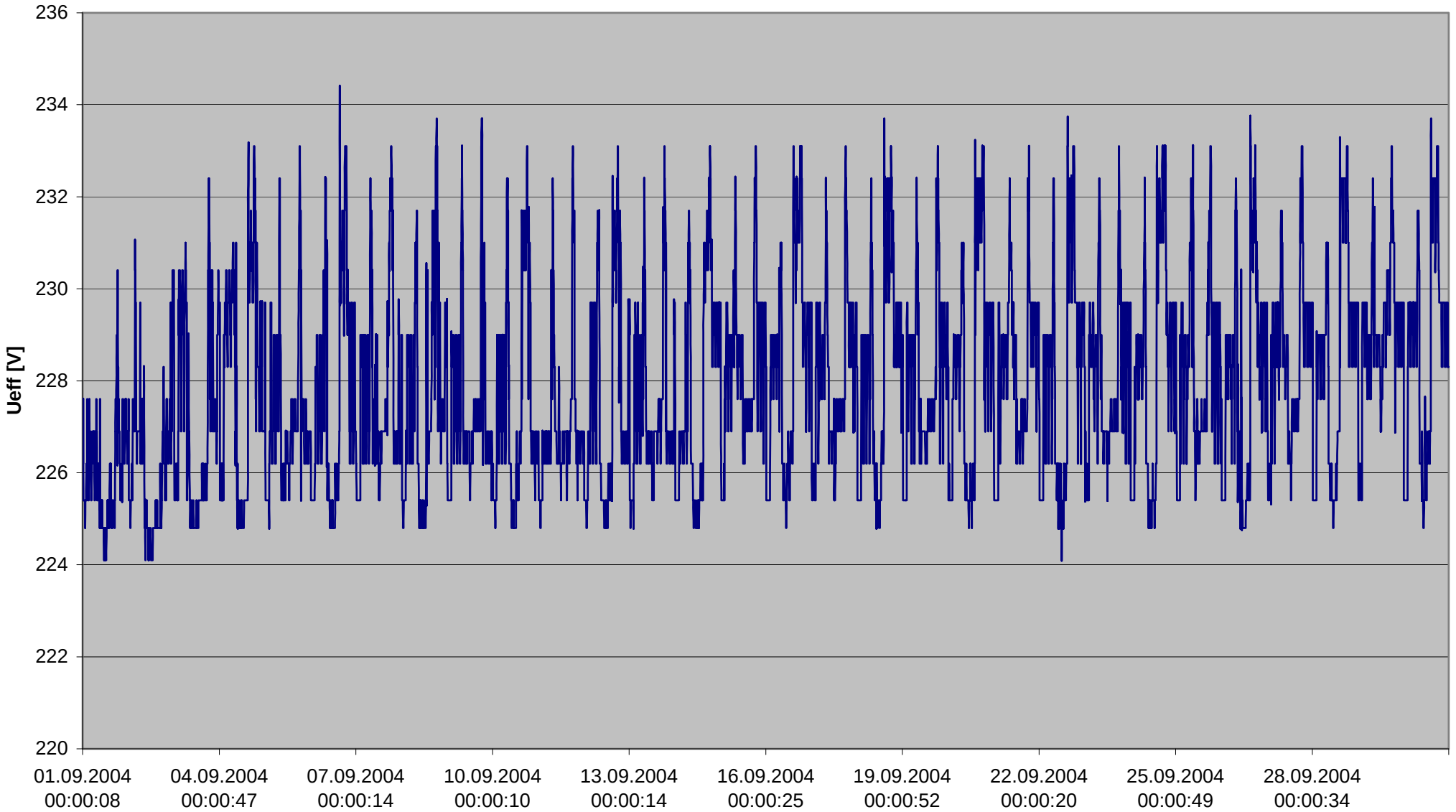
Ueff [V]
236
234
232
230
228
226
224
222
220
01.09.2004 00:00:08
04.09.2004 00:00:47
07.09.2004 00:00:14
10.09.2004 00:00:10
13.09.2004 00:00:14
16.09.2004 00:00:25
19.09.2004 00:00:52
22.09.2004 00:00:20
25.09.2004 00:00:49
28.09.2004 00:00:34

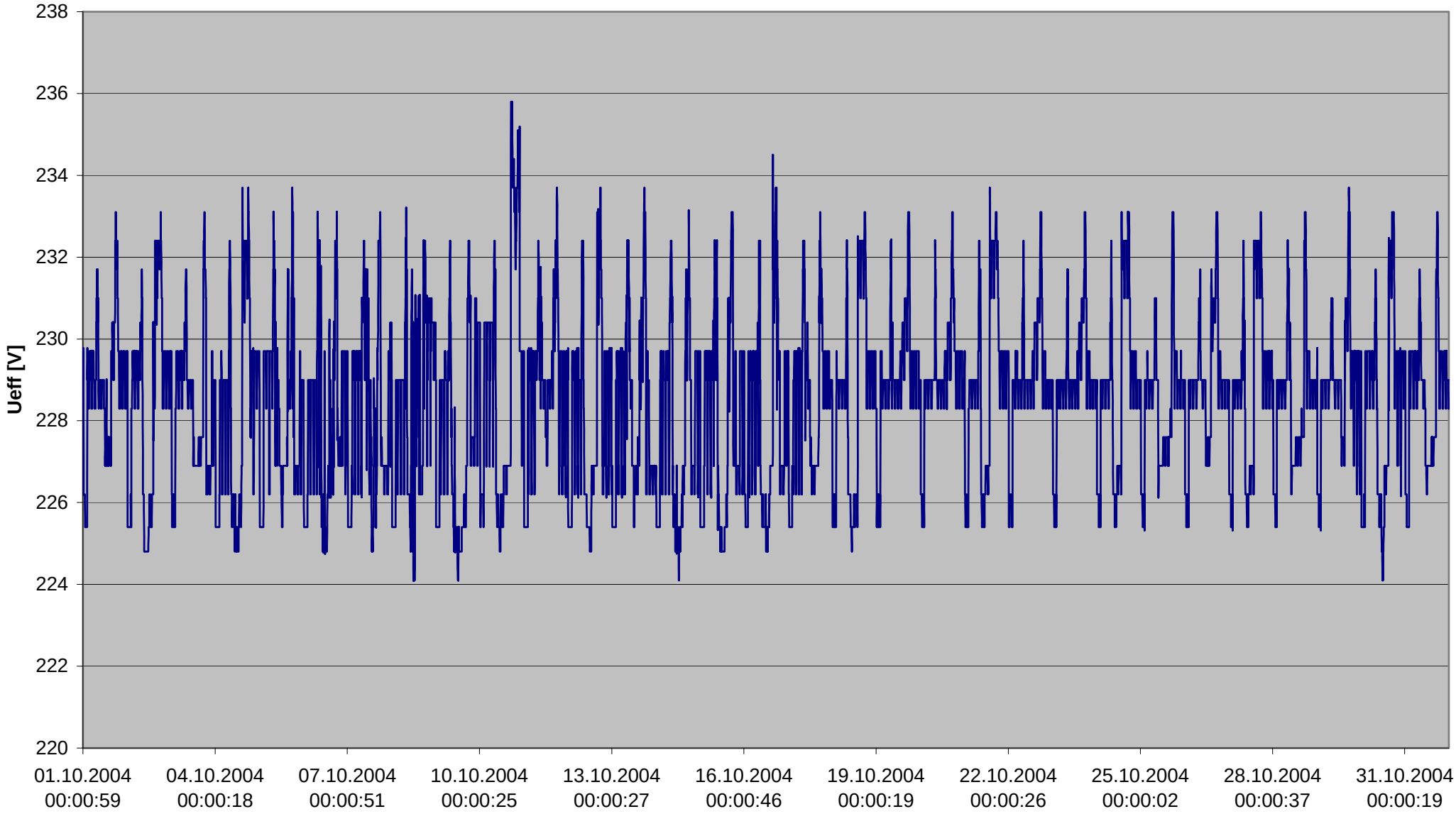
Ueff [V]
238
236
234
232
230
228
226
224
222
220
01.10.2004 00:00:59
04.10.2004 00:00:18
07.10.2004 00:00:51
10.10.2004 00:00:25
13.10.2004 00:00:27
16.10.2004 00:00:46
19.10.2004 00:00:19
22.10.2004 00:00:26
25.10.2004 00:00:02
28.10.2004 00:00:37
31.10.2004 00:00:19

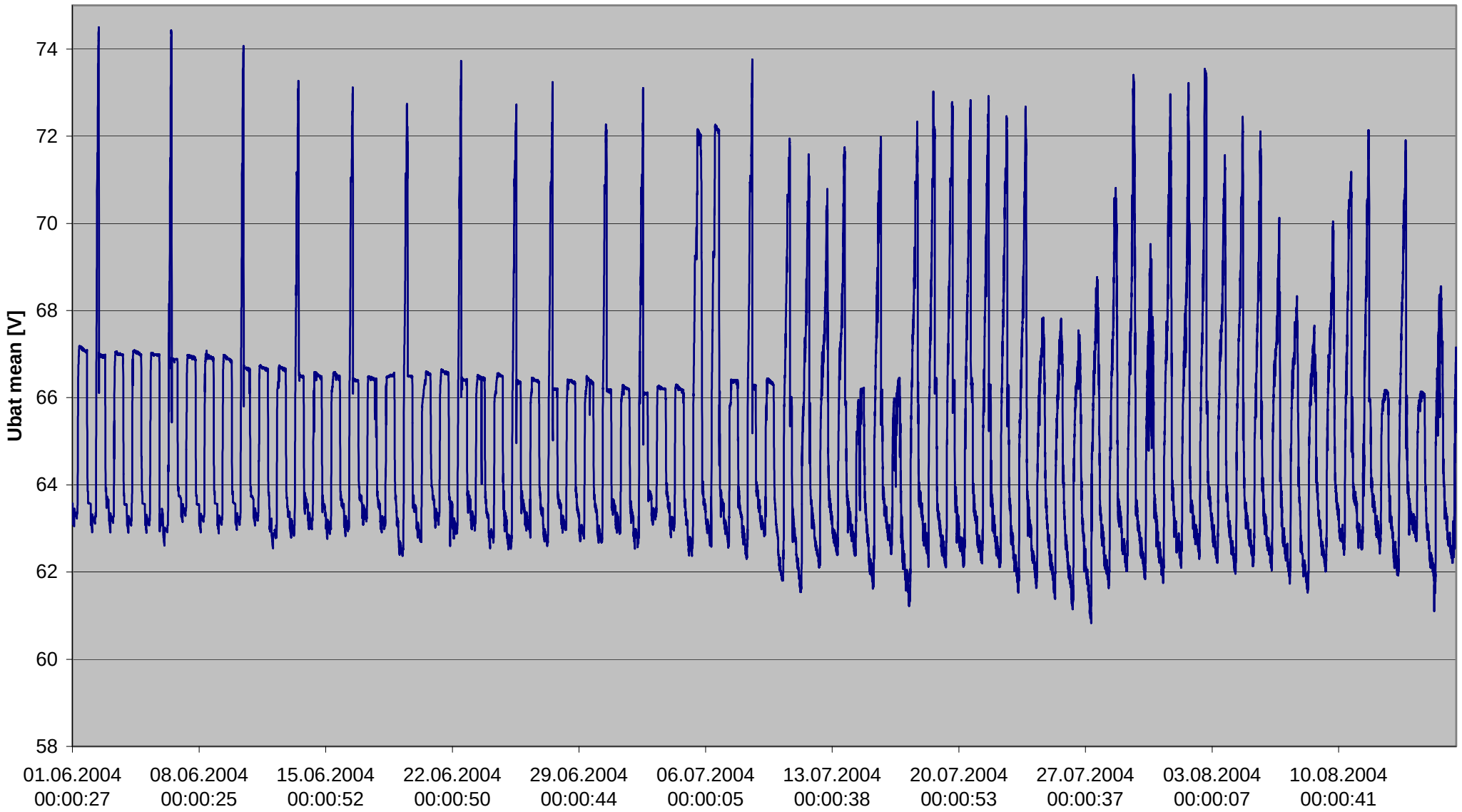
Ubat mean [V]
74
72
70
68
66
64
62
60
58
01.06.2004 00:00:27
08.06.2004 00:00:25
15.06.2004 00:00:52
22.06.2004 00:00:50
29.06.2004 00:00:44
06.07.2004 00:00:05
13.07.2004 00:00:38
20.07.2004 00:00:53
27.07.2004 00:00:37
03.08.2004 00:00:07
10.08.2004 00:00:41

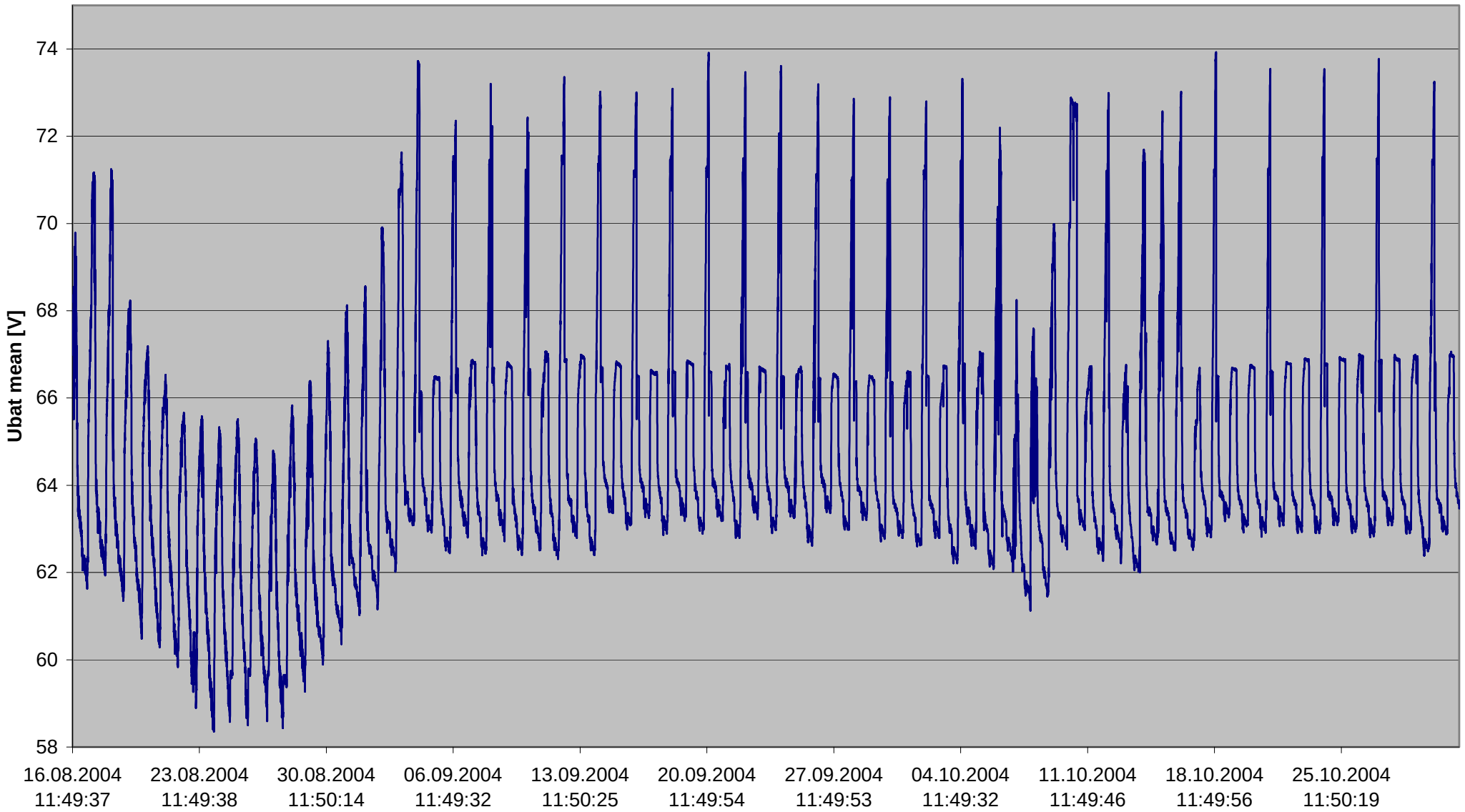
Ubat mean [V]
74
72
70
68
66
64
62
60
58
16.08.2004 11:49:37
23.08.2004 11:49:38
30.08.2004 11:50:14
06.09.2004 11:49:32
13.09.2004 11:50:25
20.09.2004 11:49:54
27.09.2004 11:49:53
04.10.2004 11:49:32
11.10.2004 11:49:46
18.10.2004 11:49:56
25.10.2004 11:50:19

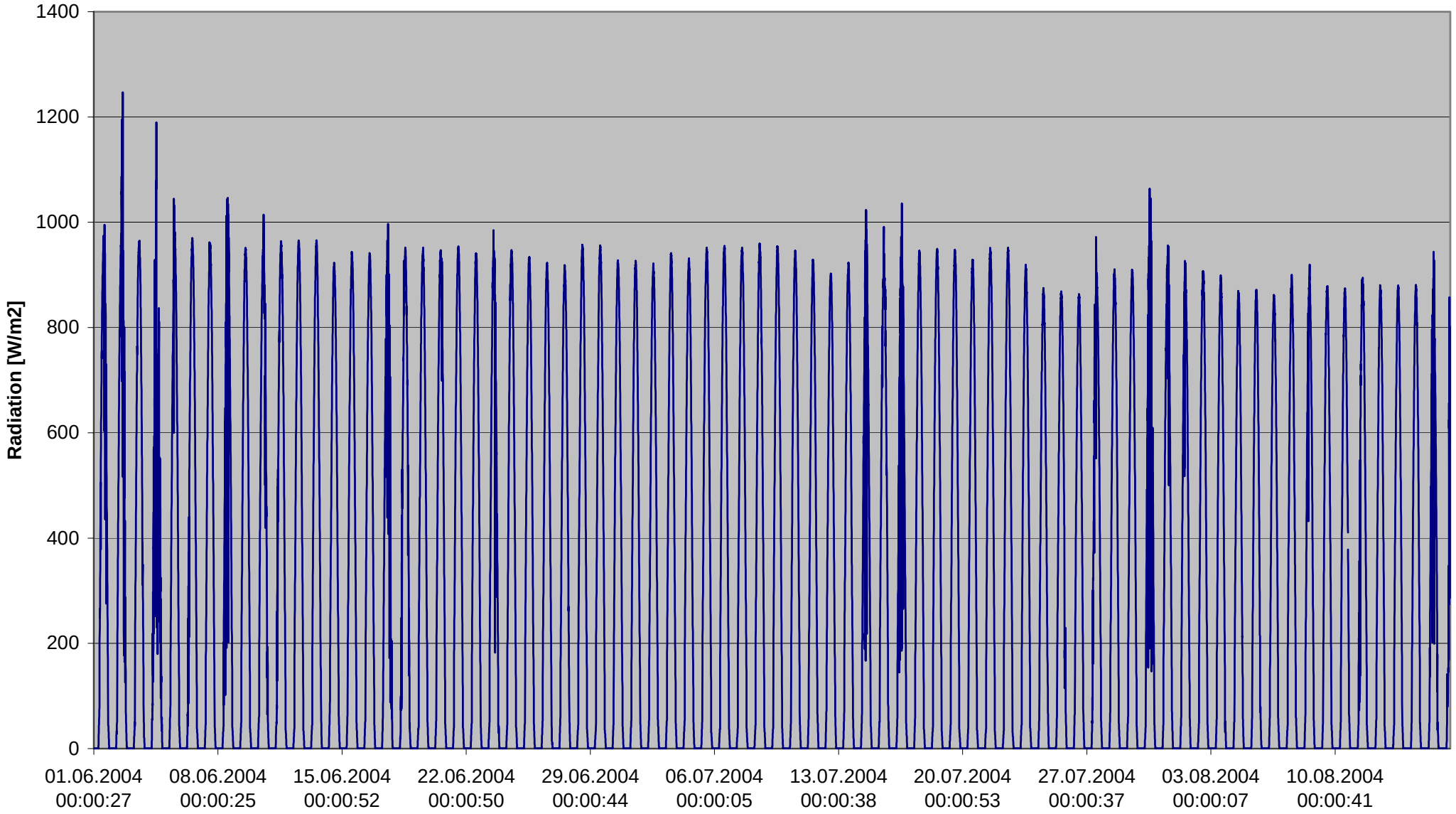
Radiation [W/m2]
1400
1200
1000
800
600
400
200
0
01.06.2004 00:00:27
08.06.2004 00:00:25
15.06.2004 00:00:52
22.06.2004 00:00:50
29.06.2004 00:00:44
06.07.2004 00:00:05
13.07.2004 00:00:38
20.07.2004 00:00:53
27.07.2004 00:00:37
03.08.2004 00:00:07
10.08.2004 00:00:41

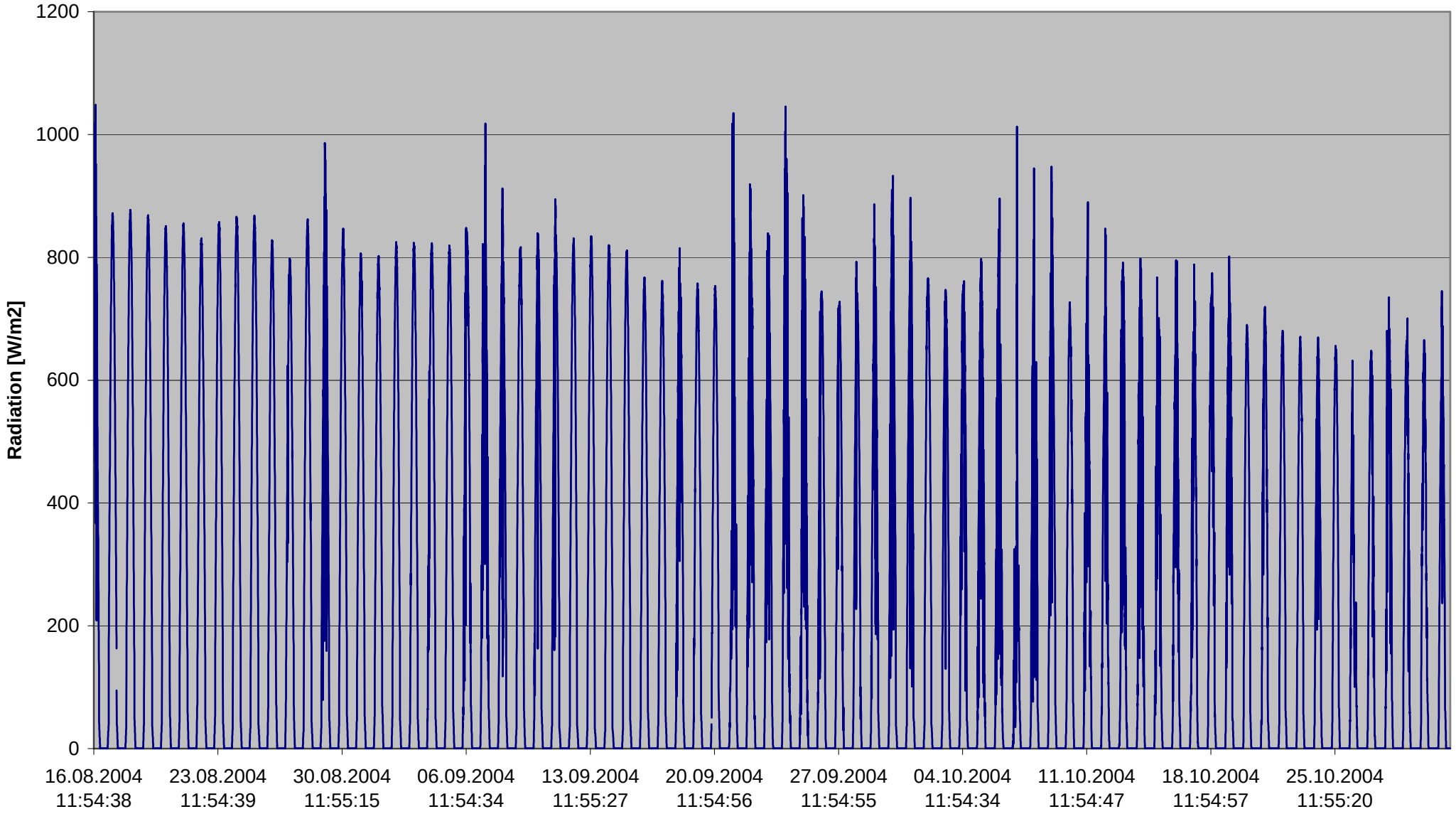
Radiation [W/m2]
1200
1000
800
600
400
200
0
16.08.2004 11:54:38
23.08.2004 11:54:39
30.08.2004 11:55:15
06.09.2004 11:54:34
13.09.2004 11:55:27
20.09.2004 11:54:56
27.09.2004 11:54:55
04.10.2004 11:54:34
11.10.2004 11:54:47
18.10.2004 11:54:57
25.10.2004 11:55:20

8.2. Frequency for grid control and energy management

As already mentioned, the variation of grid frequency is applied for organizing both primary control of the grid and energy management with distributed sources and loads. The battery inverters are synchronized, and the diesel genset applies frequency and voltage droops. This concept allows the provision of high peak power, for example for the starting of motors, and enough short-circuit currents to release circuit breakers. Peak power is shared between all operating battery inverters and the genset, without additional communication requirements.
To communicate the information coming from energy management, the set value of the grid frequency varies. The frequency window ranges from 48 Hz to 52 Hz to allow for the operation of usual consumers.

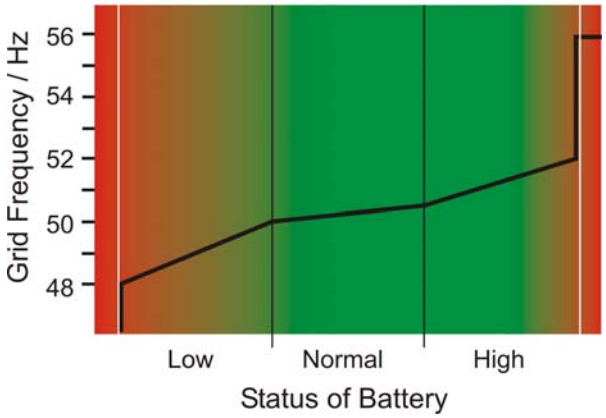

Figure 15: The battery management system is controlling load shedding and photovoltaic power via frequency

The frequency depends on the status of the battery, which is affected not only by the battery's state of charge but by historical values. A simplified graphical presentation of this dependency is shown in Figure 15. It can be seen that at times when the battery needs to be charged, the grid frequency is lowered. If necessary, the diesel genset will be started and, if the frequency drops still further (such as below 48 Hz) loads will be disconnected. If the battery is full or needs power limitation according to the implemented charge control, the distributed PV inverters that feed PV power into the AC minigrid identify a higher grid frequency and continuously limit their power output.

This control strategy is illustrated with operational results for a typical clear day in summer (Sunday 18.07.2004). On this day, the total horizontal solar radiation was 7.5 kWh/m2.

Figure 16 (a and b) show during this same day the evolution of the battery cell voltage, the total PV power (AC) and the grid frequency. During the night, the back-up power is not used, the battery is discharged and the voltage is decreasing. The lower battery state of charge is reached at about 7:30 in the morning. Till midday, the PV inverters are producing at the maximum power point (100% of MPPT operation), reaching a total AC power of 6.8 kW. At this time, the battery cells reach a first limit of 2.37 Volt and the battery inverter increases the grid frequency by 0.5 Hz. A grid frequency over 51 Hz is interpreted by the PV inverters as a signal for limiting their power proportionally to the frequency deviation. The PV inverters do not operate at the maximum power point. As long as too much solar energy is available, the battery inverter will use this control method to charge optimally the battery. After a few boost charges, the battery voltage is set to a floating level of 2.22 volts.

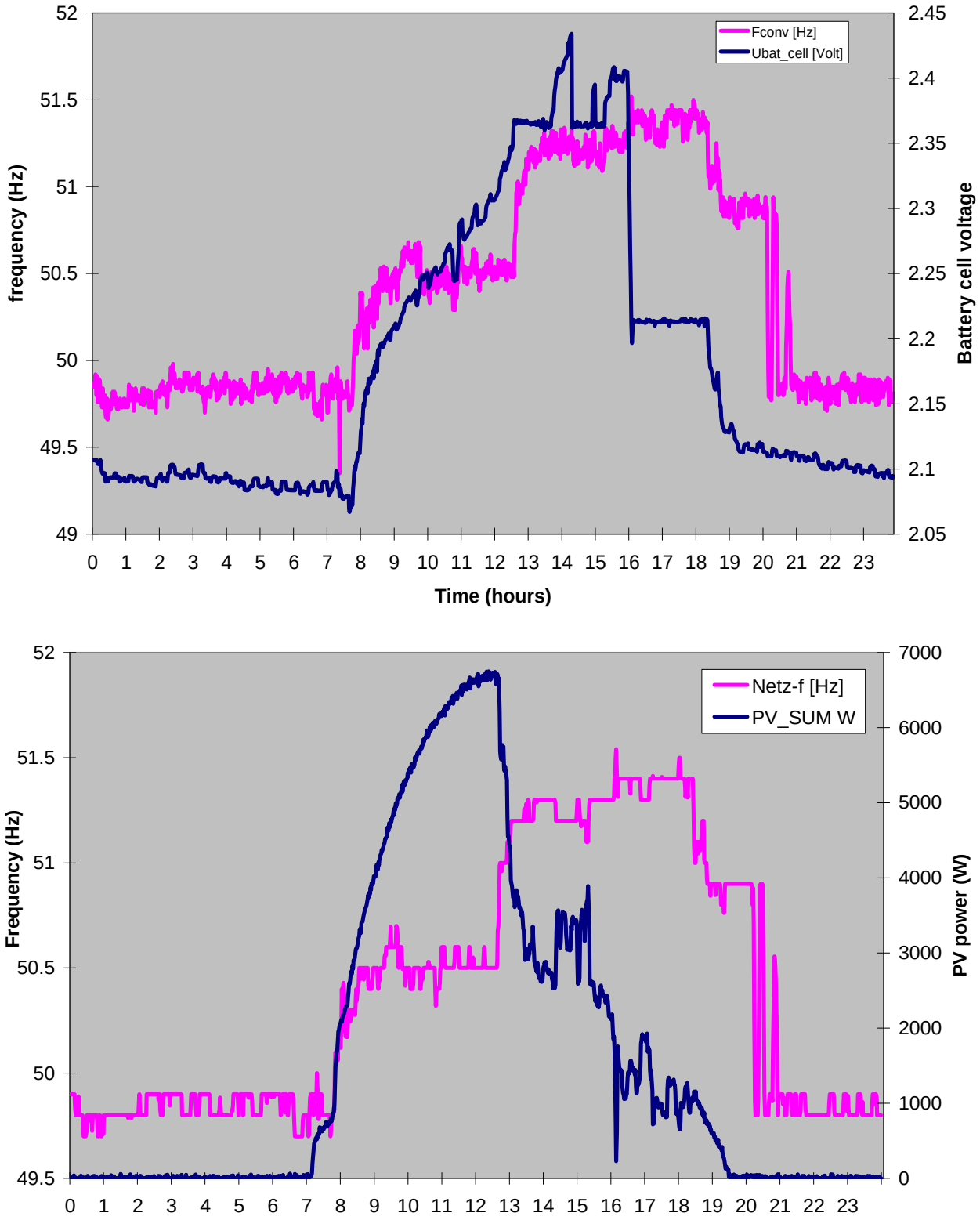

Figure 16 (a and b): The battery inverter controls the PV power by changing the grid frequency, achieving an optimal battery charging voltage (Gaidouromandra, 18.07.2004).

8.3. Energy efficient operation of multiple battery inverters on a single phase

The Gaidouromandra mini-grid can be operated as a single phase or as a three phase system. If all users have only single phase appliances, the single phase operation is more efficient. The first advantage of the single phase operation is the availability of a higher power per phase, which could be useful for starting motor loads (eg. pumps). The second advantage is a reduced standby power consumption and extended lifetime, as only one inverter needs to be always switched on. Finally, the system is redundant and the failure of one battery inverter will have a limited impact on the system operation. These advantages are summarized in Table 3. The only small disadvantage is the reduced efficiency and power of the diesel generator if operated in single phase mode.

Number of Phases	**3**	**1**
Battery inverters	3 x SI 4500	3 x SI 4500
Continuous power per phase	3.3 kVA	10 kVA
Peak power per phase	6.6 kVA	20 kVA
Stand-by operation	Not possible	Possible for 2 units

Table 3: Comparison of single and three phase operations

Figure 17 shows how the 3 different battery inverters (inv1, inv2 and inv3) are operated on the 18.07.2004. Inverter 1 is always on, while inverter 2 is most of the time in standby and used only during sunny hours.

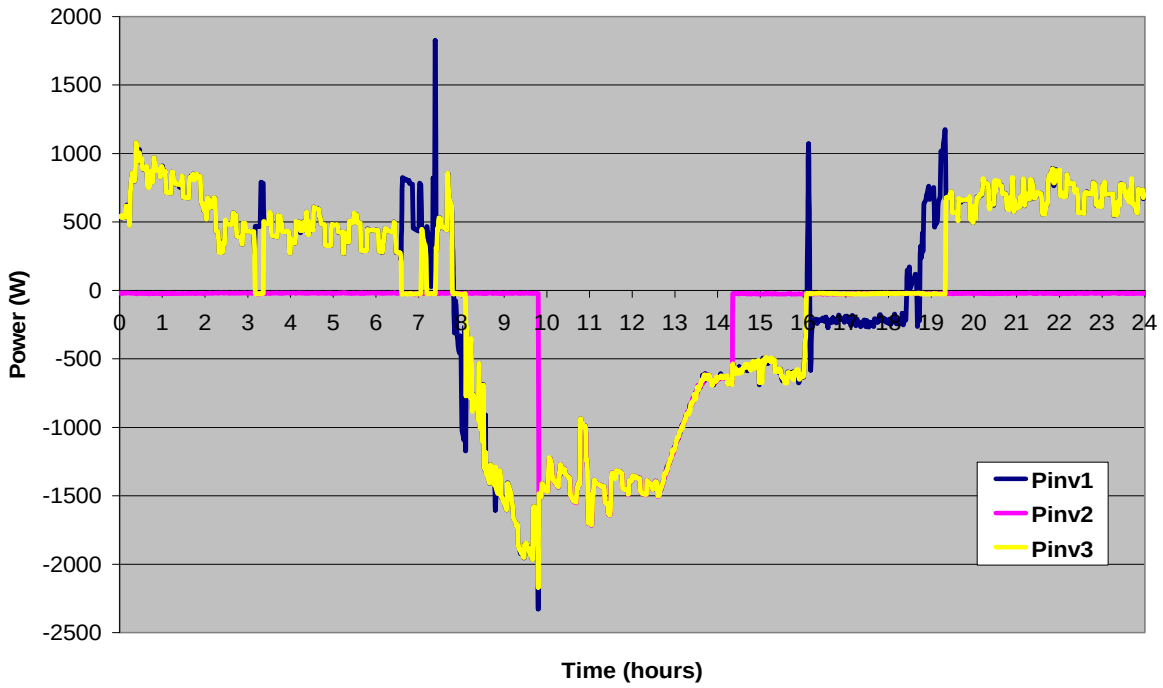

Figure 17: Power outputs of the 3 battery inverters (Gaidouromandra, 18.07.2004)

9. Analysis of summer 2008 measurements

The Gaidoroumandra system is characterized by an important seasonal fluctuation in the load profile. Although data is available since june 2007 for 2 summer periods which correspond to the highest load, the focus has been set on summer 2008, when all the monitoring was installed. The following topics have been investigated:

- Characteristic of the load (profile, un-symmetric loading of the 3 phases)
- Power quality
- Performance of the system

9.1. Characteristics of the load

Since june 2007, the power system has been redesigned as three-phase. However, all user loads are single phase, with a strong seasonal variation. This is illustrated in Figure 18 until Figure 32, which show that the phase loading is not optimal.
On phase 3, the load is nearly zero all year round. In august, the peak load on L3 is only a few hundred watts.
In winter time, the main load is the monitoring system, which is connected everyday on phase L1 from 8:30 until 17:30. If the monitoring battery needs to be recharged and the solar radiation level is not very high, the system battery can be exporting power via inverter L1 while importing power via inverters on L2 and L3. In Figure 18, a load step of P=2kW and Q=0.6kVA at 08:30 is due to the monitoring system being connected on L1. PV power is not used efficiently and losses in battery inverters could be avoided by redesigning the system as a single phase.
In summertime, the evening load profile (Figure 27, Figure 31) indicates that the main loads are probably cooling motors (refrigerator) and water pumps.
Many loads consume significant reactive power. Some loads seem to produce reactive power (eg. a refrigerator on L1 in Figure 24)

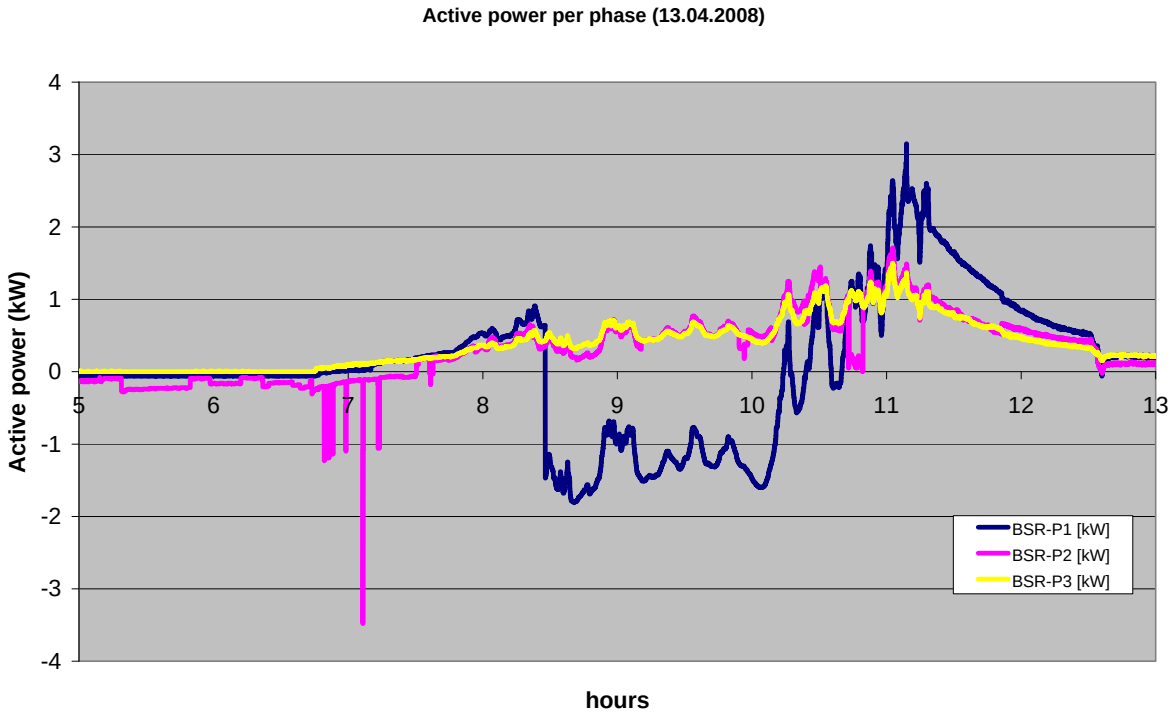

Figure 18: active power sharing between phases on 13.04.2008

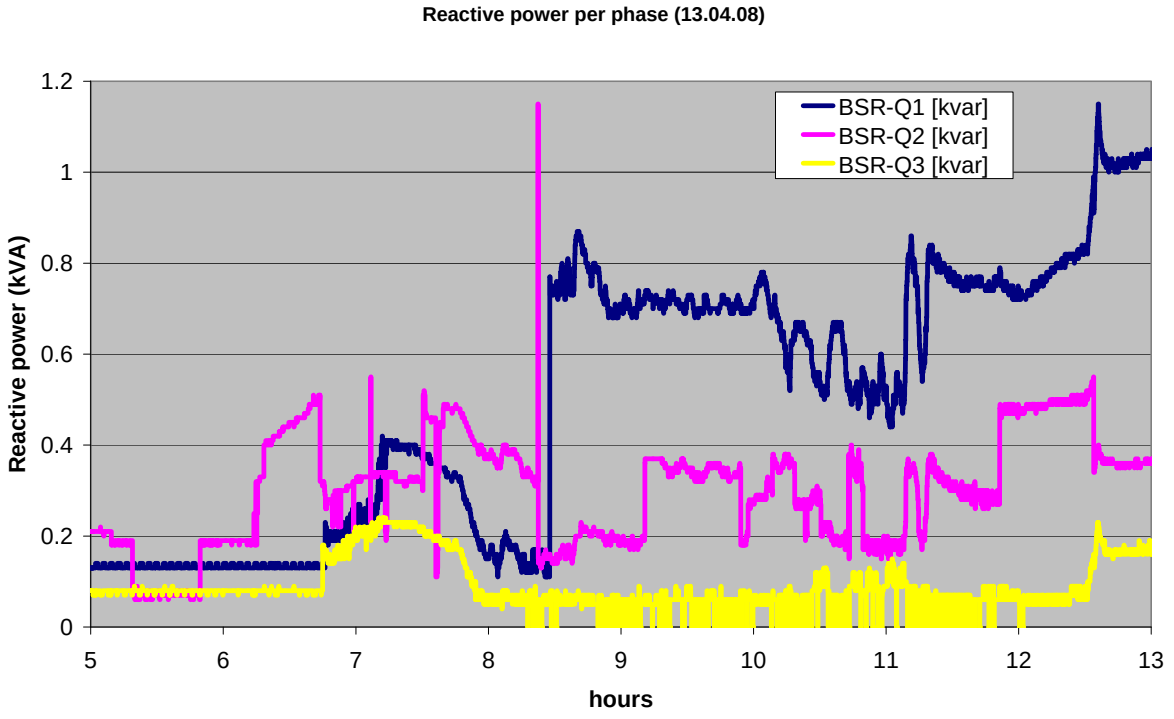

Figure 19: reactive power sharing between phases on 13.04.2008

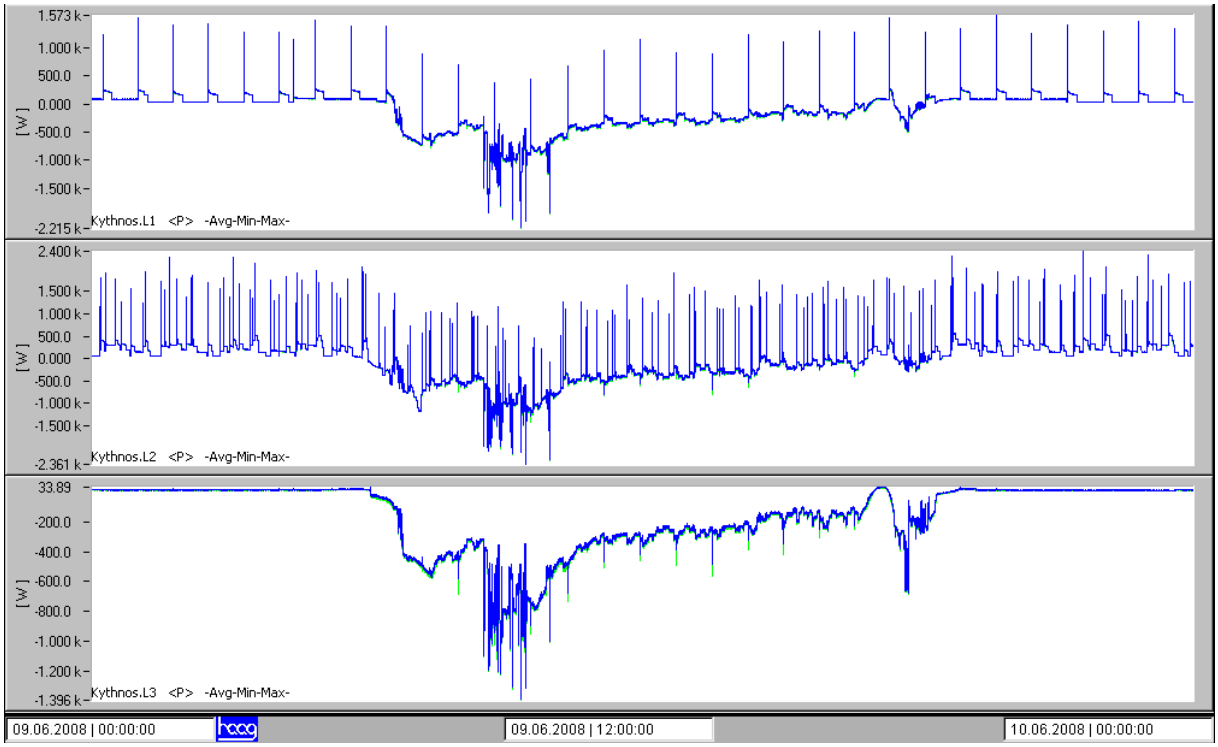

Figure 20: Phase L1, L2, L3 loading: active power on 09.06.2008

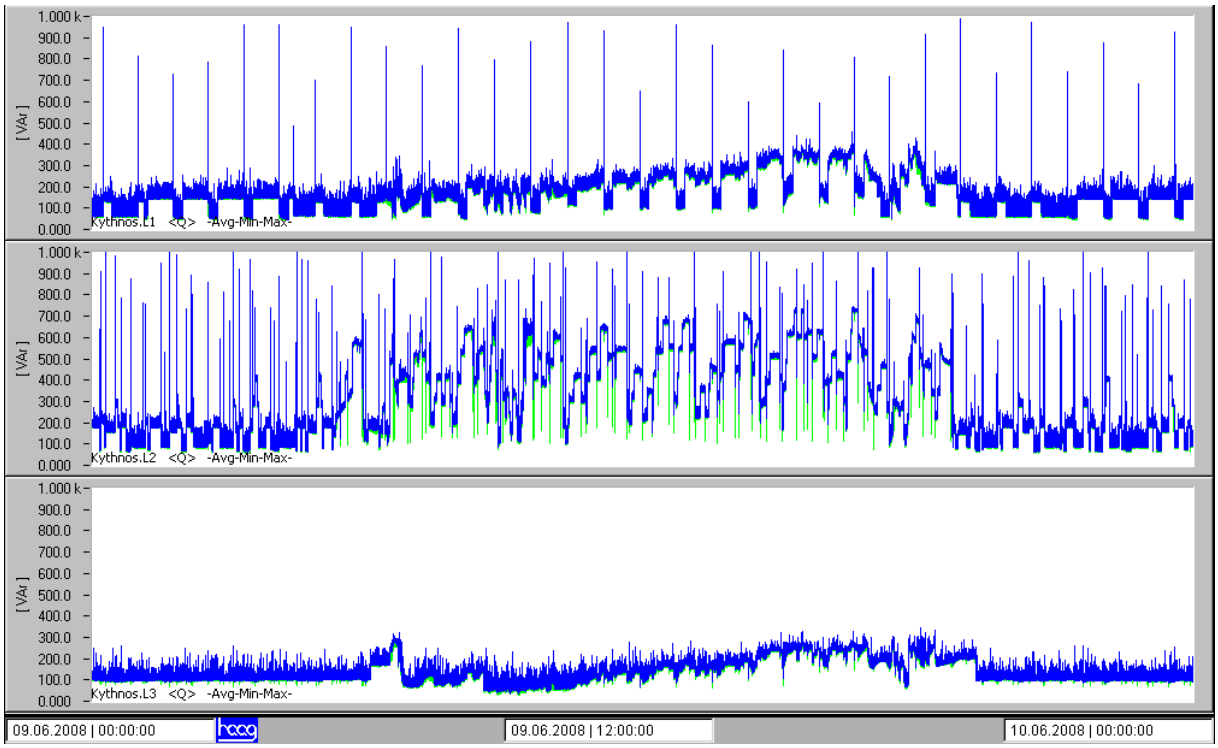

Figure 21: Phase L1, L2, L3 loading: reactive power on 09.06.2008

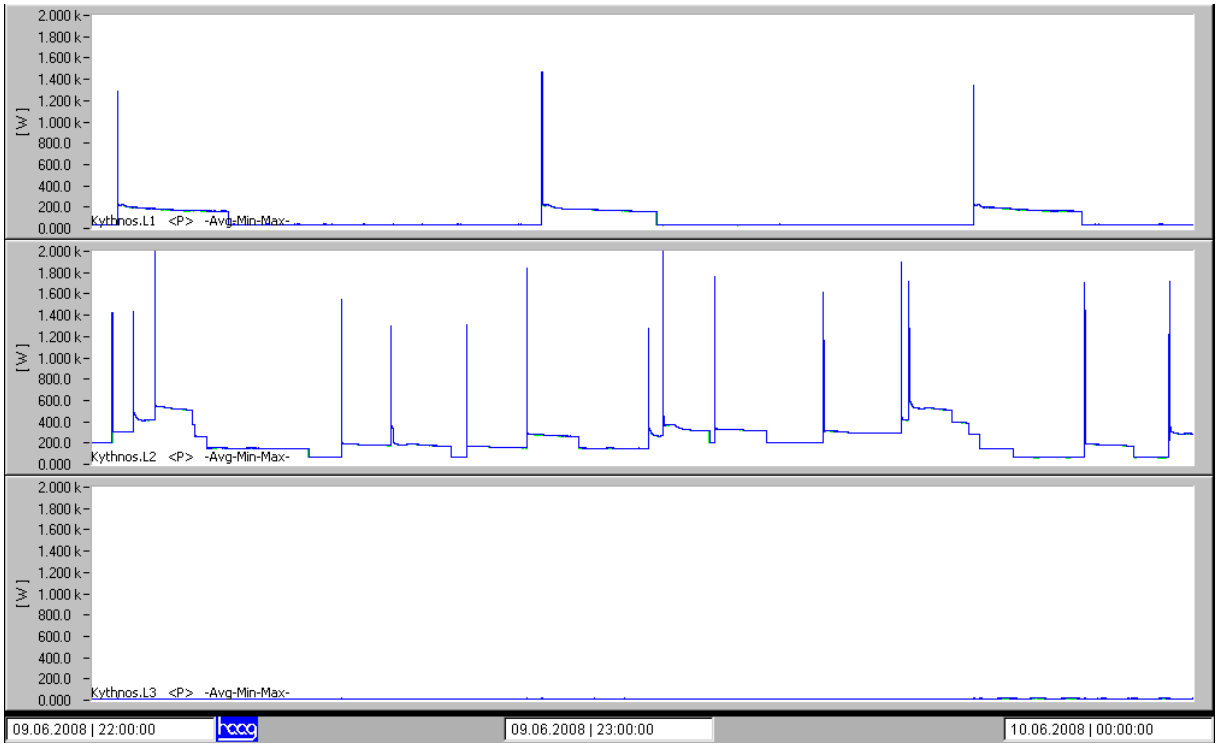

Figure 22: Phase L1, L2, L3 loading: active power by night on 09.06.2008

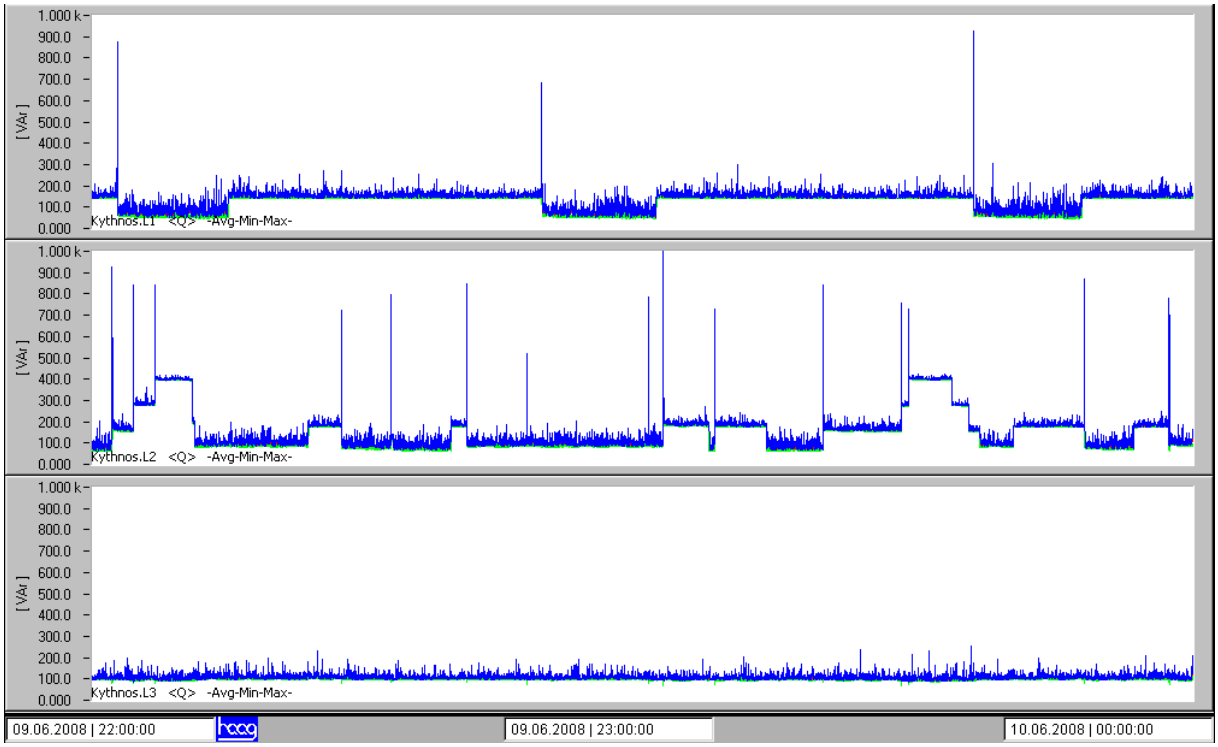

Figure 23: Phase L1, L2, L3 loading: reactive power by night on 09.06.2008

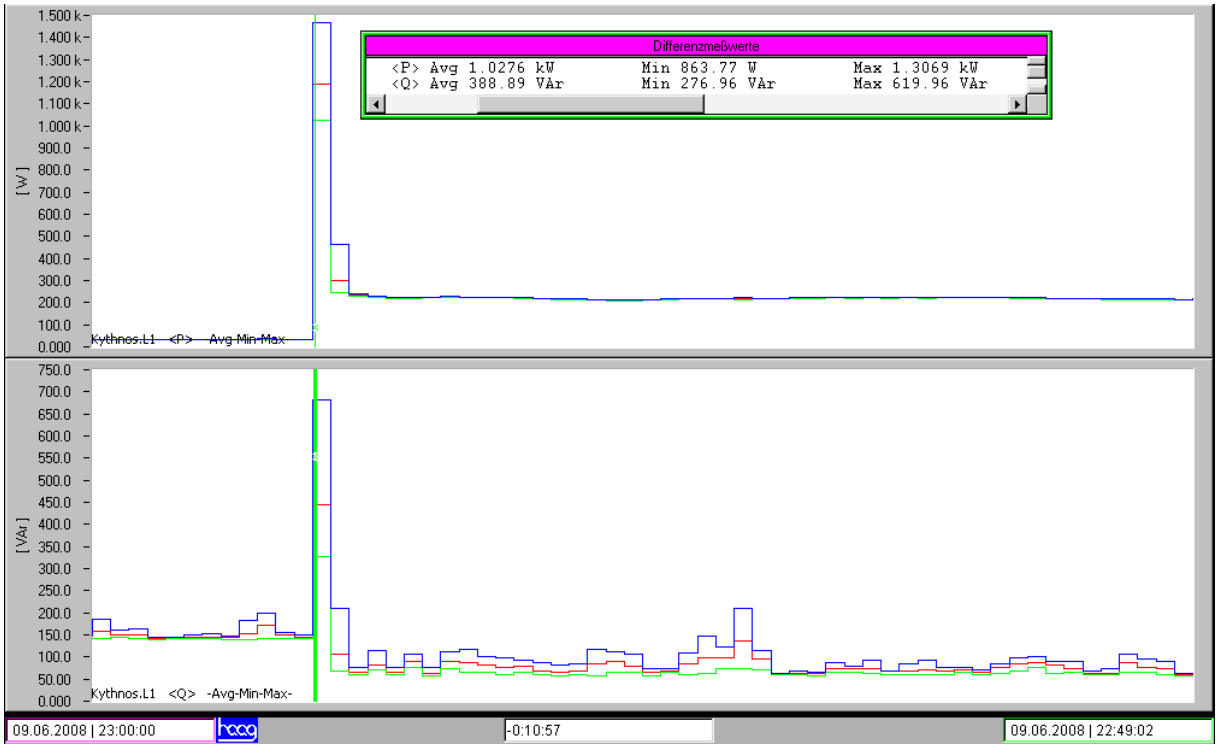

Figure 24: Active and reactive power on L1: transients due to a compressor start

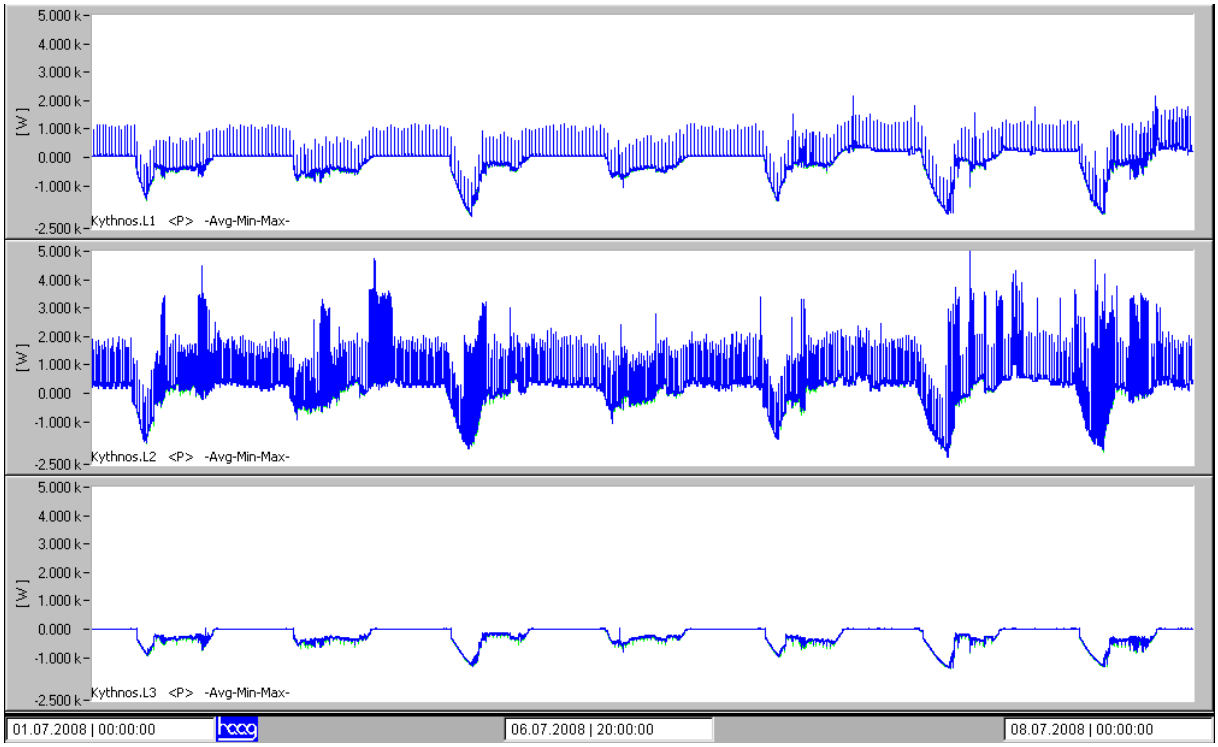

Figure 25: Phase L1, L2, L3 loading: active power during 1 week in july 2008

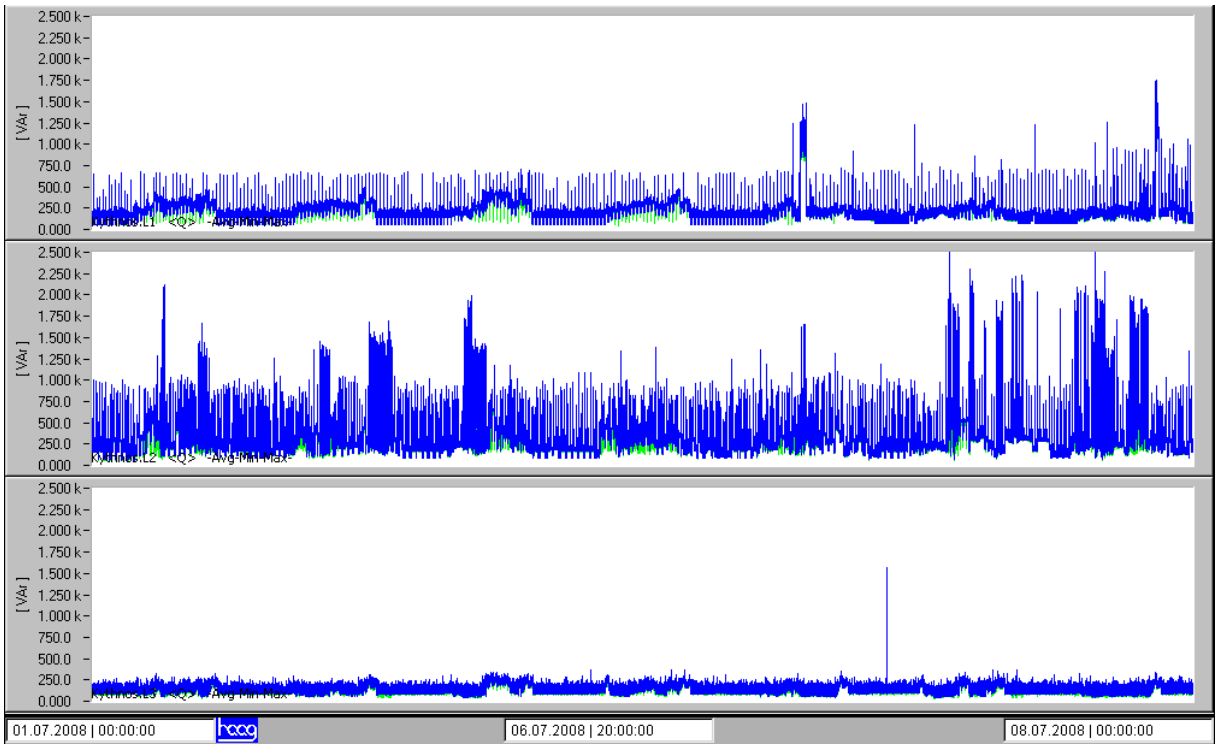

Figure 26: Phase L1, L2, L3 loading: reactive power during 1 week in august 2008

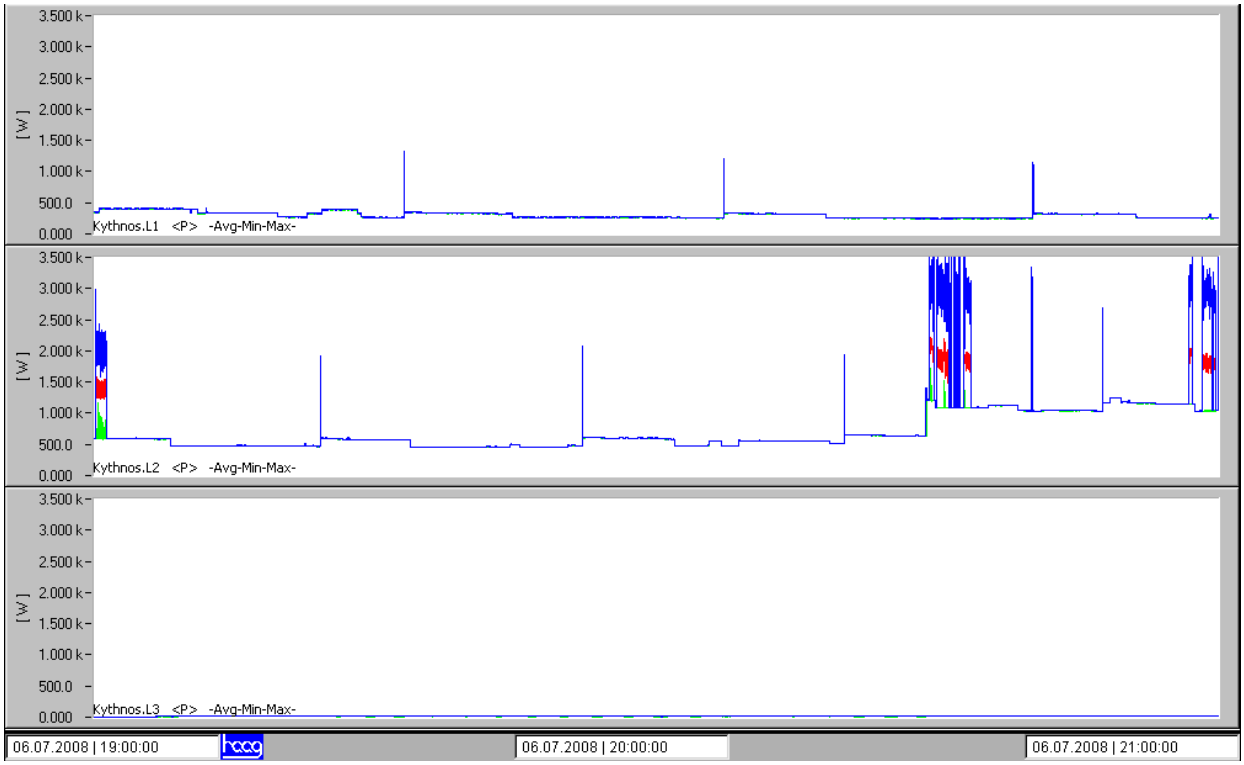

Figure 27: Phase L1, L2, L3 loading: active power in the evening on 06.07.2008

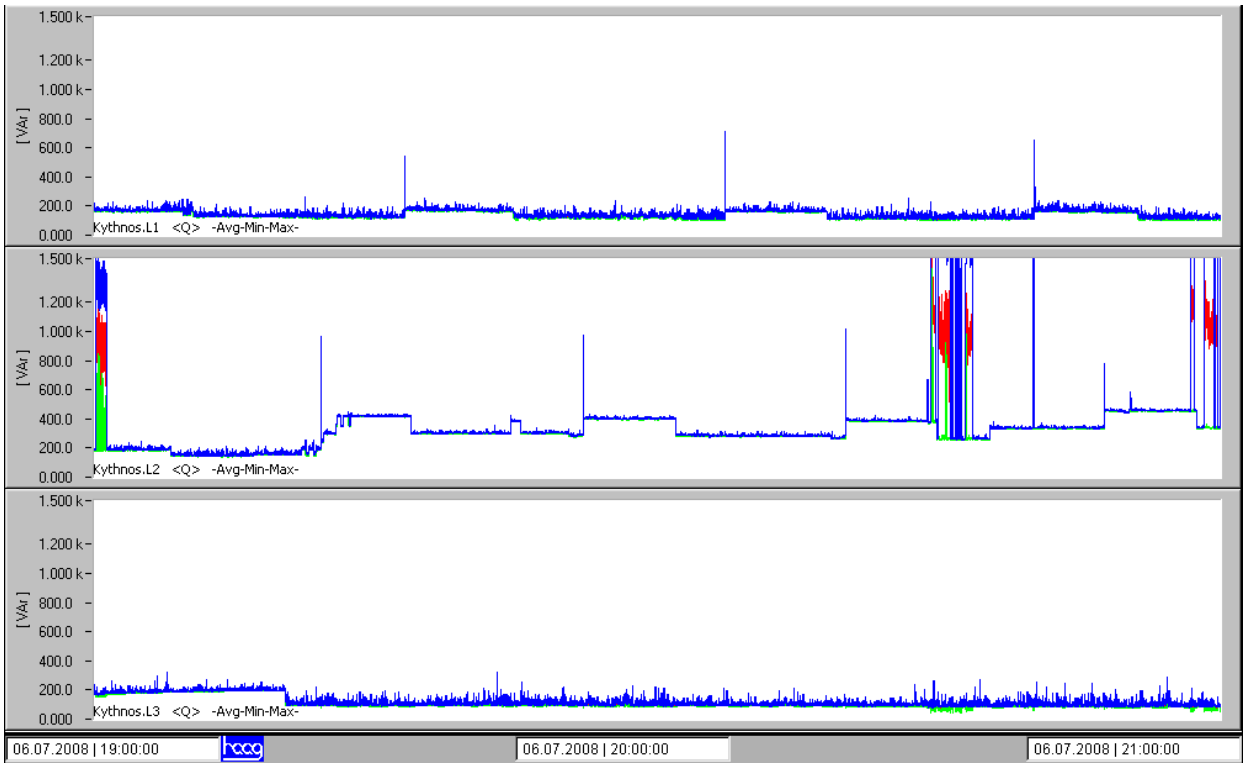

Figure 28: Phase L1, L2, L3 loading: reactive power in the evening on 06.07.2008

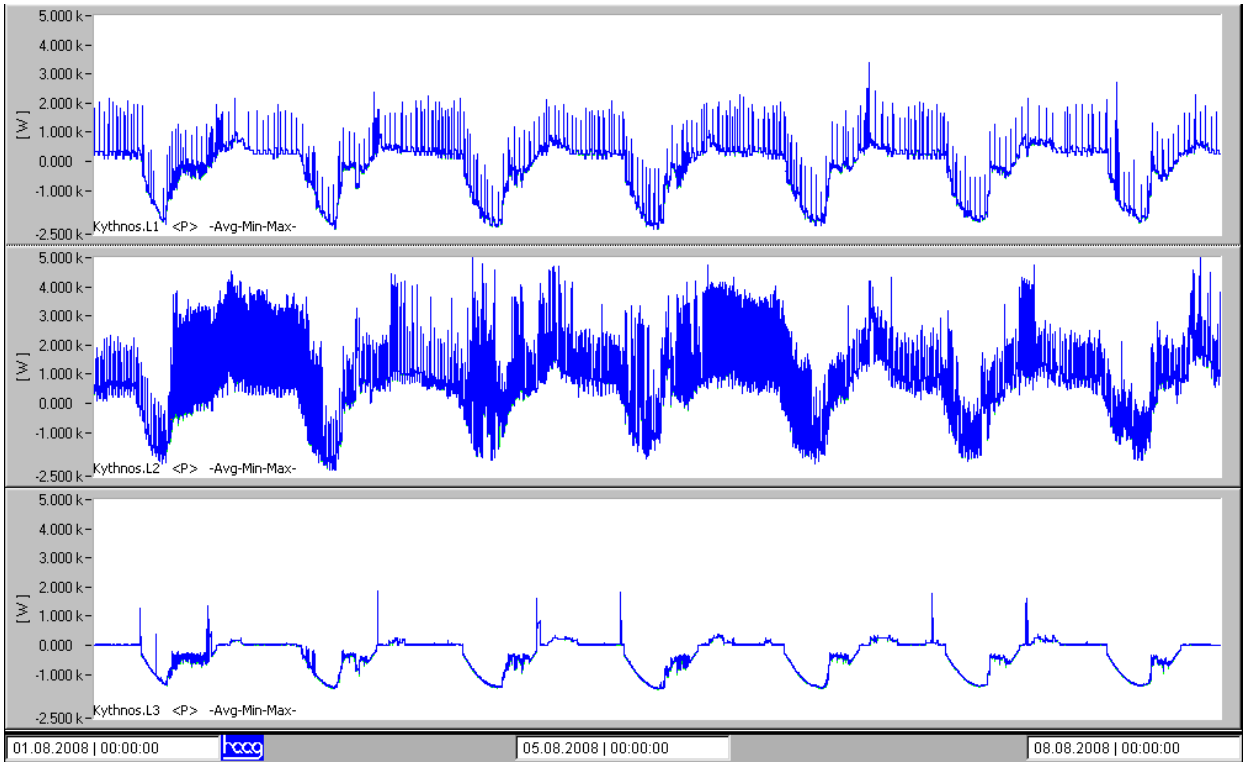

Figure 29: Phase L1, L2, L3 loading: active power during 1 week in august 2008

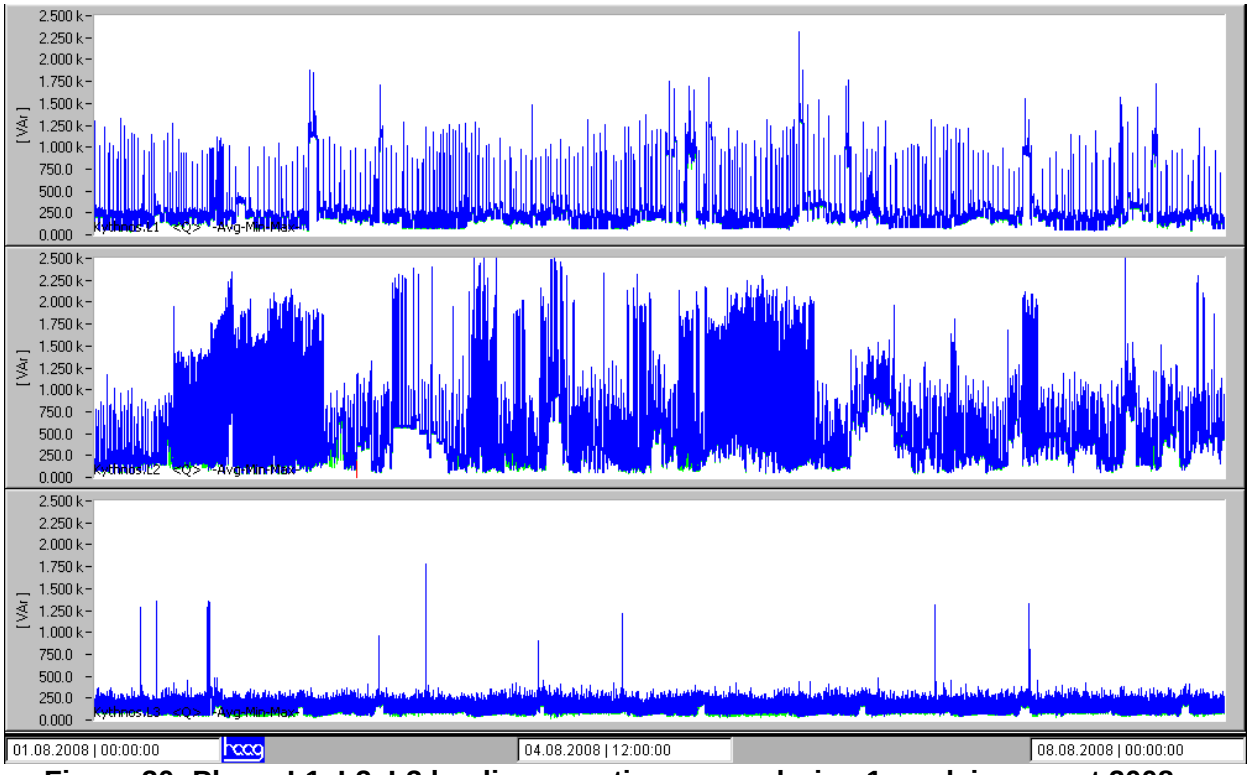

Figure 30: Phase L1, L2, L3 loading: reactive power during 1 week in august 2008

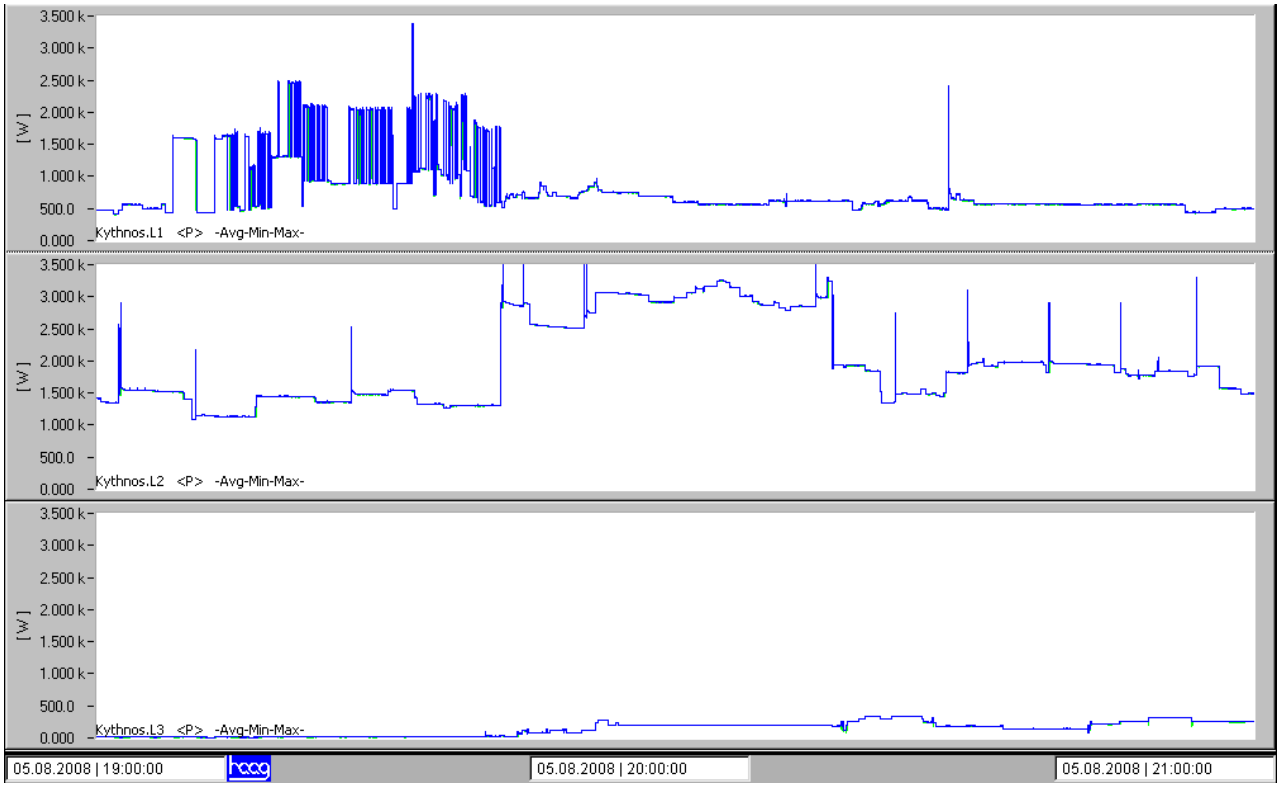

Figure 31: Phase L1, L2, L3 loading: active power in the evening on 05.08.2008

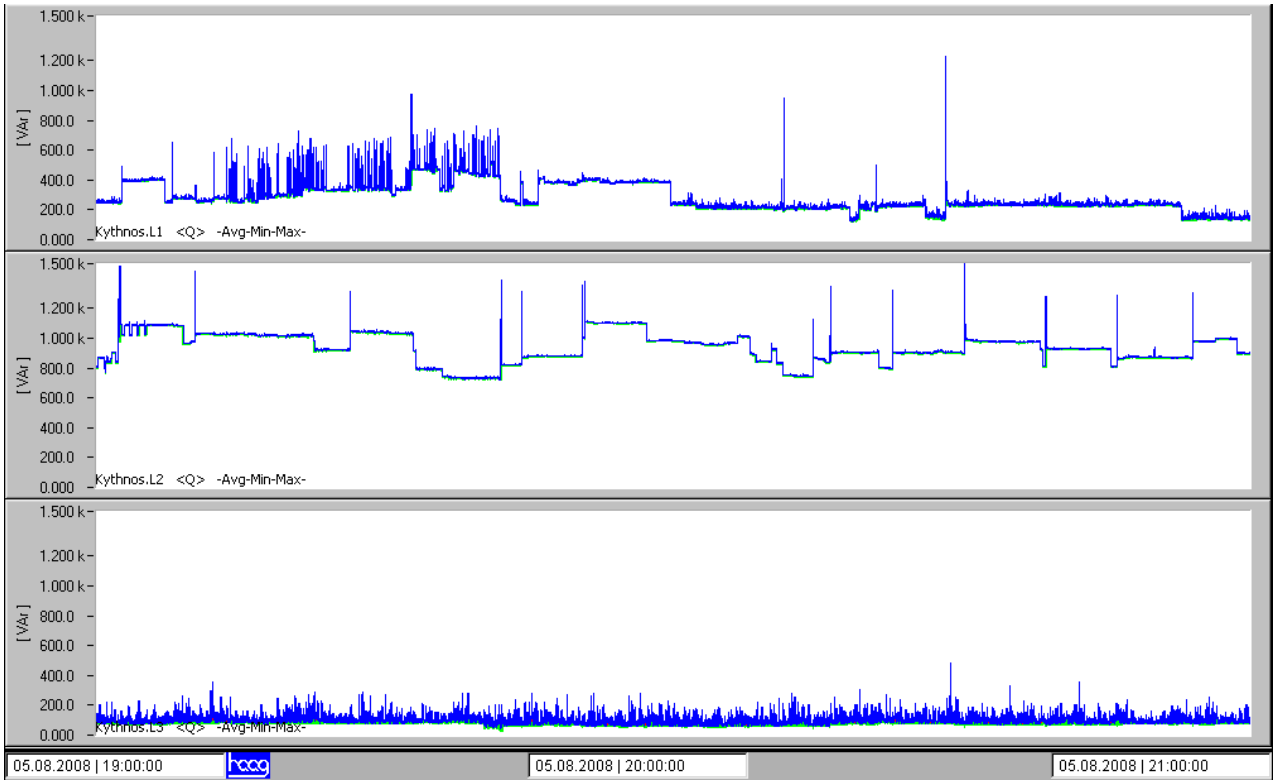

Figure 32: Phase L1, L2, L3 loading: reactive power in the evening on 05.08.2008

9.2. Measuring power quality

Power quality has been evaluated according to standard EN50160 during one week in august 2008. The evaluation report [5] indicates that the following parameters were outside tolerance more often than allowed.

- Grid frequency (18.6% of the time)
- Long term flicker on L1 (14.5% of the time)
- Long term flicker on L2 (51.8% of the time)
- Harmonic U9 on L1 (6.5% of the time)
- Harmonic U6 on L2 (12.6% of the time)

Reasons for these deviations have been investigated. The following explanations could be found:

1. Grid frequency: as the load of the Gaidoroumandra system is not very high compared to the size of the PV fields, the battery has to be protected from being overcharged and the PV power is reduced by not operating the PV inverters at the maximum power point. The derating is proportional to the frequency value above 51 Hz
2. Long term flicker on L2 (Figure 36, Figure 37): The voltage flicker is due to a big load with an active power P=2.5 kW and a reactive power Q=1.6 kVAr, which operates in periods of only 15 minutes. Other smaller loads seem to contribute also to the flicker.
3. Harmonic U9 on L1 (Figure 33, Figure 34) is above threshold due to a cyclic load, which is probably a cooling compressor with an active power P=150W and a reactive power Q=130 VAR
4. Harmonic U6 on L2 (Figure 35) is above the limit, when the PV inverters are operating in de-rating mode.

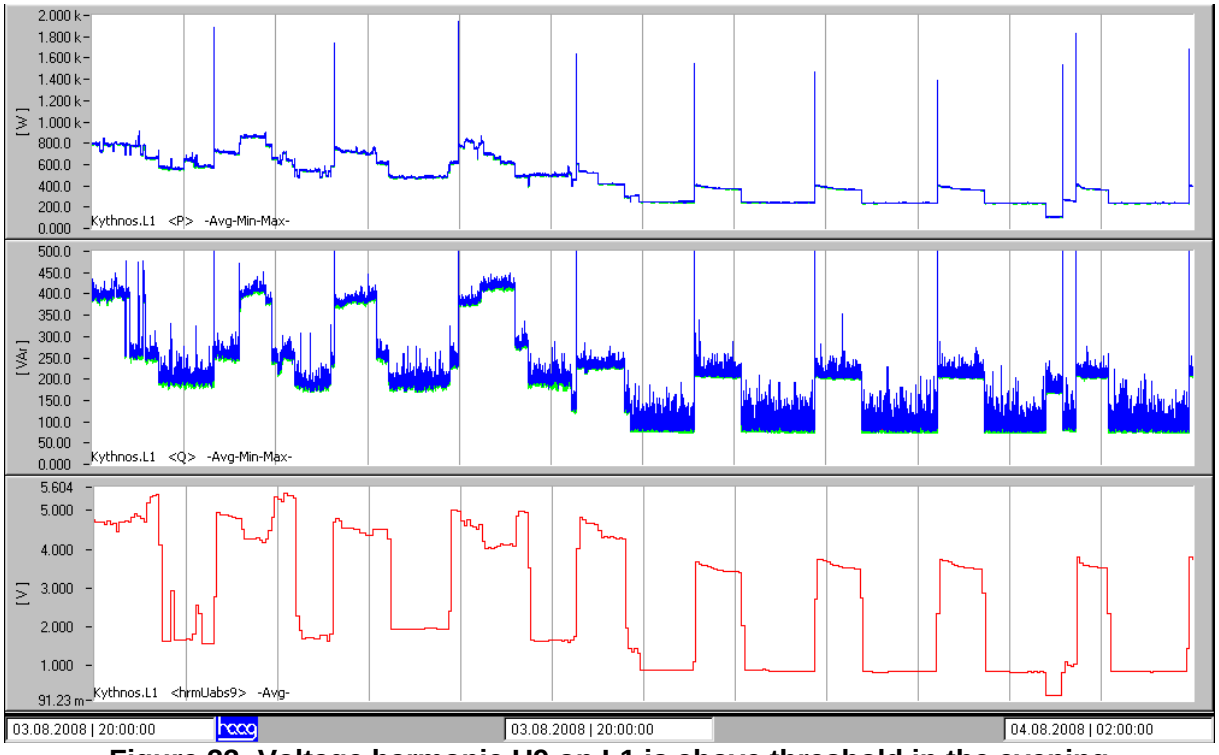

Figure 33: Voltage harmonic U9 on L1 is above threshold in the evening

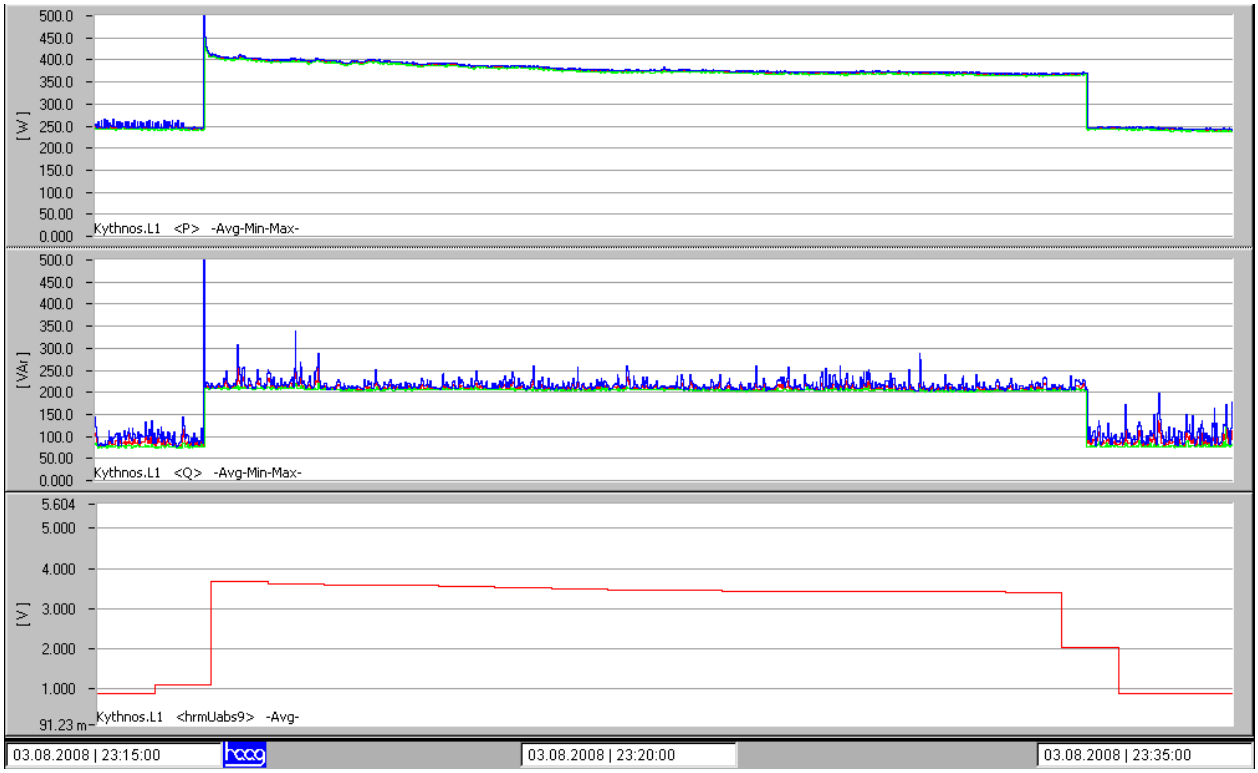

Figure 34: Voltage harmonic U9 on L1 is above threshold due to a cyclic load (probably a compressor with P=150W and Q=130 VAR)

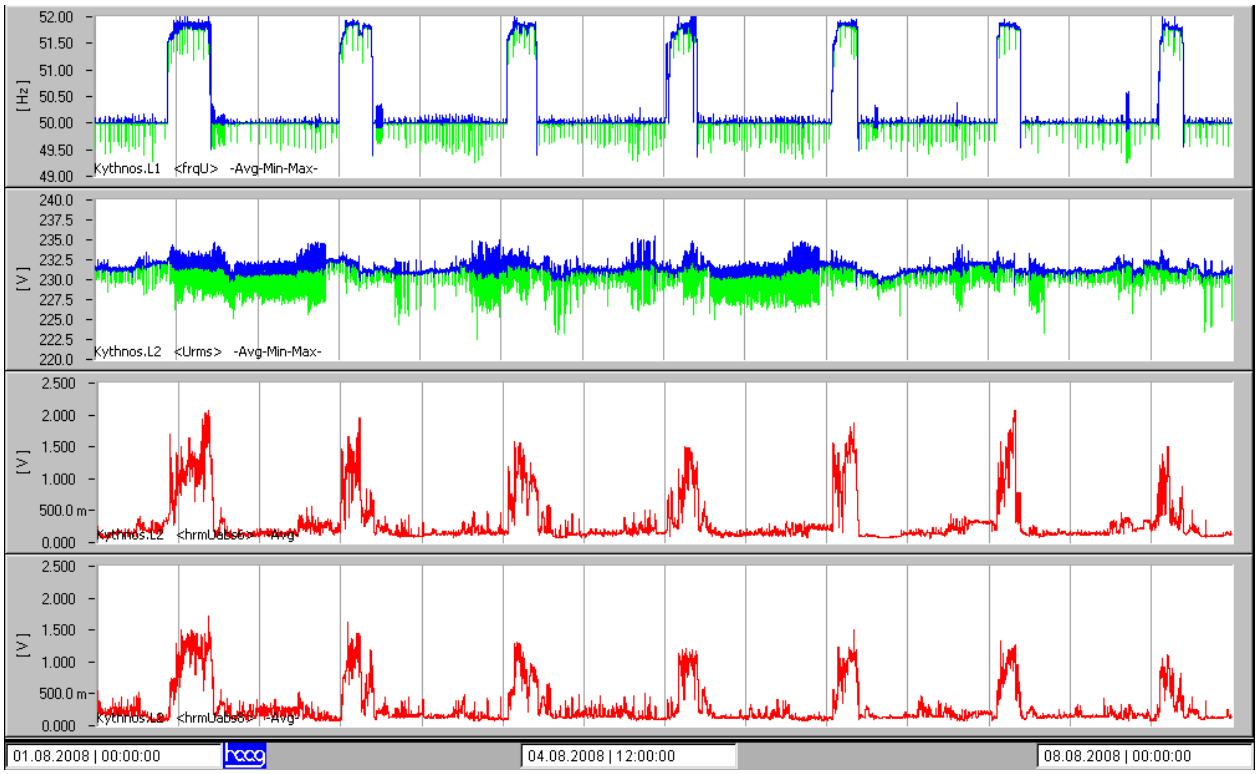

Figure 35: Voltage harmonics U6 (and U8) on L2 is above the limit, while the PV inverters are operating in de-rating mode

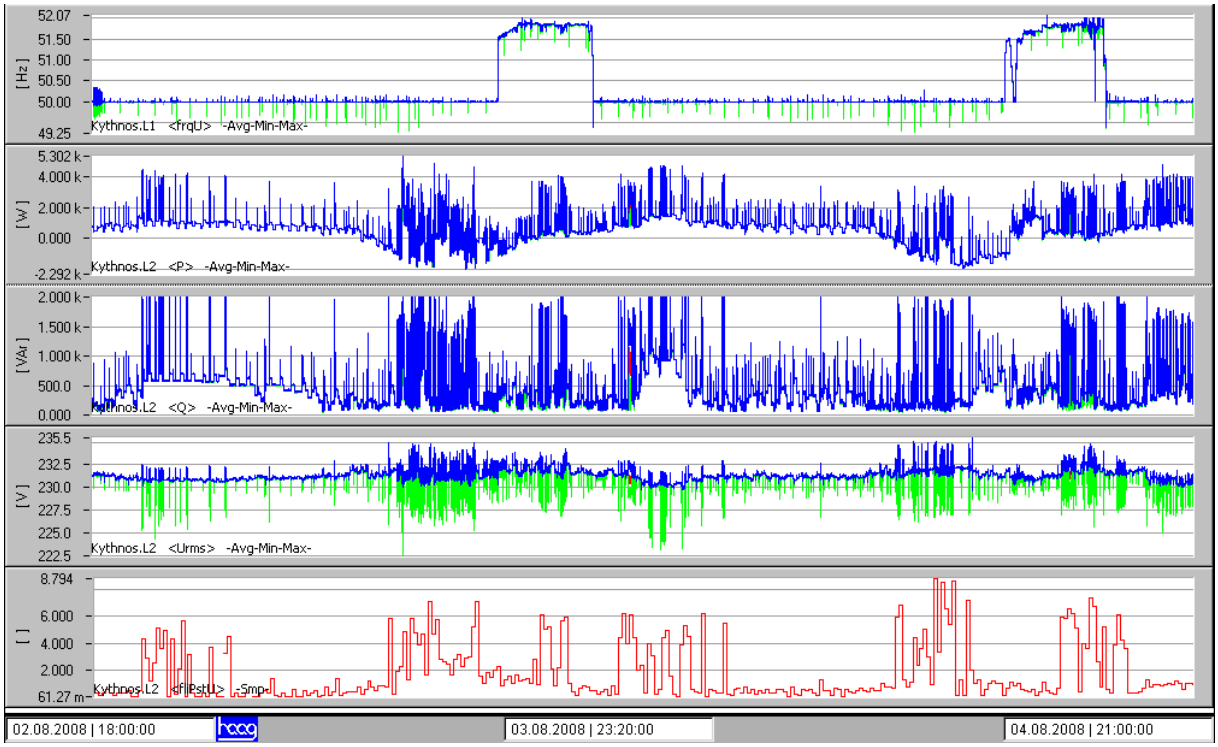

Figure 36: The flicker intensity (in red) on L2 is above the limit

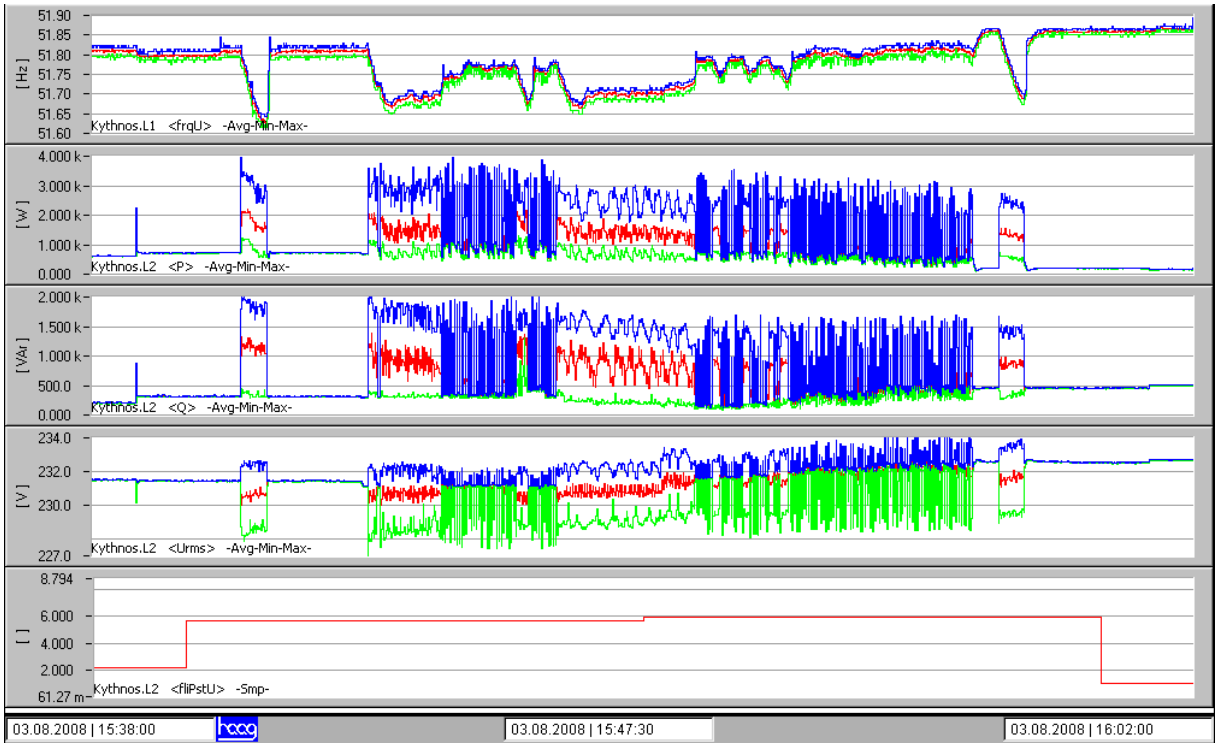

Figure 37: Voltage flicker on L2 is created by the operation of a big load (P=2.5 kW, Q=1.6 kVAr)

The precise power quality logger is measuring at only one point in the minigrid and does not provide indications about the power quality at the end of the minigrid lines.
Using the AC voltage measurement of each distributed PV inverter, it is however possible to roughly check the power quality in the minigrid. In the Figure 39, after the diesel generator was started, a serious voltage drop occurs. The AC voltages at every house were always higher than at the system house due to the PV power injection especially the AC voltages at the house number 8 and 10 (with SB 2500 inverter). However, clearly, all the voltage increases linked to PV injection were still in the acceptable range of +10% and -15% (195.5.5-253 Volts).

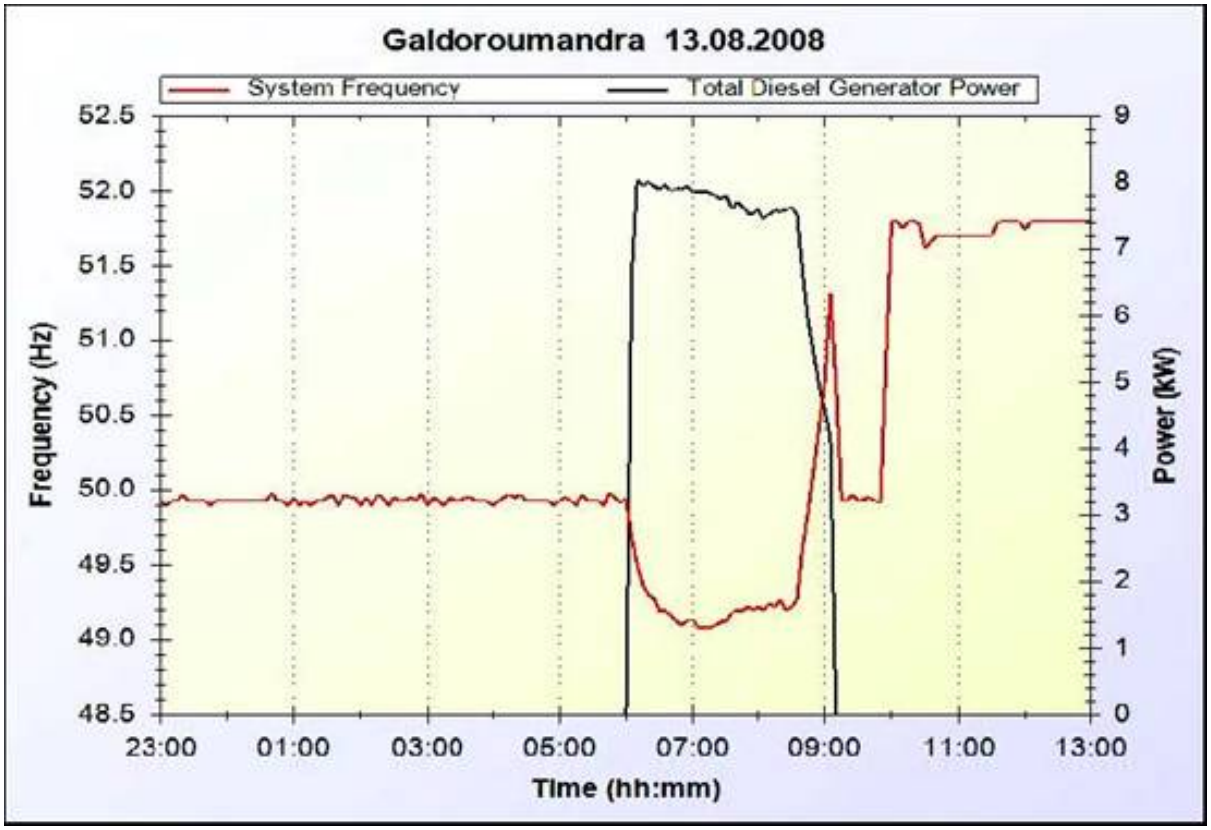

Figure 38: Grid frequency and diesel power on the 13.08.2008

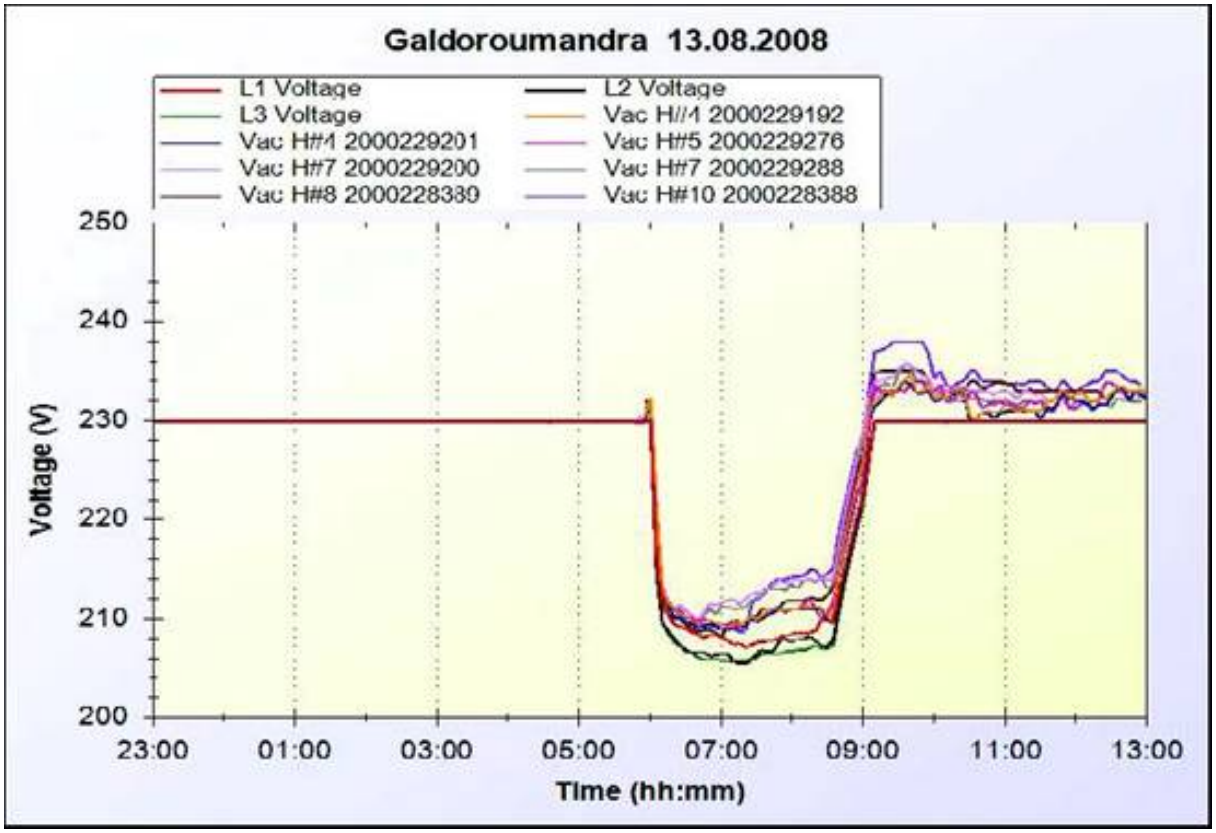

Figure 39: Voltage fluctuations in different points of the minigrid on the 13.08.2008

9.3. System performance

In this section, daily parameters calculated by using the data of Gaidouromandra minigrid on the period 1-31 August 2008 had been analyzed, using data from the webbox. Not all data (with 5 minutes timestamp) were available. In the daily plots, the circles on some data represent the data missing more than 12 times on that day.

9.3.1. Energy used in the system

The Figure 40 indicates that the amount of energy to the load in the first two weeks of august 2008 was relatively high (over 30 kWh per day). Then it was decreasing gradually in the last two weeks to be around 10 – 20 kWh a day.

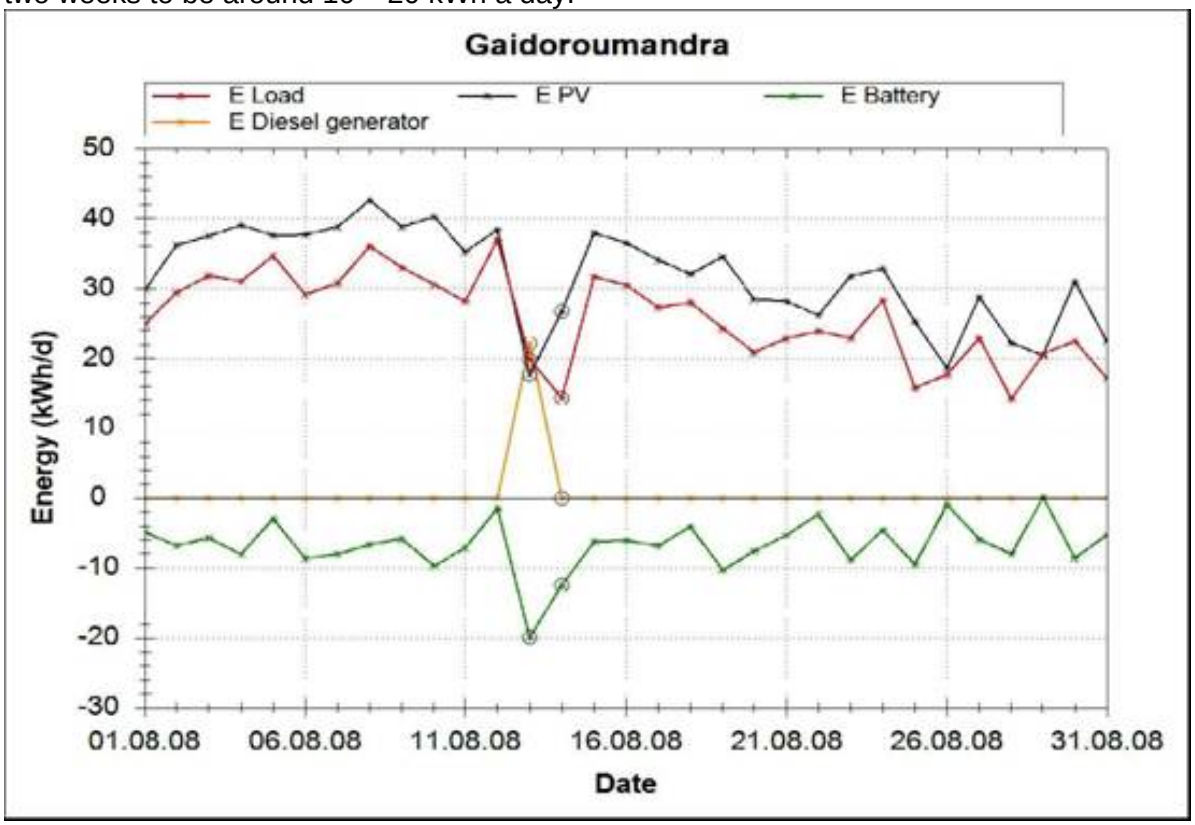

Figure 40: Daily energy production in august 2008

Remarkably, the energy generation in the system was mainly from the PV fields and battery while the diesel generator was used only on 13.08.2008 for 3 hours. The highest load in this month was on 12.08.2008 with 37 kWh. Unfortunately, the minimum load of the month cannot be calculated due to data missing on 13.08.2008 and 14.08.2008. This is the reason why on these 2 days the energy to the load and energy produced from PV seemed to be the lowest of the month.
The negative values of battery energy represented that the charging energy was more than the discharging energy (charging energy is negative, discharging is positive). Around 5 -10 kWh had to flow daily into battery as battery losses and battery loading. Since the morning state of charge of the battery in the system was changing everyday, the daily battery losses cannot be calculated precisely. Only the summation of the battery losses and battery loading can be calculated. We assume however for the calculation of the performance indicators that the impact is not significant.

9.3.2. Performance Ratio

In August 2008, the daily performance ratio was diversely from 0.2 – 0.6. The highest performance ratio was on 12.08.2008 when the peak load occurred and the lowest PR was on 13.08.2003 when the diesel generator was operated. As already mentioned, the performance ratio represents how the potential energy of the PV system is used. The higher

the performance ratio is, the better the system uses its potential. The Figure 41 shows that the less hours of frequency over 51 Hz occurred, the higher PR was calculated and vice versa. In Gaidoroumandra system, to protect overcharging battery, the system frequency was used to communicate and control the PV field production. Consequently, when the battery was full, the PV fields did not operate at the maximum power point (The PV inverter is in de-rating mode). The less hours of frequency over 51 Hz happen, the longer the PV work with maximum power point which leads to the higher performance ratio and the system can use more energy as it has higher capacity to produce more energy.

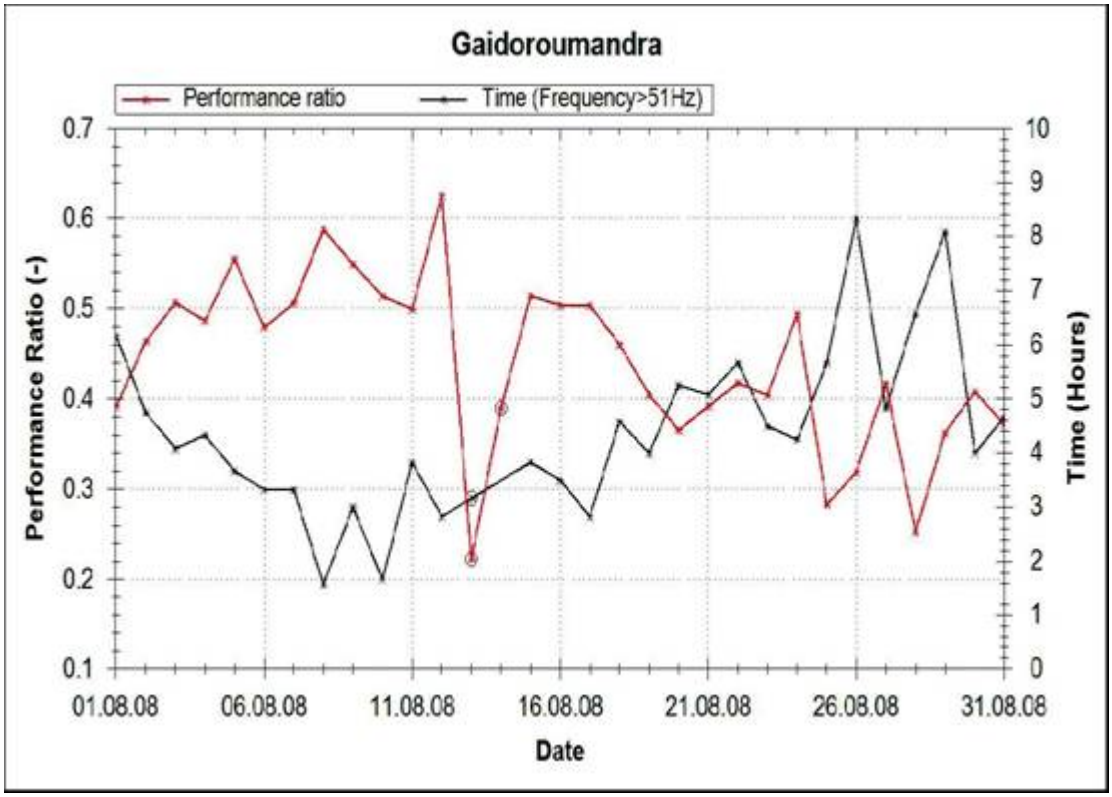

Figure 41: performance ratio and time duration with frequency over 51 Hz

9.3.3. System Losses, Capture losses

In the Figure 42, the system losses were around 1 kWh/kWp per day while the capture losses were around 2-4 kWh/kWp per day except the day when there were data missing. Compared to the final yield and system losses, the capture losses were relatively high. The reason why the capture losses were quite high is shown in the Figure 43. The longer the frequency over 51 Hz, the higher are the capture losses. It should be noted that the capture losses include the losses from de-rated power. As already mentioned, the grid frequency is increased in order to avoid overcharging the battery. Thus, the capture losses (or the de-rated power in the system) could be decreased if there would be more load.

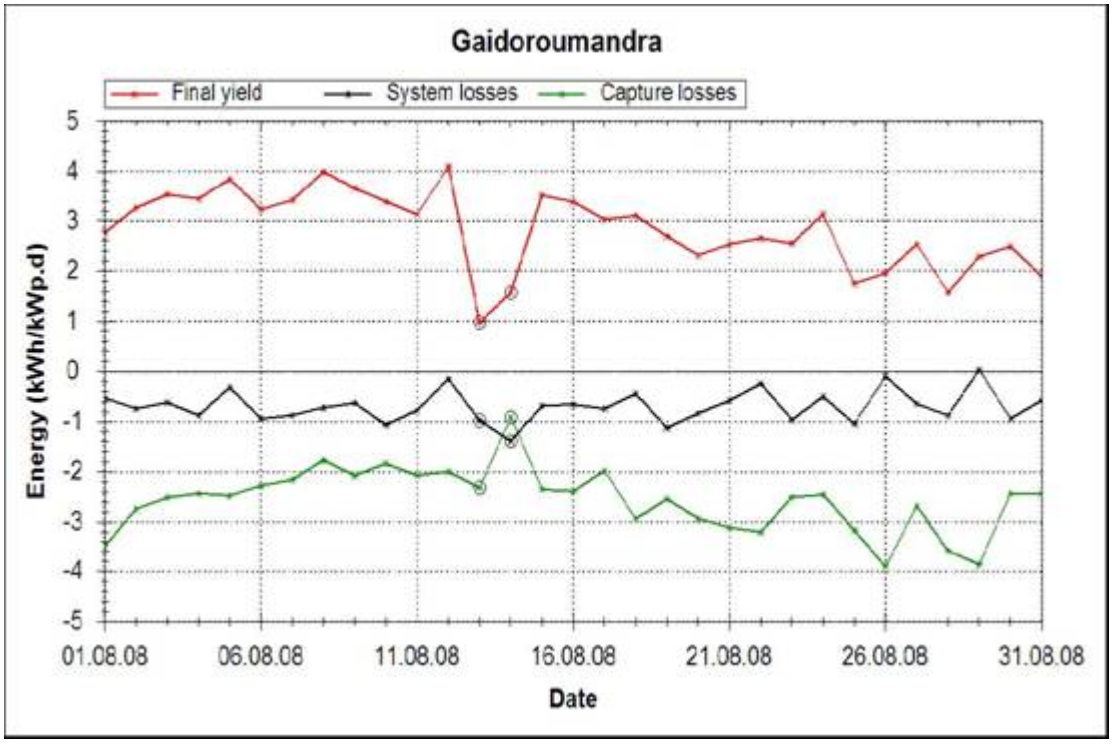

Figure 42: The daily final yield, system losses, and capture losses in August 2008

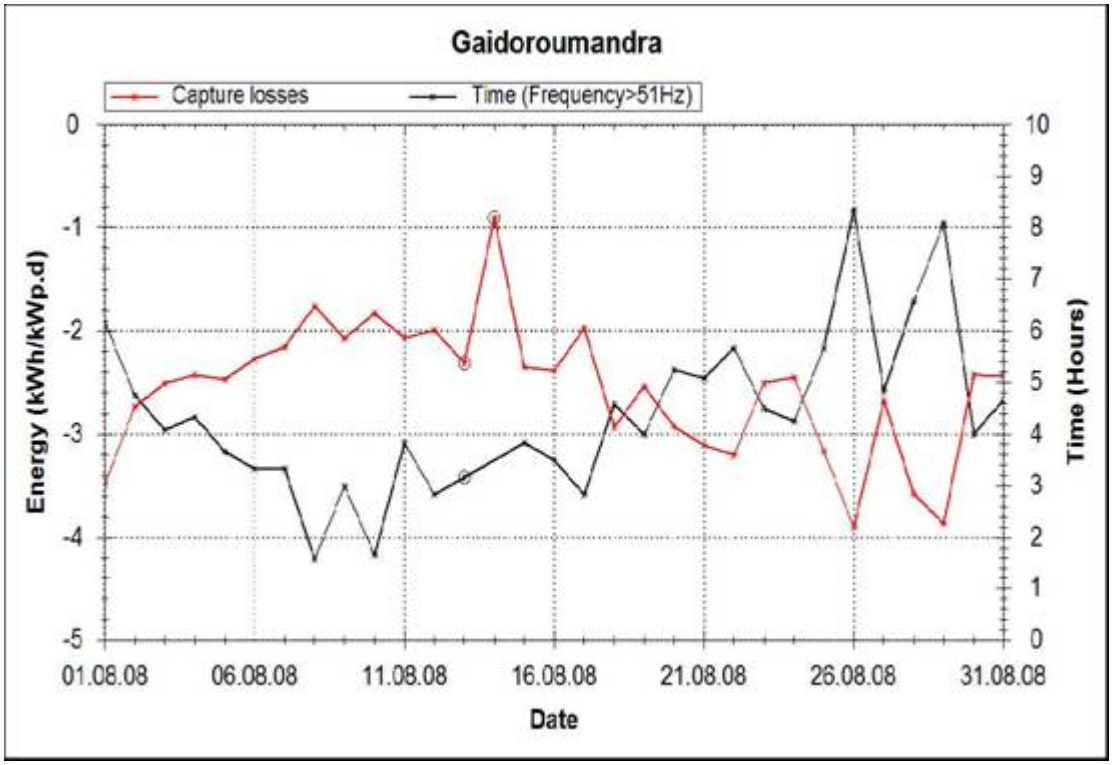

Figure 43: Capture losses and time duration with frequency over 51 Hz

9.3.4. PV inverter efficiency

There are 2 types of PV inverters in Gaidouromandra minigrid:

- Sunny Boy 1100 inverter which is installed at the house number 4 (Serial no. 2000229192, 2000229201),at the house number 5 (Serial no. 2000229276), and at the house7 (Serial no. 2000229200, 2000229288)
- Sunny Boy 2500 inverter which is installed at the house number 8 (Serial no. 2000228389) and at the house number 10 (Serial no. 2000229288)

Daily efficiencies of the PV inverters in August 2008 are plotted in Figure 44.

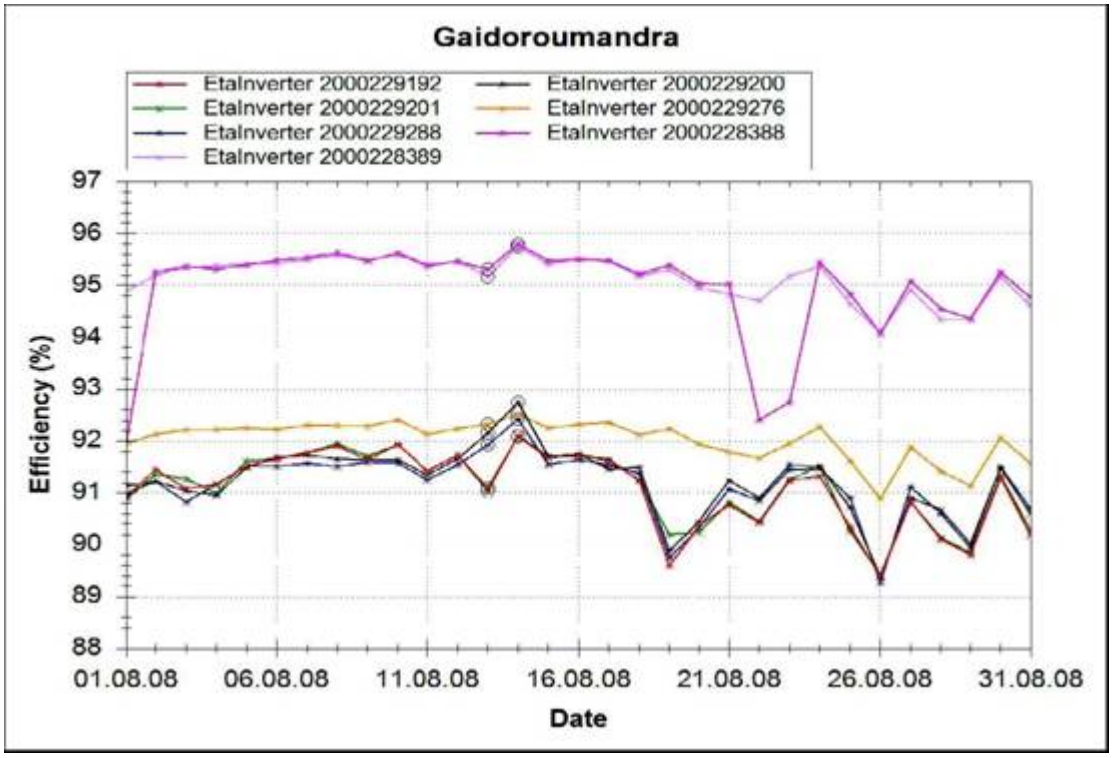

Figure 44: Daily efficiencies of PV inverters in August 2008

Obviously, the PV efficiency curves were separated into two main groups. The upper two curves were the efficiency curves of PV Inverter Sunny Boy 2500 which had approximately 95% daily efficiency. Another group was the efficiency curves of PV inverter Sunny Boy 1100 which had roughly 91% daily efficiency.
Noticeably, the 2000229276 PV inverter (Sunny Boy 1100) installed with 1.160 kW peak PV field had approximately 92 % daily inverter efficiency while the other Sunny boy 1100 inverters worked with 0.928 kW peak installed PV fields and had a lower efficiency (91%).
Although all PV inverters have the same rated power and react on the same grid frequency signal for the de-rating, they do not produce the same AC power (Figure 45). Differences are due to different tilt and azimuth angles for the PV fields, to different PV field installed power.

The PV efficiency of the PV inverter serial number 2000229200 was less than the other installed at the same house (house number 7). In the Figure 46, the DC power produced from the PV field with inverter's serial number 2000229200 was less than the DC power produced from that of 2000229288 during 8.00-11.00. The peak power produced from the first PV was around 600 W while the latter was about 750 W although they should produce the same amount of power.

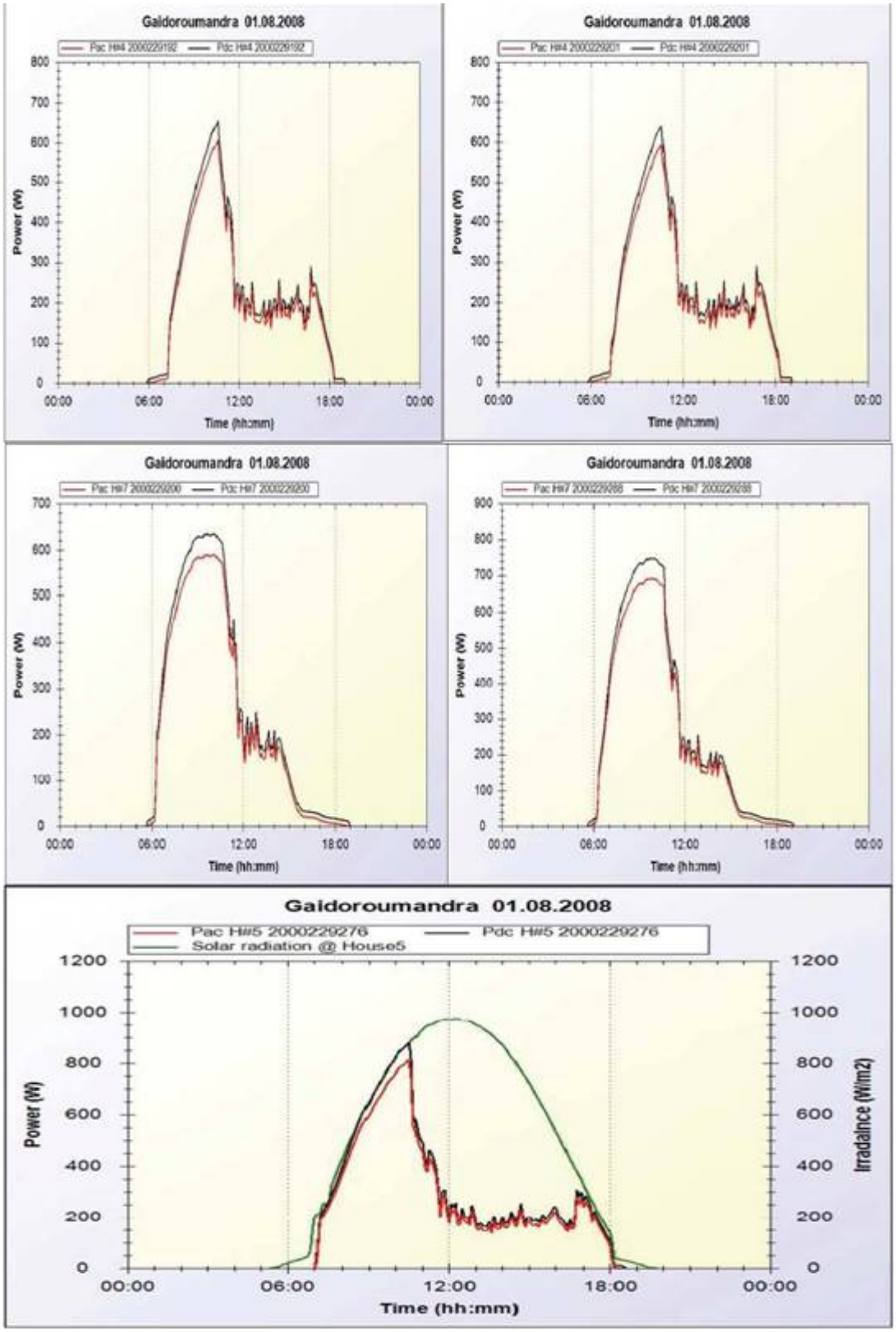

Figure 45: AC and DC power production of PV inverters (SB1100) on the 01.08.2008

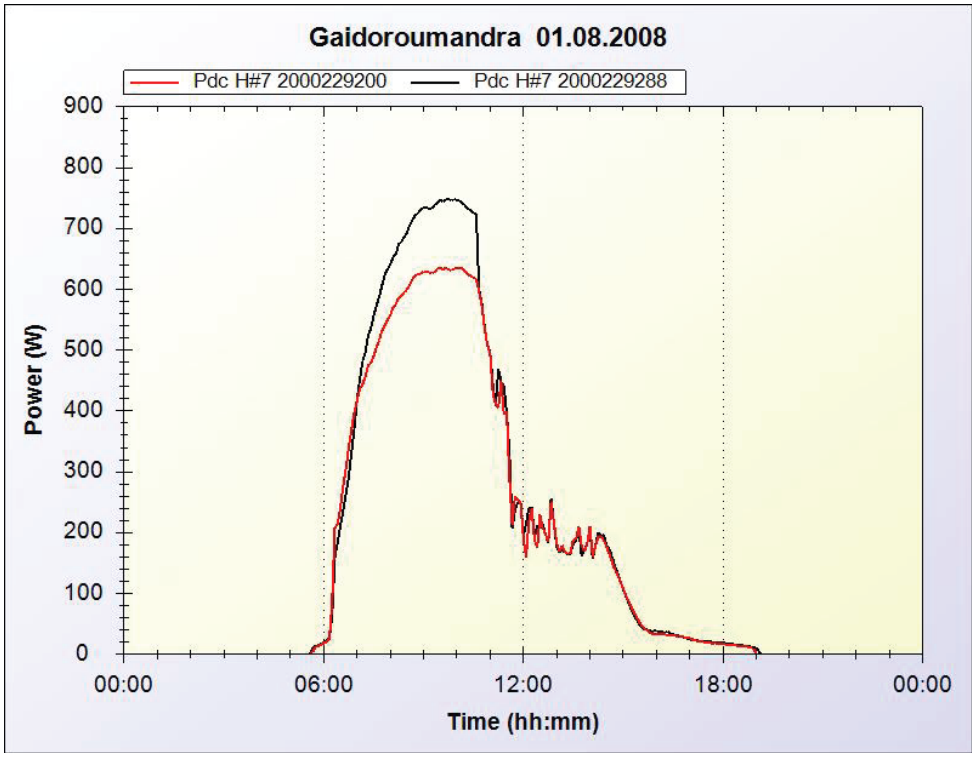

Figure 46: The DC power of the two PV fields installed near house 7 on 1.08.2008

9.3.5. Daily energy flow

The daily energy flow can be separated into two groups:

- Energy flow without the diesel generator operating as in the Figure 47.
- Energy flow with the diesel generator operating as in the Figure 48.

The Figure 47 represents the energetic performance of the Gaidouromandra minigrid on the 1.08.2008. At this day, the diesel generator was not operated. The energy captured by the PV compared to the reference yield was only 50.7%. The rest was capture losses which was around 49.3%. The performance ratio of the system was 39.2%. The amount of 16.7% of the reference yield has been provided directly from the PV fields to the load which was around 42% of the total energy to the load while the rest was provided by the battery. Around 33% of the PV energy was sent to the load, about 60% was sent to charge the battery and 7 % was the PV inverter losses on that day. The summation of the capture losses (49%) and PV inverter losses (4%) was around 53%. The total losses in the system cannot be calculated since the battery losses were tied to the battery loading.

To calculate energy flow in the system when the diesel generator was operated, the assumption is if the energy produced from PVs is as same amount as the energy from the diesel generator, then the same amount of energy from PVs and the diesel generator will be sent to the load. In other word, the energy to the load will be proportional to its input energy.

In the Figure 48, the energy flow on 13 August 2008 is presented. As we can see, on this day, the diesel generator was operated and produced approximately 35.7% of the total energy (=sum of reference yield and diesel energy). The PVs provided 30.5 % while 33.8 % was capture losses. At the PV side, there were 3 energy flows out of the PV; PV energy to the load, PV energy to charge the battery and the PV inverter losses which was around 7.4%, 21% and 2% of the reference yield or was around 24 %, 69% and 7% of the PVs energy relatively. At the load side, there were 3 sources of energy to the load; from PVs, diesel generator, and battery which were 7.4%, 9.3% and15.4% of the total energy from reference yield and diesel energy or 23%, 29% and 48 % of the total energy to the load relatively. About the energy produced from the diesel generator, 26% of diesel energy flew directly to the load while 74% flew to charge the battery in the system.

The summation of the capture losses (33.8%) and PV inverter losses (2%) was 35.8%. It is to be mentioned that the total losses in the system cannot be exactly calculated since the battery losses were tied to the battery loading.

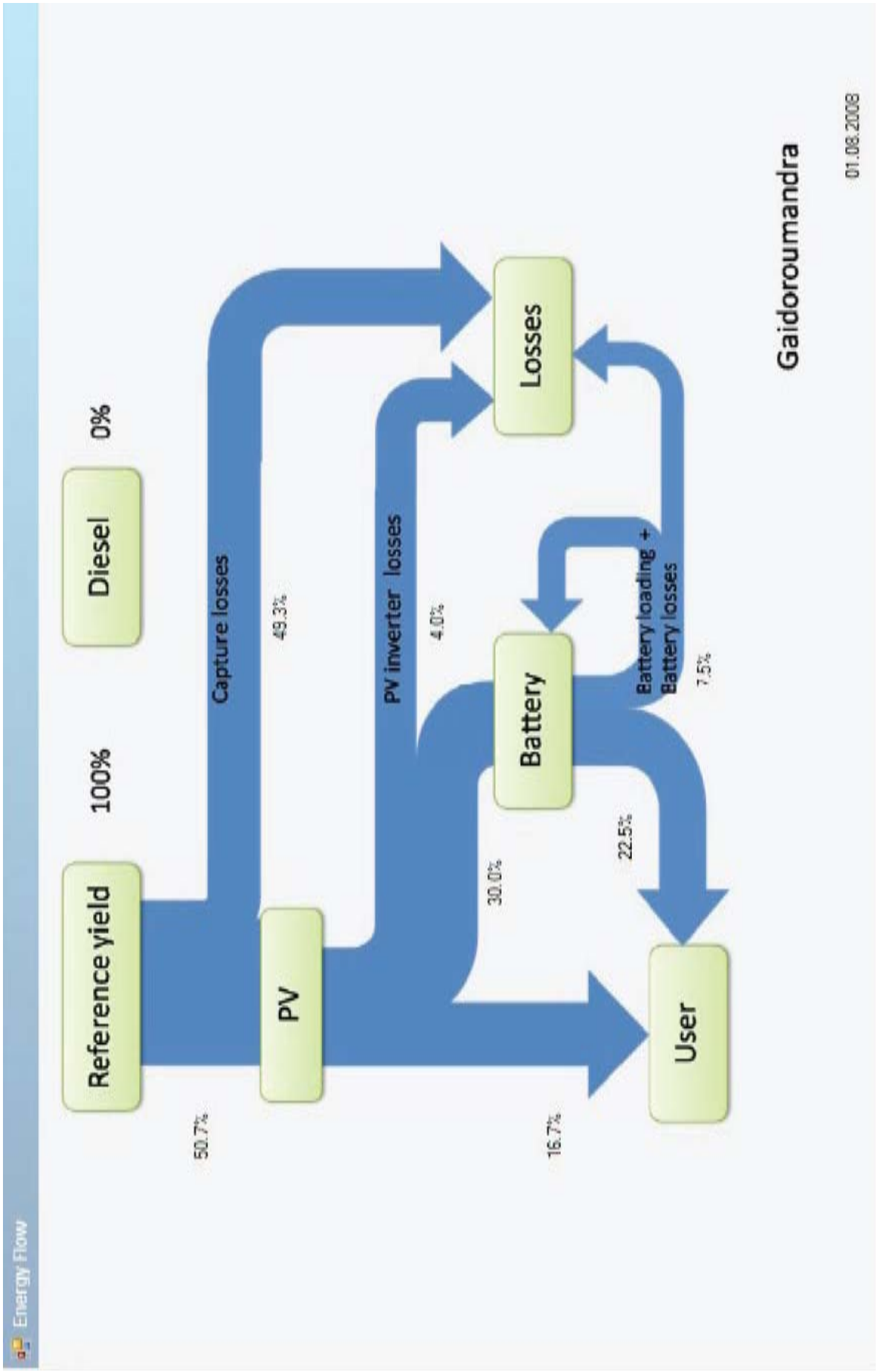

Figure 47: Energy flow diagram in the Gaidoroumandra minigrid without diesel generator on 1.08.2008

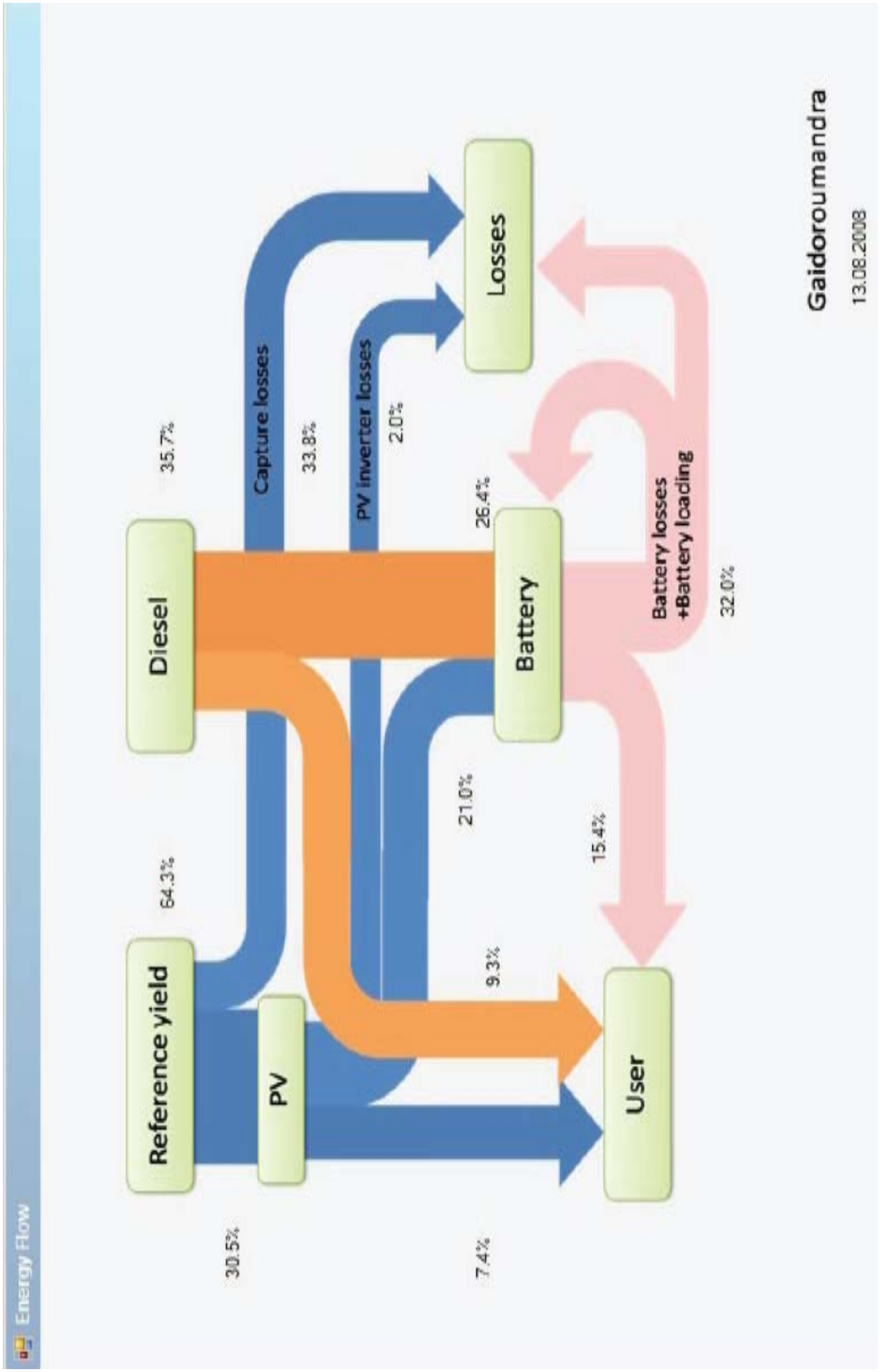

Figure 48: Energy flow diagram in the Gaidoroumandra minigrid with diesel generator on 13.08.2008

9.3.6. System frequency, battery SOC and battery voltage

In the Figure 49 and Figure 50, the system frequency was increased at 15:15 from 50 Hz to be over 51 Hz while the SOC was increasing over 90% and the battery voltage was increasing to its maximum battery voltage (57.6 Volts). As already mentioned, the grid frequency variation is applied to the system in order to control the battery charging. Compared to the 2004 plots, it can be seen that the new Sunny Island battery inverters operate differently. As far as no PV de-rating is necessary, the grid frequency is now kept constant at about 50 Hz. The grid frequency variation operates only to avoid overcharging the battery.

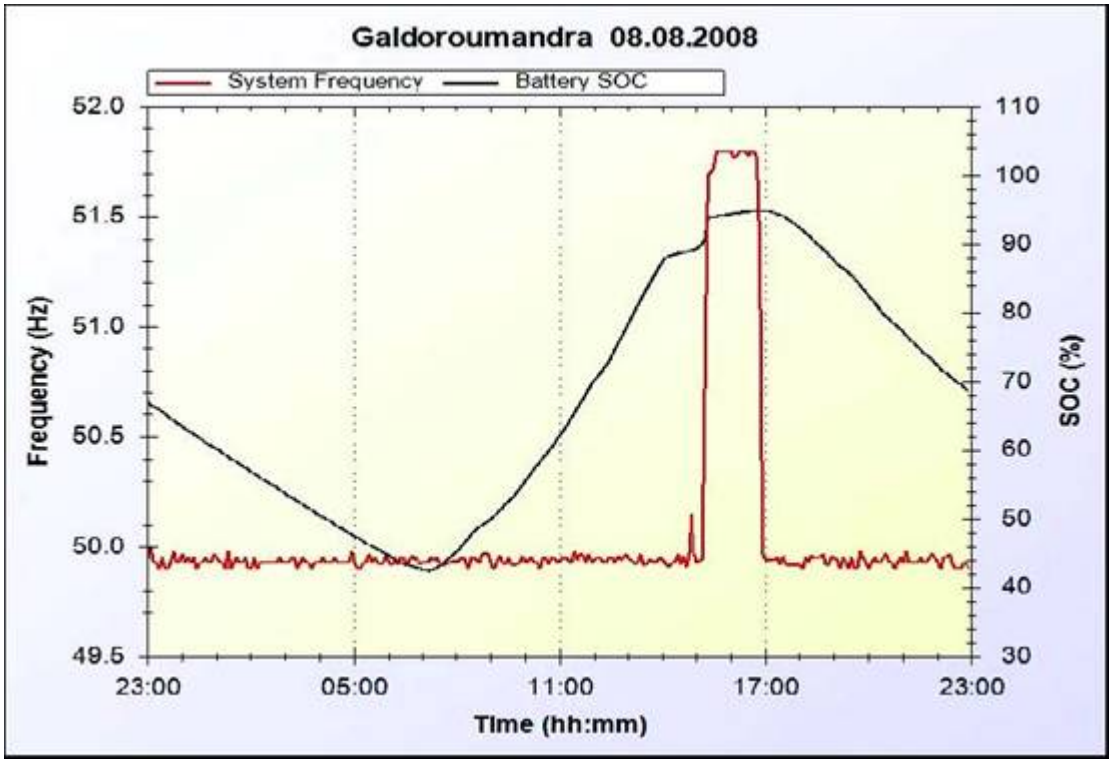

Figure 49: The system frequency vs. Battery state of charge on 8.08.2008

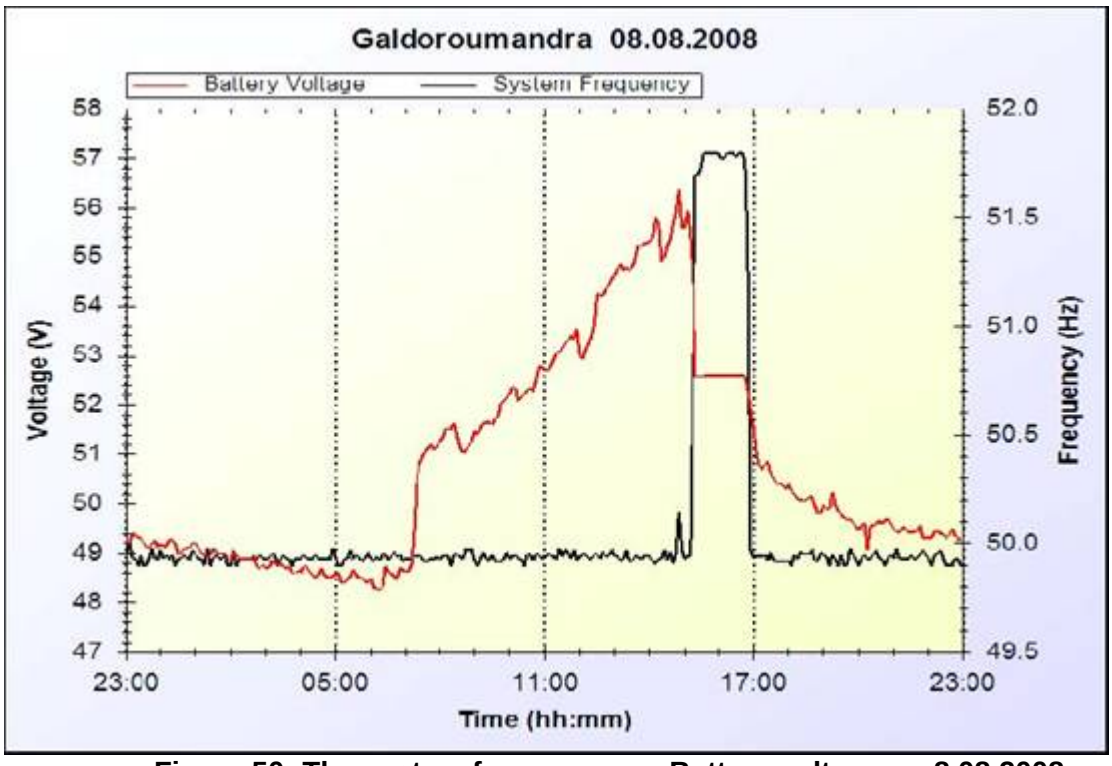

Figure 50: The system frequency vs. Battery voltage on 8.08.2008

10. Conclusions

10.1. Monitoring system re-design

Within the frame of the MMG project, the monitoring system has been upgraded by the addition of the WEBBOX which centralizes all data from SMA components, of the power quality analyzer HAAG, of a local communication network allowing easy integration of additional components (as the load management PC from NTUA) and of a new GPRS link. The final modifications took place in the first week of june 2008, so that the new system was fully operational for summer 2008 season.

10.2. Performance evaluation software

For the evaluation of the performance of the Gaidouromandra minigrid, a software tool based on Visual Basic language had been written and used to analyze the system. The program is able to read daily data files in Comma Separated Values (CSV) format provided by WEBBOX monitoring from SMA and calculate hourly and daily variation of parameters. The software can also roughly examine the system's power quality and data integrity of each daily data point sent by WEBBOX. Moreover, the software can analyze the data and present the results in 3 formats; 1)In text boxes of the software 2) In graphs 3) In CSV files.

10.3. Re-analysis of 2004 data

Upon request from project partners, data from summer 2004 has been made available. This data can be used to evaluate the load evolution and the different management strategies between the first and second generation of battery inverters.

10.4. Energy performance in august 2008

Using the software to analyze one-month of data for the Gaidoromandra minigrid from the beginning to end of August 2008, it was found that the overall performances of the Gaidouromandra minigrid system were acceptable but some points could be improved.
The daily performance ratio is ranging from 0.2 – 0.6. The highest performance ratio was on 12.08.2008 when the highest load occurred while the lowest performance ratio was on 13.08.2003 when the diesel generator was operated. The maximum daily power production from the PVs in the system in August 2008 was approximately 42 kWh/day while the energy to the load was around 37 kWh/day and the total available solar energy was around 62 kWh/day on the 8th of August 2008. The capture losses were around 26%. Moreover, the duration that the frequency was over 51 Hz on that day was only 1 hour and 35 minutes which was the minimum of the month.
Conversely, the maximum daily duration of the grid frequency over 51 Hz was around 8 hours on the 26th August 2008 with only 18 kWh/day PV energy produced, and around 17 kWh/day energy to the load while the total solar energy on the PV system was around 56 kWh/day. The capture losses were around 65% which was very high.
The battery tends to be fully charged everyday (the grid frequency is over 51 Hz aiming to communicate to the PVs for de-rated power in order to protect the battery from overcharging), which leads to more capture losses and a lower performance ratio.
The following items are suggested in order to improve the system performance.

10.4.1. Additional load for better performance ratio

The Gaidoroumandra system had a diverse performance ratio from 0.2 to 0.6 which means the performance ratio of the system can be improved to a higher value. Since the PR depends strongly on the duration of the system frequency over 51 Hz has its potential to produce more energy but more load and/or a larger battery is required. To improve system's performance ratio, excess energy in the system should be used such as for water pumping, water Desalination, or gardening, etc.

10.4.2. Coupling of battery inverters on a single phase

The minigrid loads are all single phase. The existing 3-phase is highly un-balanced. A more optimal loading could be achieved with all battery inverters operating on the same phase.

10.4.3. Additional solarimeters for measuring correct irradiance on each PVs

Only one solarimeter was installed on the system house in the middle of the valley while the PV fields were installed on the different places such as some were installed on the hill.
To calculate the PV efficiency in a short time, the input solar irradiance must have very high accuracy. If short term PV efficiency is needed, the recommendation would be to install additional solarimeters on each PV fields or only install additional solarimeters on the houses number 7 and 10 which were built on the hills.

10.4.4. Create a database

The data measured should be collected in a database for convenient analysis because currently the software works only with a specific pattern of input data. To avoid problem from incorrect pattern file, a database should be built to support it.

10.4.5. Maintenance/check of the 2000229200 PV inverter at the house no.7

Since two PV fields installed at the same place (house no.7) have not produced the same amount of DC power, it is recommended to check the 2000229200 PV inverter performance.

10.4.6. Maintenance/check of the module temperature measurement

There is a problem in the module temperature data (no difference with ambient temperature) and checking the module temperature sensor is necessary.

10.5. Power quality issues

Power quality in the minigrid presents a few weaknesses according to EN50160.
Grid frequency is above threshold because of the derating of PV inverters, which is proportional to the frequency value above 51 Hz.
High values for voltage flicker on L2 is mainly due to a big load with an active power P=2.5 kW and a reactive power Q=1.6 kVAr, which operates in periods of only 15 minutes (probably a pump).
Harmonic U9 on L1 is above threshold due to a cyclic load, which is probably a cooling compressor with an active power P=150W and a reactive power Q=130 VAR
Harmonic U6 on L2 is above the limit, when the PV inverters are operating in de-rating mode.

11. References

[1] Unchalee Parinyacupt: “Performance evaluation of Gaidouromandra minigrid”, Master thesis – Postgraduate Programme Renewable Energy, 21.01.2009

[2] M. Vandenbergh, R. Geipel, M. Landau, P. Strauss, (2006), Performance evaluation of the Gaidouromandra minigrid with distributed PV generators, 4th European PV-Hybrid and Mini-Grid Conference, 29th-30th May, 2008, Athens, Greece

[3] ISET: Dataset Gaidouromandra 2004 - 5 months from 01.06.2004 to 31.10.2004, data prepared for MMG project

[4] ISET: Dataplots Gaidouromandra 2007-2008. Daily plots of power measurements prepared with the INTOUCH monitoring system

[5] ISET: Power quality reports for Gaidoroumandra, prepared with the HAAG monitoring system.